NASA TN D-1188

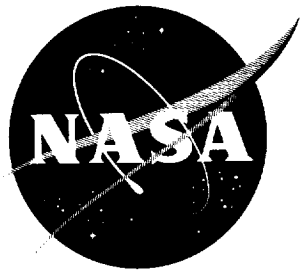

TECHNICAL NOTE

D-1188

GOVERNMENT-INDUSTRY CONFERENCE ON MERCURY CONDENSING

APRIL 18, 1961, PASADENA, CALIFORNIA

NATIONAL AERONAUTICS AND SPACE ADMINISTRATION

WASHINGTON

February 1962

CONTENTS

INTRODUCTION[1]

Considerable effort is currently being expended in the development of systems for the production of electric power for space applications. Many of these systems are based on Rankine dynamic engine cycles employing mercury as the working fluid. Principal developments are the Sunflower solar turbogenerator system sponsored by the National Aeronautics and Space Administration and the SNAP 2 and 8 nuclear turbogenerator systems sponsored, respectively, by the Atomic Energy Commission and the National Aeronautics and Space Administration. In addition, the Air Force has been supporting programs in demonstrator units and component research for mercury power systems.

An important aspect in the development of these systems is the successful execution of the boiling and condensing functions of the working fluid. Boiling and condensing in space power systems have become significant considerations because of the requirement of startup and operation in a zero-gravity environment and because of the strong influence of these functions on the system weight, reliability, and operating stability. Furthermore, questions are raised in the effective simulation of space operation in ground-based laboratory experiments.

Particular attention has been given recently by the principal system contractors to the study of mercury condensation. In addition, research programs in support of these efforts were being sponsored by both the Air Force and the National Aeronautics and Space Administration. Accordingly, a meeting was held among representatives of the various government agencies and industrial contractors actively involved in mercury condensation studies. The purpose of the symposium was to facilitate an exchange of information, coordinate efforts, and provide guidance for formulation of future programs. The format of the meeting consisted of presentations of current activities and results, followed by a general round-table discussion of pertinent technical topics and questions. Some of the specific topics discussed were gravity effects and ground testing; test apparatus and measuring techniques; prediction of pressure drop; flow stability; physics of condensing; and effect of noncondensable gases.

This report presents the proceedings of the symposium and includes the individual prepared presentations and a summary of the important results of the general discussion. To avoid any further delay in making the information available to those who did not attend the meeting, this report has been assembled without technical or editorial review. It should also be noted that the conclusions and recommendations presented herein are those of the authors of the individual papers and they do not necessarily reflect the opinions of the NASA or the other participating agencies.

---

[1]INTRODUCTION and SUMMARY by Seymour Lieblein of the NASA Lewis Research Center, who served as chairman of the symposium.

THOMPSON RAMO WOOLDRIDGE INC.

New Devices Laboratories, Tapco Group

MERCURY CONDENSER RESEARCH AND DEVELOPMENT

Presented by A. Koestel and J. J. Reinmann

OBJECT AND SCOPE

The object of this report is to present a summary of mercury condensing research and development effort conducted at Thompson Ramo Wooldridge, New Devices Laboratories over the past 4 years. This report is the result of the NASA request for an interchange of information between the AEC, NASA, and WADD contractors on the topic of mercury condensing. Condensing research and development has been supported at New Devices Laboratories under the following Government contracts:

Contract	Contract No.	Government Agency
SNAP 1	AT(30-3)-217	Atomic Energy Commission
SNAP 2	AT(11-1)-GEN-8	Atomic Energy Commission
SPUD	AF 33(616)-7979	USAF-WADD
OFFBACE	AT(11-1)-GEN-8	Atomic Energy Commission
Sunflower	NAS 5-462	NASA
Space Radiator	AF 33(616)-7368	USAF-WADD

TRW Corporate Sponsored Projects related to condensing mercury vapors are:

Project	Project No.
1. Consulting heat transfer studies	523-007411-08
2. Two-phase flow nitrogen-mercury fluid dynamics	523-007538-08

These contracts encompass not only mercury condenser research and development but also radiator design and development applied to the optimum integration of the condenser-radiator components into space vehicles.

Mercury condensing research and development has included the following:

(1) Laboratory bench experiments to define problem areas, to determine design criteria for operation in a space environment, to obtain basic design data, and to develop mathematical models describing the hydrodynamics of condensing mercury

(2) Design and tests of experimental condensers

(3) Design, test, and delivery of prototype condenser radiators

(4) Zero-gravity testing of condenser design concepts in the C131B and KC135 aircraft

Presented in this summary report are space condenser design criteria, basic design data, a description of condensing mercury research test apparatus with related analysis, and test results for both ground and zero-gravity tests.

Conclusions and recommendations for future mercury condenser research and development are also included.

CONDENSER PERFORMANCE CRITERIA

Six major factors must be considered in the design of condensers for operation in a space environment:

(1) Condenser-subcooler demarcation zone stability (liquid-vapor interfacial stability)

(2) Condenser two-phase flow regime stability

(3) Condenser pressure drop and pump inlet net positive suction head

(4) Condenser inlet and outlet manifold design

(5) Multiple or parallel tube operation

(6) Condenser-radiator heat transfer

It is sometimes overlooked that some power conversion systems for space applications have the relatively severe performance requirement of operation under accelerations up to 1 g in any direction as well as the usual zero-gravity operation. With these requirements in mind, the condenser design is primarily condensing hydrodynamics while heat transfer plays a secondary though by no means a negligible role.

In conventional condensers gravity plays a predominant role in separating the liquid regions from vapor regions. Gravity holds liquid in the "hotwell" and provides the net positive suction head for the condensate pump. It can readily be visualized that if a conventional earth bound condenser were turned upside down the liquid in the "hotwell" would be dumped into the vapor inlet line and vapor would enter the pump inlet line causing pump failure. Similarly, a glass of water when

inverted will spill its contents, although sufficient barometric pressure is available to support a 34-foot water column. Instability and wave formation at the interface between liquid and gas cause the liquid surface to deform and break up permitting the less dense gas to displace the liquid. Determination of criteria for obtaining a stable liquid-vapor interface is obviously of utmost importance.

The interacting dynamics of liquid and vapor phases flowing concurrently through passages determines the form in which the two phases will coexist. These flow forms or flow regimes are classified as bubble flow, plug flow, stratified flow, mist flow, wavy flow, slug flow, annular flow, and many others as discussed in the following sections. These various flow regimes require different inventories of liquid and vapor, and if the flow regime is of the pulsating type, the condenser inventory could also pulsate. For a fixed inventory system such as the closed Rankine vapor cycle, this means that if any external or internal disturbances, such as vibration of solid boundaries or fluid disturbances, produce a new flow regime, the heat-transfer area of the subcooler and condenser or preheater and boiler will be altered. This phenomenon not only causes pressure fluctuation because of the dynamics of moving liquid slugs but also causes thermodynamic pressure fluctuations because of changes in equilibrium condensing temperature with condensing area. In a condenser operating at low pressure levels, pressure disturbances caused by a liquid slug may be a relatively large fraction of the absolute pressure and may cause erratic operation of the pump and turbine connected to the heat exchanger. It is of no small consequence that the flow regime be made relatively insensitive to external disturbances and be reasonably free of large scale pressure and inventory pulsations.

Once the design criteria are established for providing a steady supply of liquid condensate with the required net positive suction head to the pump, refinements should be made in pressure drop and density data. To design a condenser with maximum allowable pressure drop and minimum weight, pressure drop associated with the two-phase flow mixture must be accurately determined.

When more than one condenser tube is to be operated in parallel, it is desirable to produce equal loading and similar conditions in each tube. Distribution of vapor flow to each tube is controlled by the manifold design. If flow distribution is unequal, condenser and subcooler lengths will vary from tube to tube. Variations in condenser tube inlet pressure, tube diameter, condenser pressure drop, and tube heat rejection rate all lead to variations from tube to tube that may cause unequal inventory distribution. Special attention must be paid to manifold design procedures and quality control of condenser tubes and radiator fabrication.

The location and stability of the subcooled liquid legs during multiple tube operation of a condenser depends on manifold flow distribution, heat-transfer characteristics, tube geometry, and of most importance, the slope of the flow-pressure drop curve.

Flow of the condensing mixture in a direction opposite that of gravity is the most likely to lead to instability of multiple subcooled liquid legs since this approaches the conditions of an inverted U-tube manometer which is statically unstable. Zero-gravity operation may yield liquid-leg instabilities under certain conditions; whereas if the body force and flow are in the same direction, no instability can be expected since the body force would have a powerful stabilizing effect. Hydrodynamic design criteria must be developed to prevent parallel-tube liquid-leg instabilities.

Condensing heat-transfer coefficients for mercury have been found experimentally to be in the range of 1000 Btu per hour per square foot per ^{o}F and greater, and as such represent a negligible heat-transfer resistance in the design of direct radiant cooled condensers. Compact mercury condensers cooled by a secondary fluid, however, require accurate knowledge of heat-transfer coefficients for purposes of weight minimization. Since all hardware contracts at TRW utilize direct radiation cooling, little emphasis has been placed on the determination of mercury condensing heat-transfer coefficients.

HYDRODYNAMICS OF SPACE CONDENSERS

Required condenser performance can be attained by intelligent application of the forces available in forced convection condensation in the absence of gravity or in the presence of adverse gravity effects. The physics of two-phase systems is based on hydrodynamic stability, a very difficult and complex engineering science. Usually very little progress can be made solely on an analytical basis, so that experimentation must be used to fill in the gaps. In the following sections are presented descriptions of those tests performed to obtain the necessary condenser design criteria. A summary of the analysis and the results related to these tests is also presented.

The keyword to the hydrodynamic study of condenser design for zero gravity is stability. First, a stable flow regime is necessary to maintain a nonshifting condenser inventory and condenser-subcooler demarcation zone. This ensures correct condenser pressure level and required subcooling. Next, the liquid-vapor interface must remain stable when subjected to internal and external force disturbances, e.g., fluid turbulence, partial slugging, rotating machinery vibrations, and meteroic impact loads. Stability of the interface prevents vapor from reaching the pump inlet. Finally, pressure drops and pressure fluctuations must

be held within tolerable limits. High condenser pressure drops may cause faulty pump performance and raise the turbine back pressure sufficiently to render cycle efficiency unduly low. Pressure fluctuations resulting from condenser heat-transfer area variations and high turbulence levels in two-phase flow systems could lead to erratic pump operation.

At Thompson Ramo Wooldridge mercury-condenser performance problem areas were defined, and a series of separate tests was devised to study these problems. These tests yielded design criteria for mercury condensers as well as data for devising mathematical analyses of forced convection mercury condensing. Condensers were fabricated and tested under ground conditions and in zero gravity to verify and improve these design criteria. Figure 1 is a flow sheet outlining the various tests and the manner in which these tests were integrated to yield condenser design data.

Adiabatic two-component flow tests utilizing nitrogen gas and liquid mercury were conducted to determine the possible flow regimes in a condenser. These same tests were used to investigate the critical gas velocities required to entrain mercury droplets of various diameters. Pressure drop and liquid hold-up measurements provided detailed insight into the flow mechanics of liquid mercury in vapor.

Conditions for maintaining a stable liquid column at the inlet of the condensate pump (subcooler) in zero gravity and ± 1 g were experimentally investigated. This is referred to as interfacial stability. Both static and dynamic tests were made on mercury columns in glass and stainless-steel tubes. Stability limits were defined.

An early Mark I OFFBACE single tube condenser experiment was designed from the above empirical data and tested on ground and in the WADD C131B aircraft during zero-gravity flight maneuvers. Primarily, these tests provided the critical Reynolds number for flow regime stability and verified the critical diameter tests for condenser-subcooler interfacial stability. The influence of noncondensable gas on flow performance in mercury forced-convection condensers was experimentally observed in these tests. The danger to system performance induced by gas plugs in the subcooler lines was recognized and means for gas removal suggested.

When the basic hydrodynamic stability of single-tube condensers had been verified, experimental determination of condenser pressure drop was initiated. This work was divided into several phases with each phase aimed at refining pressure drop prediction and determining sensitivity of pressure drop to external body forces. Pressure drop data were taken on the ground in constant diameter and tapered tubes, in horizontal positions, and in positive and negative inclined positions. Pressure

drop data were also obtained in the Mark II OFFBACE rig on board the KC 135 aircraft during zero-gravity maneuvers. Most recently pressure drop data were obtained on the ground for an 8 foot long stepped-tapered tube condenser in both the vertically upward and vertically downward orientations.

To support theoretical analyses of pressure drop and particle entainment sensitivity to body forces, tests were conducted to determine the minimum angle of inclination to the horizontal at which various size mercury droplets would roll down a flat plate. In the adiabatic two component flow test rig, critical gas velocities were determined for which various size droplets were swept from a static position in a glass tube inclined at various angles to the horizontal. These tests formed the basis for understanding the dynamics of mercury drops in a gravity-flow field.

Since there is a possibility of noncondensable gas accumulation near the condenser-subcooler interface, a porous plug gas removal device was designed, fabricated, and tested. Removal of a gas plug was accomplished by means of a porous tube wall having pore sizes sufficiently small to prevent the nonwetting liquid mercury from flowing out while the low surface tension gas flow was practically unrestricted.

Both a tapered and a constant diameter condenser inlet manifold were tested to determine the effect of manifold design on parallel tube condenser performance. The inlet manifold fed four parallel condenser tubes that emptied into a common subcooled liquid header. Since the condenser assembly was located in a horizontal plane for test purposes, gravity effects were minimized. The test results agreed with manifold design predictions and also demonstrated that unequal flow distribution and/or heat-transfer rates in condenser tubes created variations in condenser and subcooler lengths.

A limited amount of parallel tube stability testing was accomplished with the manifold test rig. Perturbations on the subcooler liquid lengths were introduced and their dynamic response noted. A somewhat restricted criterion for parallel tube stability was suggested.

Culminating all these tests was the zero-gravity performance test of the OFFBACE Mark II system, a simulated closed mercury Rankine cycle engine. The Mark II system was designed specifically for installation and operation in the WADD KC 135 aircraft where approximately 32 seconds of zero gravity was obtained during each zero-gravity flight maneuver. (See fig. 2 for a program of the zero-gravity maneuver.) Mark II consisted of a sealed electric motor-driven pump that recirculated mercury from a multiple glass tube condenser to an electrically heated boiler. A choked nozzle and desuperheater provided a load for the boiler. Since this system did not incorporate a prototype turbomachinery package, mercury flow rates were not dictated by turbine or bearing requirements.

This fact allowed the use of a system having lower flow rates and, therefore, lower energy requirements than prototype systems. The apparatus provided opportunity to examine the effects of orbital flight on the boiler, condenser, and pump characteristics. Condenser performance evaluation was emphasized because of its sensitivity to body forces, and because variations in its performance directly affects both turbine and pump performance.

Besides pressure and temperature measurements at strategic locations in each component, motion pictures were made of the condenser-subcooler to obtain visual stability information about flow regime, condenser-subcooler interface, and parallel tube operation.

Interfacial Stability Tests

When one fills a tube with liquid, closes one end, and inverts the tube, the liquid may or may not leave the tube. Small tubes tend to retain the liquid, while larger tubes allow the liquid to run out. The maximum size tube that will retain the liquid is customarily called a critical diameter tube. It is usually arrived at through a dynamic formulation although it can be arrived at from static stability considerations alone.

To make the discussion simple, let us first consider the two-dimensional problem. Imagine a plane interface in a vessel with vapor below and liquid above as illustrated in figure 3. As long as the surfaces are precisely plane, the conditions of static equilibrium can be satisfied.

Now let us pose the question of what will happen if the interface is disturbed with some small wavelength. The result of the disturbance will be to reduce the potential energy of the displaced liquid. This will release energy. At the same time the length of the interface formed will be increased. This will absorb energy. For sufficiently small waves in a gravity field, the amount of energy released by displacement will be less than that absorbed by new surface formation and the interface will tend to oscillate about its neutral position if released. However, for a sufficiently long wave, the distribution is clearly unstable as the amount of new surface created does not appreciably change while the mass of liquid moved to a position of lesser potential energy clearly increases. This critical wavelength for the two-dimensional case is

$$\lambda = 2\pi \sqrt{\frac{\sigma}{(\rho_f - \rho_g)g}} \qquad (1)$$

where

g local gravitational acceleration

ρ_f liquid density

ρ_g vapor density

σ surface tension

An interface between two parallel vertical planes is stable if the spacing between the plates is less than $\lambda/2$. For a cylindrical, rather than plane, geometry the critical wavelength would be slightly different from this value. From a static and dynamic stability analysis, the effect of contact angle can also be included (ref. 1). Figure 4 is a plot of critical diameter against contact angle for a cylindrical container. Two regions are identified, stable and metastable. In the metastable region, a tube that begins to empty, because of a disturbance, will continue to empty as once the wall is covered by liquid the interface would have a contact angle of zero. If the tube diameter is reduced below the critical value for 0° or 180°, a bubble should not rise, no matter what the disturbances are or what the contact angle is. Design in the metastable region may be too unreliable, thus the recommended diameter limit is

$$D \leq 1.835 \sqrt{\frac{\sigma}{g(\rho_f - \rho_g)}} \tag{2}$$

The maximum diameter $D_{critical}$ for a stable interface between liquid mercury and mercury vapor is 0.136 inch as computed from the above equation.

Experiments were conducted to test these critical diameter relations and to establish parameters needed to maintain a stable liquid column in the subcooler and the inlet to the pump in the presence of various disturbances. These investigations were divided into two areas: static stability tests and stability tests with internal and external disturbances.

Static tests. - When a stable interface exists between a liquid and a gas, it is possible to compute the column of liquid h that can be supported against body forces by pressure and surface tension forces. This equation is

$$h_{max} = \frac{p_l - p_v}{\rho g} + \frac{4\sigma \cos \theta}{D\rho g} \tag{3}$$

where

D tube diameter

p_v vapor pressure of liquid at closed end of column

p_l pressure of liquid at interface

ρg body force, lb/cu ft

This equation was verified with experimental test data obtained on mercury columns with glass tubes of diameter 0.076 and 0.139 inch. A schematic diagram of the experimental setup is shown in figure 5. Mercury was placed in a glass tube and the pressure p_l varied until the mercury column fell into the mercury trap; p_l and h_{max} were recorded. The test glass tube was bent as shown so that the mercury would "tear" at the bend and not part from the glass as would be the case in a straight tube. A straight tube was tested, but no noticeable difference between a bent tube and a straight tube could be detected.

The significance of this static analysis and supporting tests in condenser design is as follows: If a disturbing body force resulting from impact with meteoroids or from maneuvering of the space vehicle is such that liquid tends to be forced from the subcooler into the condenser, the maximum restraining force on the column of subcooled liquid is given by

$$\left[(p_l - p_v) + \frac{4\sigma \cos \theta}{D}\right] \frac{\pi D^2}{4} \qquad (4)$$

Hence, a subcooler section could be designed to withstand the expected impulse and body forces.

Interfacial stability tests were first performed at room temperature using four straight Pyrex glass tubes of 0.1696, 0.1797, 0.1908, and 0.209 inch diameters, respectively, and two tapered tubes. The straight tubes were sealed at one end and filled with a short column of mercury. The tubes were than inverted, both slowly and also with a sudden movement. Only the smallest of the four straight tubes would hold a column of mercury, and this tube did not hold consistently, indicating that the critical tube diameter should be just under 0.1696. This diameter was marked on the tapered tube as a guide. The tapered tube was then filled with mercury to a diameter somewhat smaller than 0.1696 and small increments of mercury were added until the column would just support itself in the tube, that is, the addition of just one more drop of mercury would cause the column to spill or break loose from the tube, as shown in figure 6. The measured diameter was 0.157 inch.

Repeated tests showed that moisture or any foreign matter on the inner wall of the tube prevented reproducibility of test results. The critical diameter of 0.157 inch was observed consistently during several tests on both tapered tubes when they were clean and dry. However, for a contaminated tube, the mercury column would not support itself. After the tapered tubes had been cleaned and thoroughly dried, the critical diameter was again obtained.

These tests were repeated in Type 316 stainless-steel tubes. To obtain a range of inside diameters, holes were drilled and reamed in bar stock. The tubes were cleaned with alcohol and dried. The following diameters were tested: 0.118, 0.133, 0.140, 0.149, 0.158, 0.165, 0.168, 0.176, and 0.180 inch. The largest tube which held a stable interface was the 0.168-inch-diameter tube. Behavior similar to that observed in the glass tubes was observed with the 0.168-inch-diameter tube, that is, the tube had to be thoroughly clean and dry or the mercury would not hold in the tube.

To determine the effect of temperature on the critical diameter, the five largest stable steel tubes were filled with mercury and placed inverted in glass test tubes containing a few drops of mercury. The mercury in the test tube was to provide a mercury vapor atmosphere in contact with the interface. The five test tubes containing the inverted mercury-filled tubes were then placed in a small oven and the temperature was slowly increased. Thermocouples welded to the outside of the tubes indicated the tube temperature. Figure 7 is a schematic of the test apparatus. As the temperature was increased, the mercury dropped out of the tubes. Sometimes all the liquid spilled at once, while at other times it slowly dripped out. When the mercury spilled, the tube temperature was recorded. The test procedure was repeated nine times. The first few test results showed no definite trend in temperature against tube diameter. Erratic results were believe to be caused by air entrapped in the mercury, which expanded on heating and pushed the mercury out of the tube, and by the possibility of contamination of the tubes.

After every test the tubes were cleaned and dried, filled with mercury, placed in a vacuum chamber and gently tapped to remove the air which was trapped in the tube. The tubes apparently became cleaner and the degassing technique improved with each test. In the last three tests, all five of the mercury columns spilled when the tube temperature reached 672° F, which is the mercury boiling point at atmospheric pressure.

As mentioned above, before interfacial stability can be considered, the mercury vapor pressure must be less than the pressure at the interface. This condition was present in the inclined condenser tests discussed in a later section of this report. Apparently the mercury drops which originate on the condenser wall are subcooled before reaching the

interface. Subcooling is also caused by conduction of heat back through the liquid and by surface tension which increases pressure at the interface.

The maximum stable diameter of 0.168 inch holds only for the particular tube material and surface finished tested. The reamed hole in the Type 316 stainless-steel tube had a surface finish measured as 40 microinches rms. The effect of materials is evident in a comparison with the Pyrex glass tube where the critical diameter was 0.157 inch. The effect of surface finish was observed by attempting to hold mercury in a Type 316 stainless-steel tube of 0.133-inch inside diameter which had been vapor blasted.

The tube could not hold a mercury column when inverted. The inside surface was measured at 65 microinches rms. This indicates that the inside of a condenser tube should be smooth in the vicinity of the interface. Specifying an rms value for the tube may not be sufficient because the finishing process may also have an effect.

During the OFFBACE zero-gravity flights, five test capsules of different diameters filled with water, and five filled with mercury were observed in zero gravity. Figure 8 lists the diameters tested. Figure 9 shows the nature of the body force fluctuations during the zero-gravity trajectory. It was deemed desirable to establish definitely the stability of the liquid interface contained in small diameter tubes in zero gravity with whatever extraneous disturbances might be present.

All liquid interfaces in the test capsules were observed to be stable except during one instant when the test platform struck an object during zero gravity at which time the water interface in the largest tube (0.625-in. diam.) was disrupted. Figure 8 shows the range of disturbances, as obtained from figure 9, as a shaded area. The curves are the stability limits as computed from figure 4 ($\beta = 139^{\circ}$ for mercury and 60° for water). The range of disturbances and the size of the capsules were such as to fall within the stable region in figure 8. According to figure 8, instability would have been noted in the larger tubes of $\eta = -0.22$ (mercury) and $\eta = -0.4$ (water). Since the maximum negative body force disturbance encountered was $\eta = -0.02$, a diameter of 1.75 inches (mercury) and 3.25 inches (water) would have produced incipient interfacial instability as predicted by capillary stability analysis. However, gravity waves may produce instabilities for lower diameters than stated above. A photograph of the interfacial stability mercury test rig obtained during zero gravity is shown in figure 10. All interfaces are observed as stable since the diameters and disturbances were such as to fall within the stability limit shown in figure 8.

Interfacial stability with external disturbance. - The previous section shows that static stability can be guaranteed against small disturbances by proper choice of tube diameter at the interface. However, since forced vibrations on a statically stable interface could cause the

interface to break, tests were conducted to determine interfacial stability with external disturbances.

In these tests, mercury in a glass tube was subjected to vibrations of various frequencies and amplitudes and the boundaries or limits of instability were noted. The results of the tests are shown in figure 11. As expected, the test points define a hyperbolic-type curve, which indicates that at very low frequency the interface is stable to all amplitudes and at very low amplitudes the interface is stable to all frequencies. In general, smaller tube diameters result in greater stability. Sketches indicating the appearance of the interface when unstable and stable are also shown in figure 11. The surface had the appearance of a cow's udder in which the teats broke off into drops and formed a spray. At high amplitudes a single teat was observed which broke off into a single drop. From observations of the disturbed interface it was concluded that a vibrating membrane described in texts on vibration behaves in a similar manner. The nodal circles and nodal diameters referred to in these texts apparently are similar in appearance to the disturbed interface noted in figure 11. These tests were conducted on an "M.B." shaker in horizontal glass tubes. Displacement was vertical and the tubes were mounted horizontally. The glass tube was rigidly mounted on the shake table to minimize secondary vibrations.

If the power conversion system is required to operate in the presence of relatively large disturbances, a map of these disturbances can be superposed on figure 11 and the proper tube size can be chosen so that no vibrations lie in the unstable region. In constant diameter condenser tubes, stability may be obtained at the cost of pressure drop because of the small tube diameters required. This can be alleviated by the use of tapered tubes where only the diameter near the interface need be necessarily small for stability. For more accurate predictions of stability limits with external disturbances, the tests described should be repeated with mercury in steel tubes and at 600° F in order to duplicate as closely as possible actual condenser conditions. This would be important if the condenser were required to operate under vehicle launch conditions where vibrations may be appreciable.

Internal disturbance. - The effect of vapor velocity and mercury droplets impinging on the interface was studies in single tube condenser tests. Actual prototype conditions were produced in the condenser section upstream of the interface. The type of disturbance was identified by the heat flux loading of the inside surface of the condenser and the vapor velocity. The heat flux and the vapor velocity determine the number, size, and velocity of the condensation droplets impinging on the interface.

The internal heat flux ranged between 4000 to 6000 Btu per hour per square foot of inside surface, and the vapor inlet velocity varied from 100 to 15 feet per second. Mercury vapor was condensed against a slope of 0.182. The magnitude of the heat flux simulated a condenser tube with fins in a space environment. A stable interface was observed within the range of conditions tested.

Figure 12 is a schematic diagram of the experimental setup. Both the boiler, which was placed in a molten lead bath, and the condenser were made of Pyrex glass. A vacuum was maintained on the downstream side of the mercury column (subcooler). The vacuum was measured by means of a Stokes gage down to a level of approximately 200 microns. The pressure on the condenser-subcooler interface was then found by the vertical displacement of the mercury leg in the subcooler.

During the testing it was observed that the condensation droplets adhering to the walls of the condenser varied in size along the tube. The larger ones were near the interface and the smallest ones near the condenser inlet. This indicates that the vapor velocity, which varies from a maximum value at the inlet to zero at the interface, determines the drop size. This has been verified by data obtained from the mercury-nitrogen test rig. This leads one to speculate that high vapor velocities held constant in a tapered tube will produce the closest thing to a fine spray or fog.

The apparatus shown in figure 12 was also run in the vertical position. The liquid column, although oscillating in the tube, was well defined and easy to measure. The sequence of action in the condenser was as follows. With no visible liquid movement in the condenser, small drops condensed in the tube wall and grew in size. They then started to fall back into the boiler, coalescing with drops below it. When a drop became large enough to fill the tube it was thrown back up, picked up more drops, and became a large slug attempting to join the stable column. This up-and-down motion wiped all the drops from the walls and caused the slug to break up and partly fall back into the boiler. When all the slugs had fallen back into the boiler, the action repeated this sequence. This slugging phenomena is typical of two-phase fluids flowing against gravity.

Another interfacial stability test was made on a 0.197-inch inside diameter glass condenser tube in the test setup shown in figure 13. A glass bulb mercury boiler was immersed in a lead bath heated with a hot plate. The condenser tube was 4 feet long and connected to a vacuum pump. A Stokes vacuum gage in line indicated the back pressure. The condenser was in the vertical position as shown and was also run inclined at 18° with the horizontal. The mercury was degassed by heating the bath to 750° F at atmospheric pressure and then turning on the vacuum pump, which ran continuously during the run. The measured back

pressure ranged from 750 to 200 microns. At the start, mercury condensed in the tube and the condensate column grew rapidly to the stable length. The stable length is that which is supported by the pressure at the interface.

The apparatus of figure 13 was also run at an 18° incline to the horizontal. In this case the liquid column was harder to measure because it was always attached to the slugs. The sequence observed in the vertical run was not observed here. Instead the slugs continued to oscillate in the condenser, cleaning the drops from the walls before they could grow to appreciable size. The observed pattern is shown in figure 14.

Internal and external disturbances. - Interfacial stability in the presence of both internal and external disturbances was experimentally studied in the Mark I OFFBACE rig. During zero-gravity maneuvers in the WADD C131B Convair airplane approximately 12 seconds of zero gravity was attained with pull-in and pull-out body forces as high as $2\frac{1}{2}$ g's normal to the condenser tube. Engine vibration supplied the environmental disturbances in zero gravity. Mercury was condensed in a constant diameter Pyrex tube (0.136 in. I.D.) 12 in. long) oriented normal (horizontal) to the imposed body forces. At design flow and pressure, the liquid vapor interface remained stable for all body forces. Although at high g forces the interface deformed, it did not break up and admit vapor to the subcooler.

Two-Phase Flow Investigations

Two-phase heat-transfer and fluid-dynamic correlations require as their starting point a knowledge of the flow regime, or flow pattern. This is also the case in single-phase flow. Here it must be known whether the flow is laminar or turbulent before the Nusselt number or friction factor can be correlated. The mechanics of flow and heat transfer are, of course, different in laminar and turbulent flow. Thus, defining the two-phase flow regime establishes the flow and heat-transfer mechanisms and the resulting required correlation parameters.

A general classification of two-phase flow patterns is shown in figure 15. In one extreme we have vapor bubbles dispersed in a continuous phase of liquid and in the other extreme liquid droplets dispersed in vapor. Further classification is possible if droplet size or bubble size are included as variables. In between these two extremes occurs a condition where both phases are continuous. A liquid film on the wall with a vapor core or a vapor film on the wall and a liquid core are two cases. Further classification is possible if the form of the continuous interface (wavy, slug, smooth) is included.

The nonwetting property and high surface tension of pure liquid mercury is a destabilizing factor for the liquid-vapor interface, and as a result, films of pure liquid mercury are rare in a flowing system. Droplets dispersed in a vapor phase is the flow pattern observed in all two-phase flow tests made in transparent tubes using either liquid mercury in nitrogen gas or in mercury vapor. Thus, in postulating either a heat-transfer model or a fluid-dynamic model for analytical purposes, a flow pattern involving liquid drops dispersed in mercury vapor is assumed. In condensing, growing stationary surface drops are swept into the flowing vapor when they reach a certain critical size. The critical droplet size is determined by the vapor velocity and, since a condenser of constant tube diameter will have an axially varying gas velocity, droplets of different sizes will also result. Figure 16 illustrates the flow pattern encountered during condenser tests.

Adiabatic two-component flow tests. - To obtain two-phase flow pressure drop data without the complications of heat transfer and condensing, two-component flow tests were conducted using nitrogen gas and liquid mercury flowing through a transparent glass test section. Figure 17 is a photograph of the test apparatus and figure 18 is a schematic of the same apparatus.

In operation, dry nitrogen gas is metered and mixed with liquid mercury and ducted to a glass test section 4 feet long. Pressure drop was indicated on a mercury manometer connected to static-pressure taps at each end of the test section.

The two-phase mixture leaving the test section enters a separator where the nitrogen is vented and the liquid is collected and weighed. Valves control the nitrogen and mercury flow into the mixing tee. The test section had an inside diameter of 0.394 inch and all tests were run with the test section in the horizontal position. Quick-closing pneumatically operated valves were located at the inlet and exit of the test section. By closing these valves simultaneously, the liquid mercury was trapped in the test section and could be removed and weighed to determine the liquid inventory.

The most striking phenomenon observed in these two-phase flow tests was the tendency towards separation of the two well-mixed phases when a mixture of liquid mercury and nitrogen gas entered a pipe line. This phenomenon was observed by a number of two-phase flow investigators using water and air, but in the case of liquid mercury an additional phenomenon, peculiar to mercury only, was noted: as the gas flowed rapidly down the tube, the liquid mercury was left behind in drop form, being moved slowly (relative to the gas) by the drag of the gas on the drops. Since the gas phase was moving two to twenty times faster than the liquid phase, the droplets had a tendency to slow down and to accumulate in the tube. For "equilibrium" conditions, the liquid drops would

have to leave the test section at the same velocity as they entered it. Equilibrium conditions were not reached because the available tube length was not sufficient. Since such an "equilibrium" condition does not exist in an actual condenser, no special effort was made to achieve such fully developed flows. Because of the nonwetting properties of liquid mercury and its high surface tension, it was impossible to obtain a continuous liquid film or layer of mercury. The liquid phase was always in drop form of one sort or another.

The following patterns were observed with the concurrent flow of nitrogen and liquid mercury (nonwetting) and are sketched in figure 19:

(a) Caterpillar flow: The liquid phase is never continuous; it is broken into long, caterpillar-like drops that are equally spaced and move at the same velocity.

(b) Drop flow: The caterpillars are broken into smaller drops by the higher gas flow. Again the spacing between drops is fairly even and only little drop growth is noticed.

(c) Turbulent flow: The high gas rate causes turbulent movement of the drops. The drops bounce off the walls, colliding with each other and growing in size.

(d) Semiannular flow: The small drops on the bottom are moving very rapidly and closely together (to the naked eye, there seems to be a continuous liquid stream). Smaller drops are moving along the walls with some drops dispersed in the gas stream.

(e) Fog flow: The drops are picked up from the walls by the very fast moving gas and dispersed in the gas stream. The drops are so small that they cannot be seen by the unaided eye.

In addition to these main flow patterns, a few transition patterns were noted. For instance, if in turbulent flow the liquid rate was increased, the flow pattern seemed to approach the wavy pattern of wetting fluids, but such a pattern cannot be defined because no continuous liquid phase was ever observed with liquid mercury. The fast-moving large drops, being in a highly turbulent state, only appear to form a continuous layer of mercury. The transition between semiannular flow and fog flow is very sudden. No annular flow, in the strict sense of the word, was ever observed. The drops on the bottom of the tube were always larger and more numerous than the drops along the walls of the tube. This is a gravity phenomenon which will be discussed in detail later.

Figure 20 is a two-phase flow map in which the variables are the liquid and gas weight-flow rates. The transition between the flow

patterns cannot be pinpointed and for this reason, areas rather than lines were drawn as demarcation between the different zones. It may be noted that at high liquid and low gas rates, an unsteady and slugging type of flow exists. The flow map points out one important factor, namely, that for a given tube configuration and orientation, the flow patterns are functions of the two weight flows only.

Pressure drop. - The pressure drop in any two-phase flow system is greater than that for the flow of either phase flowing alone. This increase in pressure drop is due to the shear forces on the walls, the drag forces due to the particles, and the fact that the presence of the second fluid reduces the cross-sectional area of flow for the first fluid.

In presenting two-phase-flow pressure drop data, it is customary to plot the pressure drop ratio against the flowing quality. The pressure drop ratio is the ratio of the two-phase pressure drop Δp_{tp} to the pressure drop due to the gas alone Δp_g.

The flowing quality is defined as the ratio of the flow rate of the gas to the total flow.

Figure 21 is such a plot for the nitrogen - liquid mercury data. The pressure-drop ratio is seen to be greatly influenced by the gas flow rates. This is attributed to two effects: (1) gravity and (2) drop size. At low flow rates, gravity causes the mixture to desegregate, thus affecting the pressure drop. At high gas flow rates, drop sizes are reduced and the increase in drag associated with a large number of small drops causes an increase in pressure drop as contrasted to a smaller number of large drops. An increase in mercury flow (decrease in quality) also increases the pressure-drop ratio, but to a much lesser extent. We can conclude that the pressure drop is most sensitive to the gas flow.

A comparison of the pressure-drop data with the well-known Martinelli correlation is in order. Figure 22 shows this comparison for the case of viscous-turbulent flow, which Martinelli defines as the gas Reynolds number greater than 2000 and the liquid Reynolds number less than 1000. The spread in data is no greater than the spread in Martinelli's data used to obtain the curve. It is also evident that the spread is not random but that Φ_{gvt} increases with gas flow rate.

Figure 22 indicates that the Martinelli correlation (curve in fig. 22) may be valid for approximate estimates of pressure drop, but is insufficient to apply to condenser design for space powerplants. A mathematical analysis more pertinent to the specific flow pattern of condensing pure mercury is required to improve the correlation.

Adiabatic two-phase flow pressure-drop data are useful to predict pressure drop in a condenser. However, the results of such a procedure are to be considered approximate since different mechanisms are involved in the flow during condensing. In the two-phase flow test rig, liquid mercury is atomized in the flowing nitrogen and the mixture flows through the test section. In the condenser vapor enters the inlet and condensation occurs along the tube. The liquid drops grow on the surface until they are swept away by the flowing vapor. The mass flow rate of vapor is decreasing while the flow rate of liquid is increasing along the length of the condenser tube. Therefore, any one data point taken in the two-phase flow test rig represents one point in the condenser.

To use these data to predict approximate condenser pressure drop, the data from curves shown as figure 22 must be integrated to obtain the pressure drop in condensing a vapor from a quality of unity to zero keeping the total weight flow constant.

Holdup. - The liquid holdup in a system is important from the viewpoint of inventory consideration, and for determination of the ratio of liquid droplet velocity to gas velocity, which is referred to as the slip ratio. Holdup is of prime importance in formulating pressure drop equations based on the flow mechanics as defined by the slip ratio. For every nitrogen - liquid mercury test run, the liquid holdup was obtained by the quick-closing valve technique.

Figure 23 shows the liquid holdup (defined as the volume fraction of liquid in the test section) as a function of the flowing quality. On the same graph are plotted theoretical relations and semiempirical correlations for comparative purposes. The test points fall between the theoretical fog flow equation and the Martinelli liquid holdup correlation. This indicates that although fog flow was approached, it was never reached. Fog flow can be achieved only with very small drops which travel at the same velocity as the gas. The deviation from the Martinelli curve is due to the fact that the Martinelli model is based on continuous liquid and gas phases, whereas in the case of a nonwetting fluid, the liquid phase is discontinuous (drop flow of one kind or another) and only the gas phase is continuous. This means that the volume occupied by the liquid is appreciably smaller in the nonwetting case, and thus the experimental liquid holdup is less than predicted by Martinelli's curve.

Figure 23 shows that the experimental results follow the trend of the fog flow curve but are approximately ten times as large. A crude approximation of the condenser inventory can be made assuming that the liquid volume fraction will be ten times that for the fog flow case.

For fog flow the liquid and vapor have the same velocity and therefore the weight of liquid will be equal to the weight of vapor in a condenser tube. Since the volume fraction of liquid is small, it can be neglected in computing the vapor volume in the tube. Therefore the liquid weight in the tube will be ten times the vapor weight and the total weight of mixture in the condenser tube will be eleven times the weight of vapor which can be contained in the tube volume.

Flow regime stability. - The flow pattern for a two-phase flow system is determined by conduit shape, body or gravitational forces, interphase forces (normal and shear stresses), and intraphase forces (surface tension). In general, the flow patterns can be classified as (1) gas phase dispersed in a continuous liquid phase (bubbles), (2) liquid phase dispersed in a continuous gas phase (droplets or fog), (3) both phases continuous with wavy or smooth interface. The high surface tension (intraphase force) of nonwetting liquid mercury and the mercury vapor drag force (interphase force) exerted by the flowing vapor on the liquid mercury tend toward a flow regime of liquid mercury droplets dispersed in vapor. This general flow pattern can be further classified as to the size of the mercury droplets.

Pressure drop and inventory data can be correlated only if the flow pattern is defined. For example, the pressure drop in a pipe containing a single-phase fluid can be computed if it is known whether the flow is laminar or turbulent. In the design of a zero-gravity condenser, the characteristics of the two-phase flow system must be such as to be relatively independent of any body forces that may be imposed during launch, ground testing, or in orbit. At zero gravity, it is anticipated that some body force disturbances may occur. If the condenser flow pattern is sensitive to body forces, then the resulting alteration in flow pattern will cause changes in condenser liquid holdup which, in turn, causes a shift in the position of the subcooler-condenser interface and changes in the amount of subcooling. Since the two-phase pressure drop also depends on flow pattern, a change in pressure drop will occur with imposed body force disturbances. Tests have indicated this to be true. At low Reynolds numbers, the condenser pressure drop measurements will be shown to be sensitive to inclination. At the higher Reynolds numbers the differences disappeared, indicating that the flow pattern is no longer dependent on the Froude number (ratio of inertia to gravity forces).

Tests have been made in zero gravity and in the laboratory to determine the minimum design Reynolds number at which two-phase flow is independent of gravity. The following tests provided the necessary information:

(a) Critical drop size measurements: A determination of the relation between gas flow and drop size at instant of entrainment

(b) Zero-gravity tests: Visual indication of flow regime sensitivity to gravity

(c) Pressure drop measurements in mercury condensers: Dependence of pressure drop on gravity

(d) Inclined plate test: Drop entrainment in a gravity field

Measurements of critical droplet size. - A difficult flow phenomenon to analyze is that involving the motion of a dispersed substance within a flowing fluid. The dispersed substance might be solid particles, liquid droplets, gas bubbles, or immiscible droplets. The number of variables required for rigorous analysis is usually too great to be handled experimentally or analytically. As a result, the problem is to simplify without significantly detracting from the physics of the phenomenon. For a two-phase flow system, the same variables as for a single-phase fluid are used (Reynolds, Weber, Froude, Mach numbers, etc.) in addition to the ratio of the properties of the dispersed substance to the continuous fluid (viscosity, density, etc.). In the majority of cases, the following minimum number of variables should be considered:

(a) A boundary scale term, such as the pipe diameter

(b) A velocity to define the kinematics of the main flow

(c) The properties of the main flow, such as density and viscosity

(d) The dispersed phase described by a linear dimension (diameter if spherical droplets), specific weight if the effect of gravity on the flow is to be investigated, density, viscosity, surface tension of liquid-vapor interface, and the concentration

A function as follows will result:

$$f(D, U_g, \mu_g, \mu_l, \rho_g, \rho_l, \gamma, d, \sigma, C) \tag{5}$$

or in terms of dimensionless parameters, equation (5) may be expressed as

$$f\left(\frac{D\rho_g U_g}{\mu_g}, \frac{\rho_g U_g^2}{\gamma d}, \frac{d\rho_g U_g^2}{\sigma}, \frac{d}{D}, \frac{\mu_g}{\mu_l}, \frac{\rho_g}{\rho_l}, \frac{C_f}{C_w}\right) = 0$$

$$f(\text{Reynolds, Froude, Weber numbers, } d/D, \mu_g/\mu_l, \rho_g/\rho_l, C_f/C_w) = 0$$

where

C concentration (number of droplets per unit volume)

C_f concentration in flowing gas

C_w concentration on wall

D tube diameter, ft

U_g gas velocity, ft/sec

γ specific weight due to gravity, lb force/cu ft

μ_f liquid viscosity

μ_g gas viscosity

ρ_g gas density, lb mass/cu ft

ρ_l liquid density, lb mass/cu ft

σ surface tension, lb force/ft

If certain characteristics of the droplets are determined by the flow, then flow becomes an independent variable. For the case investigated, the droplet size was determined by the gas velocity. For the entrainment tests under consideration, the number of droplets in the tube was held to a minimum; therefore, droplet interference was minimized, and C in equation (5) was eliminated as a variable.

In these tests mercury droplets were sprayed onto the inside surface of a glass tube. The droplets were then measured by crosshair in a microscope. The nitrogen flow rate required to pick up or entrain the droplet into the gas stream was then determined. Figure 24 shows a schematic of the test. This test simulated the conditions in a mercury condenser in which drops grow on the surface by condensation until they are large enough to be entrained by the flowing vapor. If by chance another drop would collide with the droplet in the view of the microscope, the data would not be recorded since entrainment was caused by collision and not by the gas. This phenomenon was rare. During the tests ρ_g was not varied by much, and since ρ_f was constant, the property ratio ρ_g/ρ_f was not a major variable. Surface tension and the property ratio μ_g/μ_f were also constant.

Equation (5) now becomes

$$f\left(\frac{D\rho_g U_g}{\mu_g},\ \frac{d}{D},\ \frac{\rho_g U_g^2}{\gamma d}\right) = 0$$

where

$\frac{D\rho_g U_g}{\mu_g}$ Reynolds number

$\frac{\rho_g U_g^2}{\gamma d}$ Froude number

For a given tube inclination, the Froude number was found to be a function of the gas Reynolds number; therefore, the data can be presented as d/D against the gas Reynolds number for a given tube inclination. The purpose of the tests is to determine the gas Reynolds number at which d/D is independent of gravity, that is, tube inclination. When the term, $\rho_g U_g^2/\gamma d$ is low in magnitude, it can be expected that the droplet size ratio is influenced by gravity.

Figure 25 shows a plot of the data obtained from the nitrogen-mercury test rig of figure 24. The ratio d/D is plotted against the gas Reynolds number for tubes of different size tilted both upwards and downwards. A measurement of a critical mercury droplet size obtained in a mercury condenser in zero gravity is also shown. The source of this droplet measurement in zero gravity is discussed in the following section entitled "Zero-gravity tests." Also plotted in figure 25 is the ratio of laminar boundary-layer thickness against the gas Reynolds number in order to afford a comparison between the droplet size and the thickness of the laminar sublayer. The equation used for computing the thickness of the laminar sublayer is

$$\frac{\delta}{D} = \frac{25}{(Re_g)^{7/8}} \qquad (6)$$

which can be found in any standard text on boundary-layer fluid mechanics. Note in figure 25 that as the critical Reynolds number is reached (4000 to 2000), the laminar boundary layer fills the tube and δ/D equals R/D equals 0.5. The scatter in droplet size measurements is caused by gravity since some of the droplets were measured while clinging to the side of the tube and some were on the bottom. In figure 26 is plotted the absolute values of critical drop size and laminar sublayer thickness against relative velocity. Apparently, the force of gravity

played some role in the incipient motion of the droplet according to figure 25. In addition, the tube was oriented in three positions with respect to the gas flow direction, namely, tilted upward, horizontal, and tilted downward. In figure 25 note that the droplet measurements are greater than the laminar sublayer by several factors and that the size of liquid mercury droplet in mercury vapor in zero gravity (diamond-shaped symbol) appears to be less than the size of liquid mercury droplets in nitrogen gas in a 1-g environment. This means that data obtained in an earthbound nitrogen-mercury rig are conservative since droplets are smaller in zero gravity and that the flow regime is less likely to be affected by gravity disturbances. Support to this statement is given in figure 27 in which the ratio of the gas pressure acting on the droplet to weight force of droplet (Froude number) is plotted against the gas Reynolds number. For Reynolds numbers less than 8000, the ratio of inertia to gravity force is of the same order of magnitude, indicating that a condenser designed for Reynolds number lower than 7000 may show changes in performance (changes in inventory and pressure drop) when taken from a 1-g environment. Note that Froude numbers are in the range of 100 to 1000 for Reynolds numbers greater than 15,000. As mentioned before, indications are that the actual Reynolds numbers for mercury condensing are somewhat lower for a given Froude number.

The effect of gravity on critical droplet size is further illustrated in figure 28 in which the ratio of gravity to inertia force (reciprocal Froude number) is plotted against the gas Reynolds number for the case of upward and downward flow of gas. As expected for low Reynolds numbers, droplets are smaller for downward flow than for upward flow since gravity and gas pressure both act in the same direction and therefore both aid in droplet entrainment. As the ratio of gravity to inertia force approaches zero at high Reynolds numbers, the two curves merge, indicating that the role played by gravity becomes negligible. At a Reynolds number near 20,000 the effect of gravity seems to disappear, and according to figure 27, at a Reynolds number of 20,000 the ratio of inertia to gravity is about 300.

The reason for relating critical droplet size to gas Reynolds number in figures 25, 27, and 28 is that a relation is believed to exist between the laminar sublayer thickness - which is also a function of gas Reynolds number - and the critical droplet diameter.

The phenomenon of gas entrainment of mercury droplets is closely related to the subject of sediment transportation, which is usually covered in texts on hydraulics. Here the transportation rate of sediment is related to the tractive force of the stream. The tractive force required to cause incipient movement of sediment is referred to as the critical tractive force and is closely analogous to the vapor flow rate and the maximum drop sizes to which the condensate can grow before movement begins in a condenser. Various investigators in the fluid of

sediment transportation have noted an exponential relation between particle diameter and the critical tractive force. They noted a change in slope of the function when a certain particle diameter was attained. This was attributed to a change in boundary motion regime depending upon the magnitude of submergence of the surface particle within the laminar boundary layer. Apparently, the ratio of particle diameter to laminar boundary-layer thickness becomes the essential parameter. This ratio has the same significance as the ratio of the size of the surface roughness projections to the laminar boundary-layer thickness in the case of pipe roughness and friction factors. Many investigators in the field of sediment transportation feel that the ratio of particle diameter to the boundary-layer thickness plays an essential role in determining not only the beginning of movement but the form of the function at incipient motion. Subsequent analyses show that a surface tension force, drag, and gravity are the primary agents in establishing the entrainment drop size. Thus the Weber and Froude numbers become the important flow parameters.

Zero-gravity tests. - The zero-gravity tests were conducted with TRW test apparatus aboard the C-131-B aircraft at WADD. The tests were part of the SNAP 2 sponsored OFFBACE program investigating the fluid mechanics aspects of a Rankine cycle powerplant in a zero-gravity environment. WADD flew the airplane through trajectories which produced conditions of weightlessness (zero-gravity), 2.55, and unity g.

Figure 29 presents photographs of mercury condensing during different magnitudes of body forces acting normal to the tube axis. The photographs were produced from high-speed motion picture films taken at 500 frames per second (thirty times normal speed).

These photographs show mercury droplets produced in a 0.136-inch inside diameter tube approximately 12 inches long with inlet vapor Reynolds numbers in the range of 2000 to 4000. Droplet measurements taken from the high-speed films and presented in figure 30 show a change in drop size distribution when going from zero to 2.55 g. This means that the flow regime is sensitive to body force disturbances and that changes in mercury inventory and pressure drop would occur as a result. This sensitivity is attributed to the low vapor Reynolds number and the resulting low Froude number of the droplets. A high Reynolds number condenser would be insensitive to body force disturbance except in the region near the interface where local vapor velocity and gas Reynolds number approach zero.

Growth of droplet size due to agglomeration near the liquid interface further increases the sensitivity of the flow pattern to gravity disturbances. Tapering the tube is a means of remedying the situation since vapor velocities are maintained high along the entire tube length. Drop agglomeration, which depends on the volumetric flow ratio of liquid to vapor, becomes a problem when the mixture quality becomes low for

both straight and tapered tubes. The agglomeration effect is brought out by equation (5), which has the critical droplet size as a function of the droplet concentration ratio of moving drops to stationary growing droplets on the wall.

The spread in drop size due to gravity shown in figure 30 is caused by gravity force inducing incipient drop motion in the upper part of the tube and by gravity retarding movement in the lower portions. Therefore, droplets entrained in the upper region of the tube will become smaller while droplets in the lower region will get larger. The reason for some spread in drop size even at zero gravity is the fact that the data were evaluated near the midsection of the tube where small droplets born near the condenser inlet in a relatively high vapor Reynolds number are mixed with larger droplets originating further downstream where the local vapor Reynolds number is relatively low.

Analytical determination of drop size. - Since estimates of mercury droplet sizes are desirable if gravity effects in mercury condensers are to be computed, a detailed understanding of drop entrainment is of prime importance.

Mercury drops grow on the heat-transfer surface by condensation until they are large enough to be entrained into the flowing vapor by action of gravity and drag forces. The size to which the droplet will grow at incipient entrainment is denoted as δ_c. Critical drop size measurements were made in glass tubes with flowing nitrogen gas and on inclined plates in which only gravity effects are present.

Figure 31 shows a droplet resting on a surface under the influence of gravity and drag forces. The retarding force, which prevents movement, is attributed to surface tension. It is surmised that the only property of a real (Newtonian) fluid which can support stress without a rate of deformation is the surface tension. Without surface tension the action of any stress (drag or gravity) will immediately produce movement or flow.

The following is an equation for the force balance just at the condition of incipient movement (the momentum term is zero):

$$\frac{\pi\delta_c^2}{4} C_{d_\delta} \frac{\rho_v U_v^2}{2g_s} \pm n \sin\theta \rho_f \frac{\pi\delta_c^3}{6} = \pi\delta_c \sigma E_\sigma \qquad (7)$$

where E_σ is a constant to be evaluated by experiment. It is of the order of 1 and takes into account the effect of drop deformation, contact angle, and condition of surface on the magnitude of the retarding surface tension force. Since $\pi\delta_c\sigma$ represents an upper limit, E_σ will be less than 1. The actual perimeter of contact will be less than $\pi\delta_c$, and σ will be reduced by the cosine of the mean contact angle during deformation.

The coefficient of drag for drops C_{d_δ} is, of course, dependent on the deformation.

The values of the drag coefficients for the deformable bodies (bubbles and drops) are greater than for solid spheres and are near 1. Therefore, for simplicity, assume equal to 1 and let E_σ accommodate the deformation effect. Equation (7) becomes

$$\frac{\rho_v U_v^2}{2g_s} \pm n \sin\theta \rho_f \frac{2}{3}\delta_c = \frac{4\sigma}{\delta_c} E_\sigma \tag{8}$$

Since the E_σ is evaluated by test and its magnitude depends on the degree of deformation the drop can accommodate before it breaks loose from the surface, it is of importance to examine the shape of drops under the influence of forces. Figures 32 to 34 show the correlated results. The correlation parameters are those obtained from equation (8). For horizontal tubes equation (8) becomes

$$\frac{\rho_v U_v^2 \delta_c}{\sigma 2g_s} = 4E_\sigma \tag{9}$$

Thus, the left term becomes the Weber number.

The Weber number depends on the constant E_σ which is determined by the effect of drop distortion on the surface tension force.

For the inclined plate equation (8) becomes

$$n \sin\theta \rho_f \frac{2}{3}\frac{\delta^2}{\sigma} = 4E_\sigma \tag{10}$$

For this case the left term is a nameless group representing the ratio of gravity to surface tension.

When results are obtained from flow test in inclined tubes, both terms in equation (8) are required for correlation. Figure 33 correlates the results for horizontal tubes. Note that the ordinate values represent four times the factor E_σ. The value of E_σ varies with δ_c/D since the curvature of the tube in relation to the curvature of the drop affects the surface tension force and thus the value of E_σ. As the drop size becomes small, the tube surface approaches that of a flat plate and thus E_σ approaches a constant value as $\delta_c \ll D$. The value for E_σ for the inclined plate results is indicated in figures 32 and 33. This value should compare with the E_σ obtained from the flow test results (fig. 33) for the condition of δ_c/D approaching zero. As can be seen, the agreement is good.

Figure 34 shows the correlation for the inclined tubes and the values for E_σ are indicated.

A theoretical approach for the determination of E_σ is available if the analytical procedures of Bachforth and Adams (ref. 2) are applied. They computed the entire shape of a mercury drop in a gravity field normal to the surface upon which the drop rested. The combined effect of surface tension and gravity established the surface film curvature and thus the value of the contact angle and the contact (solid-liquid interface) surface area. This could be done in a gravity field of different orientation or a given distribution of surface forces (pressure and shear). The hydrodynamic pressure distribution on a rigid sphere is well known. This distribution of force can be used to calculate the deformation of a fluid drop. Reiteration would be required since the distorted drop would have an altered distribution of surface forces. The combined effect of surface shear and pressure forces are incorporated into the measured coefficient of drag. When once the drop shape is analytically established, E_σ can be determined by a line integral around the contact perimeter as shown in figure 31 as follows:

$$E_\sigma = \frac{1}{\pi\delta_c} \oint_S \sin \beta \, dS \qquad (11)$$

when S is the perimeter length.

The mathematical procedures appear difficult and the experimental techniques appear more fruitful.

Equation (8) together with the experimental values for E_σ can now be used to determine the value for δ_c in a combined gravity-flow field. The determined value for δ_c can be incorporated into dynamic equations for computing slip and pressure drop in a gravity-flow field.

Condenser Pressure Drop

Pressure drop in mercury condensers was measured on straight, continuously tapered, and stepped tapered tubes. These tubes were operated in several orientations: horizontal, inclined upwards from the horizontal, vertical upward, and vertical downward. Condensing temperatures ranged from 500° to 725° F. The total range of Reynolds numbers measured at the condenser inlet was from 12 to 12,000.

The ratio of condenser length to condenser inlet diameter (L/D) ranged from 24 to 155. The data were correlated over this range and found to agree with adiabatic two-component flow data at high Reynolds numbers. However, condensing data is required for Reynolds numbers above 15×10^4 in order definitely to establish a trend.

Pressure drop apparatus. - In the straight and continuously tapered tube cases, the apparatus was fabricated from Pyrex. The condenser tube was joined to a glass bulb boiler containing a pressure tap. Glass was used for ease of fabrication and to secure a leak proof apparatus. The greatest advantage of using glassware was that the condensing process could be visually observed and pressure and flow rate could be measured directly in the apparatus.

Figures 35 to 37 are schematics of typical test setups. In figure 35 the boiler was partly filled with liquid mercury and submerged in the liquid lead bath. The vacuum pump was turned on and the condenser tube was opened to the degassing line. The air was drawn off and the mercury vapor flowed into the cold condenser tube and condensed. The valve between the vacuum pump and the boiler pressure manometer was opened for an instant to draw vapor into the tube. This vapor condensed and formed a liquid plug between the U-tube manometer and the boiler (the boiler pressure manometer has an inside diameter of 0.10 inch and therefore will hold a stable liquid plug). The flow rate was measured by timing the increase in length of the condensate in the condenser tube. The pressure at the liquid-vapor interface in the condenser was measured by liquid height between the condenser tube and the liquid surface in the condensate sump. Both boiler and condenser pressures were referenced to the atmospheric pressure.

In most cases natural convection on the outside of the tube was found to cool the condenser adequately. At the high Reynolds numbers, a fan was used to blow air over the tube to achieve higher cooling rates. The flow rate in the tube could be varied by changing the effective condenser length by controlling the condensate liquid length in the condenser tube.

Three separate condenser tubes were tested. The tapered condenser tube was 39 inches long. This tube was tapered by drawing it out by hand. Consequently, the actual taper could not be predetermined. Figure 38 shows the measured inside diameter of this tube along its length. This tube was operated both horizontally and inclined at 43° upwards from the horizontal.

A straight tube of 0.157-inch inside diameter and 4 feet length was operated inclined at 15° with the horizontal. To obtain higher flow rates in the tube, a 6 feet long tube of 0.150-inch inside diameter was tested.

The range of flow rates obtained in each tube was directly proportional to the tube length. To obtain higher flow rates and, consequently, higher Reynolds numbers, tubes longer than 6 feet must be used.

A schematic of the test apparatus for an 8 feet step tapered Pyrex tube is shown in figure 39 as installed for flow upward against gravity. The tube consisted of eight 1 foot long sections stepped progressively to form a tapered tube condenser. The inside tube diameters from inlet to outlet were 0.620, 0.507, 0.436, 0.374, 0.284, 0.232, 0.127, 0.0956 inch, respectively. Pressure drop was obtained as the difference in pressures measured by the U-tube manometer at the condenser inlet and the Bourdon tube gage at the condenser outlet.

Depending on the vapor flow rate, forced convection was sometimes used to reject the latent heat without allowing the system pressure to become too high.

With the system operating at a steady level and the interface positioned with the flow control valve, the following readings were taken:

(a) Upstream pressure: This pressure is read directly from the manometer as a gage pressure.

(b) Downstream pressure: The downstream pressure gage is calibrated in place to read gage pressure at the point where the gage line is tapped into the system. The liquid height from the tap to the interface is then added to the calibrated gage reading to give the pressure at the interface.

(c) Upward flow: After the condensate passes through the flow control valve and subcooler, it is collected for a recorded time in a calibrated cylinder. From this the upward flow rate is calculated.

(d) Downward flow: During most of the testing at low flow rates some of the condensate fell down the tube because of low vapor velocities. This flow is collected in a calibrated drain tube for a measured time to obtain the down flow rate.

(e) Tube temperatures: The temperatures of the outside of each of the eight different sized tubes in the test section are measured and used to calculate the variation in the rate of heat rejection along the test section. This calculation is necessary to eventually determine ΔP_g. (Vapor "only" pressure drop.)

Figure 40 is a schematic of the test setup for vertical downflow in the stepped tapered condenser. The method of operation and the data taken are essentially the same as for the vertically upflow case with the exception of (1) there is only one flow measurement, and (2) the correction to the gage pressure (downstream) to obtain the interface pressure is of opposite sign.

Condenser pressure drop test results. - A convenient way to present two-phase flow pressure drop data is as a ratio of the actual pressure drop to that which would occur if one phase were flowing separately. This ratio is defined as Φ.

The minimum value of Φ is 1 since the addition of a second phase into a duct having a flow of fluid cannot decrease the pressure drop to a value less than that occurring for the original flow.

For condensing, Φ is defined as the ratio of the pressure drop for condensing a vapor of unity quality, excluding momentum pressure recovery, to the computed pressure drop which would occur for the vapor alone flowing without liquid present. Thus,

$$\Phi \equiv \frac{\Delta p_{tp}}{\int_{x=1}^{x=0} f \frac{dL}{D} \frac{(Gx)^2}{\rho_v 2 g_s}} \tag{12}$$

where

D	diameter
f	friction factor
G	total mass velocity
L	length
Δp_{tp}	two-phase pressure drop
x	quality
ρ_v	vapor density

and Δp_{tp} represents the frictional two-phase pressure drop corrected for momentum effects.

The differential length dL can be replaced by a differential quality change dx if the condensing load is defined along the tube length. Vapor density, friction factor, and diameter can all vary along the tube. The Φ as defined by equation (12) is different from the Φ defined in the section entitled "Pressure drop." In this section Φ is a local value defined as $\Delta p_{tp}/\Delta p_g$ and Φ defined by equation (12) is an integrated mean value as obtained by a condenser which in effect is an integrating device giving integrated measurements.

The pressure drop for vapor alone is computed as though the reduction in vapor fraction along the tube were accomplished by extraction of the vapor rather than by condensation. For these tests where the upstream pressure is measured at the boiler and the downstream pressure is measured after the liquid-vapor interface, the measured pressure drop must be corrected for the acceleration at the condenser inlet and the momentum pressure recovery must be accounted for so that the pressure drop represents only the drag forces due to the liquid droplets and the wall shear stress on the following liquid-vapor mixture.

By dimensionless analysis, it can be shown that for two-phase flow

$$\Phi = f\left(Re, Fr, \frac{\rho_g}{\rho_l}, \frac{\mu_g}{\mu_l}\right)$$

For liquid mercury, the properties may be considered as constants over the range of temperatures for which pressure drop data were obtained. The effect of the Froude number was investigated by changing the attitude of the condenser tube. Therefore the liquid properties do not enter the correlation. From condenser pressure drop data, it was found that Φ could be correlated by

$$\Phi = f\left[Re_o\left(\frac{\bar{v}_g}{10}\right)^{1.25}\right]$$

where

Re_o inlet vapor Reynolds number

$\bar{v}_g$ mean vapor specific volume evaluated at average condenser pressure, cu ft/lb

This equation was determined experimentally. Further work is being done to develop an analytical expression so that gravity effects can be included. This work will be described subsequently.

To present results, the vapor specific volume is normalized by dividing by 10, which is near the liquid specific average value for all the test data. The mean specific volume is the specific volume at the average of the inlet and outlet condenser pressures.

Figure 41 shows the resulting plot of Φ against the Reynolds number - specific volume parameter. Data on the Mark II OFFBACE rig are also included. Also shown on this plot is the Martinelli correlation for viscous-turbulent flow, for an average quality of 50 percent and properties evaluated at 600° F. It is remarkable that the parameter $Re_o(\bar{v}_g/10)^{1.25}$ which was found to fit the condenser data may also be factored from the Martinelli parameter.

The large value of Φ at the low Reynolds numbers is caused by the presence of large stationary liquid drops. As shown in the section entitled "Flow Regime Stability," drop size increases rapidly with decreasing Reynolds numbers. The large drops result in a large liquid inventory, which raises the pressure drop. At high Reynolds numbers, the drop size is smaller than at low Reynolds numbers and the effects of the drops on the pressure drop are less important when compared with the shear stresses produced by the vapor, as indicated by Φ approaching a value of 1. As the drops become smaller with increasing Reynolds number, the drag associated with a large number of drops should again increase as was evident in the nitrogen-mercury bare tube test data plotted in figure 42. This trend must still be confirmed by condensers operating at high inlet Reynolds numbers. At extremely high Reynolds numbers, drops can become small enough that the flow acts as a single-phase fluid (fog flow). These limits must still be experimentally verified. Also evident in figure 41 is that values of Φ are higher for the inclined tubes than for the horizontal tubes at the lower Reynolds numbers. This is due again to the fact that at low Reynolds numbers gravity forces become important because of the relatively large drops. The drops are larger in the inclined tubes than in the horizontal tubes because gravity force opposes the drop movement in the condenser.

The merging of the data at a value of 10,000 for $Re_o(\overline{v}_g/10)^{1.25}$ indicates that at this point pressure drop is no longer greatly influenced by the gravity force. Since the average value of the specific volume of the mercury vapor in the tests was near 10, the Reynolds number is the same order of magnitude as the parameter $Re_o(\overline{v}_g/10)^{1.25}$. As shown in the section Flow Regime Stability, gravity influences become small at Reynolds numbers near 10,000. Therefore, all indications are that at Reynolds numbers appreciably lower than 10,000, gravity force variation between 1 and zero gravity will have an effect on the pressure drop. These results are also verified by the Froude number relations of figures 25, 27, and 28. There at Re_o above 10,000 the inertia forces are much larger than the gravity forces.

As the drops become very small at the high Reynolds numbers, Φ appears to be approaching a constant value. When the drops become so small that the liquid-vapor mixture can be treated as a homogeneous fluid, the flow regime is defined as fog flow. In fog flow the liquid and the vapor have the same velocity and the specific volume is that of the mixture. The value of Φ for fog flow in a straight tube is 1.5.

The spread in the data of figure 41 is not excessive compared with other two-phase flow data. Martinelli's data have a spread of ± 50 percent and data of other investigators compared with the Martinelli curve shown even larger spread as shown in the next section.

A theoretical analysis has been carried out to determine the sensitivity of Φ to body forces. This analysis assumes the flow regime shown in figure 16. Liquid holdup measurements used postulate drop dynamics for computing the slip ratio. Critical drop sizes from the two-component flow tests and the flat plate tests are used to determine the droplet size distribution in the following mixture. Critical drop sizes are also used to obtain condensing surface drop population, which allows calculation of the tube wall friction factor.

This above information is combined to yield relations between Φ and the condenser flow parameters as follows:

For a constant diameter condenser tube in a gravity flow field, Φ can be computed from the equation

$$\Phi = \frac{2}{f}\epsilon\left[\frac{4D}{L} \pm \frac{16n \sin\theta}{\epsilon^2 Re_o^2}\left(\frac{g_s D^3 \rho_v^2}{\mu_v^2}\right)\right] + \frac{f_\delta}{f} \pm \frac{8n \sin\theta}{\epsilon f\, Re_o^2}\left(\frac{g_s D^3 \rho_v^2}{\mu_v^2}\right) \qquad (13)$$

where ϵ is computed from the equation

$$\frac{\frac{3}{128} Re_o^2 \left(\frac{\mu_v^2}{g_s \rho_f D\sigma}\right) C_{d_\delta}\left(\frac{1}{\epsilon} - 1\right)^2}{\frac{4D}{L} \pm \frac{16n \sin\theta}{\epsilon^2 Re_o}\left(\frac{g_s D^3 \rho_v^2}{\mu_v^2}\right)} \pm \frac{n \sin\theta}{6}\left(\frac{\rho_f D^2}{\sigma}\right)\left[\frac{\frac{3C_{d_\delta}\rho_v}{4\rho_f}\left(\frac{1}{\epsilon} - 1\right)^2}{\frac{4D}{L} \pm \frac{16n \sin\theta}{\epsilon^2 Re_o^2}\left(\frac{g_s D^3 \rho_v^2}{\mu_v^2}\right)}\right] = E_\sigma \qquad (14)$$

and f_δ is computed from

$$\frac{1}{32}\frac{\rho_f}{\rho_g} Re_o^2 \left(\frac{\mu_v^2}{g_s \rho_f D\sigma}\right)\frac{\delta_c}{D} \pm (n \sin\theta)\frac{1}{6}\frac{\rho_f D^2}{\sigma}\left(\frac{\delta_c}{D}\right)^2 = E_\sigma \qquad (15)$$

and

$$f_\delta = \frac{0.14}{\left(\frac{p}{\delta_c}\right)^{0.307}} \quad \text{for fully rough conditions} \qquad (16)$$

These equations are tentative and are currently being refined to include additional test data. When fully substantiated, these equations will replace the empirical correlations of figure 41.

In figures 43 and 44 are plotted theoretical values of Φ computed from the equations against Re_o with $\overline{v}_g$ as a parameter. Included are

the zero-g and ground test data for comparison. An error analysis has indicated that the data in these figures could have errors ranging from 20 to 200 percent; the most accurate data are represented by the largest specific volume.

Comparison of condenser drop results with other data. - Any correlation for particular data can be evaluated by comparing results to published data. As shown in figure 41, condenser pressure drop data agree with the Martinelli curve at high Reynolds numbers. Figure 42 compares the curves in figure 41 to two other sets of mercury data and to mercury-nitrogen two-phase flow data for bare tubes and for tubes with internal springs.

Mercury-nitrogen two-phase flow data obtained in a bare tube deviate from the Martinelli curve. This trend from the Martinelli curve agrees with two-phase flow results of other experimenters and can be attributed to gravity effects (relatively low Froude number). Decrease in drop size and increasing droplet drag with velocity contribute to the increase in Φ with flow rate.

Figure 45 reproduced from WADC Technical Report 55-422 is an example of a comparison of experimenters' data with some proposed correlation such as Martinelli's. As explained in the report, "This figure [fig. 45] indicates clearly that the correlation proposed by Martinelli does not predict the data as completely as one would like. In addition, these data confirm the objections of Jenkins, i.e., that a definite trend with liquid rate exists which is not accounted for in the correlation. The correlation is seen to be partially successful in predicting the data at high air rates (low value of abscissa). At low-air-water ratios the data deviate to such an extent that the correlation is considered useless even though the two assumptions on which the correlation was based are fulfilled." In figure 45 agreement with Martinelli's correlating curve is reached at the higher flow rates where the Froude number becomes relatively large.

The effect of gravity was also noted in mercury condensation tests at TRW. In the low Reynolds number range where the droplet Froude number is low, the inclined tube indicated higher pressure drops than the horizontal tube. At the higher Reynolds numbers (above 10,000), the difference between the inclined and horizontal tube disappeared because inertia is large compared with gravity.

Mercury-nitrogen test data for the bare tube without swirl inserts show increasing values of Φ with Reynolds number, resembling the curve of figure 21. The appearance of flow at low Reynolds number indicated stratification of mercury droplets near the lower portion of the tube. At higher Reynolds numbers the droplets are small and are homogeneously dispersed throughout the cross section of the tube thus increasing Φ because of drag.

Rig sensitivity is a contributing factor to the effect of gravity in the mercury-nitrogen rig. Evidently, the mercury atomizing nozzle and the mixing length between nozzle and test section establish a good deal of the two-phase mechanics. This was verified in the theoretical development of equations (13) to (16).

Data obtained in the mercury-nitrogen rig for tubes with spring inserts did not exhibit gravity effects (see fig. 42). Because acceleration forces produced by the spring inserts are radial and are large enough to mask out the 1 g due to gravity, Φ remains relatively constant with Reynolds number. An exact correlation cannot be expected since a slightly different flow pattern is produced, that is, droplets are swirled and forced to the tube wall in a tube with swirl inserts and are randomly distributed in a bare tube.

Local low vapor velocities and droplet Froude numbers will make any condenser somewhat sensitive to body forces as the quality approaches zero. This sensitivity can be minimized by tube tapering. Visual observation during tests in tapered tubes showed a uniform cloud of mercury droplets moving steadily, without evidence of slugging, toward the interface in both inclined and horizontal tubes.

Manifold Test

When more than one condenser tube is to be operated in parallel, it is desirable to produce equal loading and similar conditions in each tube. This can be done by making all tubes the same and by providing a source and sink plenum on each end of the tube. A plenum is a large chamber that makes the flow conditions the same at each end of the tube. In order to reduce weight and increase compactness, plenums of relatively small size are incorporated into parallel flow systems. These plenums also referred to as manifolds and require careful design in order that they produce as near as possible uniform conditions to each attached tube. A manifold of relatively small size will have frictional flow losses, thus it is impossible to have a constant total pressure along the axis of the manifold. However, if it is assumed that the manifold velocity head is lost as the flow turns normal to the manifold axis into the tube, near uniform conditions will be obtained if the static pressure is maintained constant throughout the manifold. This design criterion is well known to designers of flow systems and can be found in appropriate engineering handbooks. The design procedure utilizing the criterion is referred to as the static regain method. This method of manifold design is commonly used in air duct design where a constant static pressure is desired at the duct outlets. This type of design attempts to control the static-pressure regain due to loss of fluid velocity when fluid is removed at the manifold outlets. It is desired that this static-pressure regain be equal to the static friction pressure drop in each section so that a constant static-pressure manifold is obtained.

In order to substantiate the static regain design method as applied to mercury condensers, a test rig was designed as shown in figure 46. The tubes were horizontal so that gravity would be eliminated as an agent in establishing liquid levels and liquid level stability. Thus zero-gravity conditions are simulated. The tubes were supplied by mercury vapor generated in a pot boiler. A superheater was added to the inlet line in order to minimize moisture carryover and condensation. Two different types of test were run. One test was made with the drain valves closed, which produces a condition where the liquid level is independent of pressure. Here it is possible to study the effect of condensing length on flow rate and to compare the four tubes operating at approximately the same temperature. Another test was run with the drain valves open. The liquid level here is established by pressure drop considerations. This test simulated actual condenser operation with the exception that flow was allowed to build up in the tubes for metering purposes.

Two manifolds were tested. One was stepped as shown in figure 47 and the other was of constant diameter (fig. 48). The liquid buildup pattern for a typical run with a stepped manifold is shown in figure 47. The drain valves were closed. The liquid level buildups in the first three tubes are about equal, but in the fourth tube it is slightly higher. This is believed to be caused by moisture carryover in the inlet lines. The liquid buildup pattern for a typical run with a constant diameter manifold and with drain valves closed is shown in figure 48. Again the first three tubes received about equal flow, and the last tube received some moisture carryover. These tests demonstrate that flow rate is not determined by manifold configuration, but rather, by the condenser tube lengths. If equal condenser lengths produce equal flow rates, flow rate must be proportional to condenser length. This agrees with the usual analytical heat-transfer model based on uniform heat transfer and equal tube diameters.

With the drain valves open another degree of freedom for the liquid inventory is introduced. Here actual condenser performance is simulated. The interface pressures are all equal since the liquid manifold pressure losses are negligible. Figure 49 shows the liquid level positions and the buildup when a step manifold is used. The liquid levels are different because the manifold was not fabricated exactly to the dimensions specified by the constant static-pressure design and as a result there was a static-pressure change in the manifold. A calculation of pressure drops along the four fluid paths was made in order to determine whether the liquid level relations which were observed would agree with the liquid level relation which was predicted according to the design procedure. It was found that it is possible to predict liquid interface positions accurately by the static-regain method, namely, within 3 percent. It may be concluded that it is possible to design a manifold with the desired liquid levels by the static-regain method. The design of the

liquid manifold plays a small role as long as the liquid velocity and pressure drop are kept negligibly small. This is the case for the prototype system and for the test apparatus, and as a result a stepped liquid manifold has not been incorporated in the test setup.

The test of the constant diameter manifold with the drain valves open proved that this manifold was undesirable since the liquid levels were so grossly unbalanced and their locations were unpredictable.

Removing liquid inventory from the test apparatus made it possible to operate the parallel tube condenser with a single liquid interface in the drain tube, thus demonstrating the feasibility of this mode of operation.

In the oscillations of the liquid legs in a vertical U-tube monometer, gravity is the restoring force. In these tests large unbalances were set up frequently by allowing one or two condenser tubes to fill up with liquid. The drain valves were opened quickly, which allowed the liquid freedom to move among the tubes. In every case, the liquid interfaces returned to an equilibrium condition and no oscillation or liquid level instability was observed. Pressure forces appear to be the restoring force. In the following section the problem of parallel tube operation is further considered.

Parallel Tube Operational Problems

The location and stability of the liquid legs during multiple tube - multiple liquid interface operation of a condenser depends on several factors, namely, (1) manifold design, (2) heat removal characteristics, and (3) tube geometry. The manifold problem and the experimentation are described in the preceding section. The effect of heat-transfer unbalances and of differences in tube geometry on liquid level can be investigated analytically and the results compared with observation made during zero-gravity maneuvers on the OFFBACE Mark II test rig. The basis for the analysis is schematically shown in figure 50. The vapor and liquid manifolds are at constant pressure, hence, the pressure drop in each tube is the same.

The problem of stability of a multiple-tube flow system with liquid legs can be approached by determining when stability is a problem and then eliminating this problem. Any parallel tube system in which all tubes are identical has a possible operating point with all the tubes behaving identically. This array of tubes is stable if, when one or more tubes experience disturbances (flow, pressure, etc.), the system tends to return to its original state with all tubes again performing in an identical manner. It appears a necessary and probably a sufficient

condition for the flow - pressure drop curve always to have a positive slope. A system with such a characteristic may oscillate after a disturbance, but the oscillation will tend to die out. In an unstable system, either a persistent oscillation is set up or the system simply shifts to another operating condition. The latter condition might be a very low flow in one tube and very high flow in another with the same net flow.

Liquid leg stability analysis. - The pressure drop across the tube is

$$\Delta p_{tp} = \Phi f' \frac{L}{D} \frac{\rho_v U_o^2}{2g_s} - \frac{\rho_v U_o^2}{g_s} \tag{17}$$

where f' includes the effect of a vapor flow reduced to zero at the liquid interface.

One criterion for stability is

$$\frac{d(\Delta p_{tp})}{d(\rho_v U_o)} \geq 0 \tag{18}$$

As a result, equation (17) becomes

$$\Phi f' \frac{L}{D} \geq 2 \tag{19}$$

for stability.

For the Mark II OFFBACE condenser, $\Phi f'(L/D)$ values ranged from 2.7 to 1.8. Thus, for the lower limit condenser, conditions are such that symptoms of near instability might be detectable, such as sluggish oscillations of the liquid interfaces. However, no definite oscillations attributed to instability were detected.

SNAP 2 condenser requirements are such that the L/D ratio is about twice that of the Mark II condenser. This creates confidence in the liquid leg stability of the SNAP 2 condenser in zero gravity.

Liquid leg steady-state position analysis. - The pressure drop in a condenser tube in turbulent flow can be expressed as

$$\Delta p = \frac{K \dot{m}^{1.75} L}{D^{4.75}} \tag{20}$$

where K is a constant containing Φ, f', μ_v, and g_s.

The radiation heat transfer from the condenser surface can be expressed as

$$\dot{m}\, h_{fg} = K' \epsilon L (T_R^4 - T_o^4) \tag{21}$$

where K' is a constant containing the fin dimensions and the Stephen-Boltzmann constant.

Since the pressure drop can be altered by means of various effects,

$$d(\Delta p) = \frac{\partial \Delta p}{\partial \epsilon} d\epsilon + \frac{\partial \Delta p}{\partial L} dL + \frac{\partial \Delta p}{\partial D} dD + \frac{\partial \Delta p}{\partial \Delta T} d(\Delta T) + \frac{\partial \Delta p}{\partial T_o} dT_o \tag{22}$$

Thus, changes in fin emissivity, condenser length (liquid leg change), tube diameter, fin temperature drop, and the sink temperature are included as factors affecting the pressure drop. Combining equations (21) and (22), obtaining the above partial derivatives, and numerically evaluating them, results in the following expression:

$$\frac{dL}{L} = -0.63 \frac{d\epsilon}{\epsilon} + 1.73 \frac{dD}{D} + 2.55 \frac{d\Delta T}{T_c} - 2.55\, T_o^3 \frac{dT_o}{T_c^4} \tag{23}$$

where

$$\frac{d(\Delta p)}{\Delta p} = 0$$

for parallel tubes with constant pressure plenums.

The following approximation was made to obtain equation (23):

$$(T_c - \Delta T)^4 - T_o^4 \cong T_c^4 \quad \text{and} \quad (T_c - \Delta T)^3 \cong T_c^3$$

The Mark II test condenser contained four tubes, three of which were glass (0.137, 0.140, 0.135 in. I.D.) and one of stainless steel (0.129 in. I.D.). The greatest difference in diameter of the transparent tubes is 0.005 inch. Therefore, according to equation (23), the greatest difference in liquid leg length should be

$$dL = 1.67 \times 12 \times 1.73 \times \frac{0.005}{0.135} = 1.28 \text{ in.}$$

The difference in liquid leg length, as observed during the zero-gravity trajectory, was between 1 and 1.5 inches when the system was free of noncondensables. When the system was not well degassed, expansion of entrapped gas bubbles in the liquid legs during zero gravity produced changes in the liquid lengths; the amount depended on how much

gas was contained in each leg. The effect of noncondensables in the liquid mercury is the same as adding mercury to the system in zero gravity, that is, the gross movements of the liquid decreases the condenser area.

Liquid-length differences in zero gravity for tapered tubes can be analyzed by a modification of equation (20). For constant mass flow, the following differential equation results:

$$\frac{d(\Delta p)}{\Delta p} = \left[- \frac{2.75\ BL}{2.75(A - BL) + A} + 2.75 + \frac{2BL}{A - BL} \right] \frac{dL}{L} \tag{24}$$

where

$$A = D_o$$

$$B = \frac{D_o - D_e}{L_T}$$

A typical tapered tube may have

$$D_o = 0.67 \text{ in.},\ D_e = 0.16 \text{ in.},\ L = 104 \text{ in.}$$

and equation (24) gives, for a tapered tube,

$$\frac{d(\Delta p)}{\Delta p} = 7.85 \frac{dL}{L}$$

and, for a constant diameter tube,

$$\frac{d(\Delta p)}{\Delta p} = 2.75 \frac{dL}{L}$$

and, for equal changes in ϵ, D, ΔT, T_o,

$$dL_{D=const} = 2.86\ dL_{Tapered} \tag{25}$$

Equation (25) shows that the liquid leg movement in a tapered tube is less than for a tube of constant diameter for the same unbalances in ϵ, D, ΔT, T_o.

Equation (23) for a tapered tube becomes

$$\frac{dL}{L} = -0.22 \frac{d\epsilon}{\epsilon} + 0.60 \frac{dD}{D} + 0.89 \frac{d\ \Delta T}{T_c} + 0.89\ T_o^3 \frac{dT_o}{T_c^4} \tag{26}$$

As another example of the use of these equations, consider the variation in subcooler liquid lengths for one tube facing the sun and one tube in the shade of the vehicle. In one case the effective space temperature is approximately 687° R and in the other case it is approximately 100° R. Substitution into equations (25) and (26) gives

$$dL = 16.6 \text{ in. (tapered)}$$

$$dL = 47.5 \text{ in. (constant diameter)}$$

This illustrates the desirability of tapered tubes over straight tubes during conditions of unbalance.

CONDENSING MERCURY HEAT TRANSFER

The heat to be rejected by a condenser is related to the heat-transfer area by temperature and the overall heat-transfer coefficient. For a radiation-cooled condenser in space, the heat liberated during change of phase must pass in series through three resistances. The first is that of the condensate layer which will form on the cooled surface in the condenser. In general, the heat-transfer coefficient associated with change of phase is very high. The second resistance will be that of the metal walls. For prime heat-transfer surface where condensation takes place on one side of a plate and heat is radiated from the opposite side, the resistance to heat flow will be proportional to the plate thickness. If, however, the radiator employs a finned surface for radiation, the resistance will include the resistance of the metal enclosing the condensing fluid passages as well as the resistance of the fin material. The third resistance is that of the radiating surface. This resistance is a function of the material, the condition of the surface, the temperature of the surface, and the temperature and position of bodies which the radiator can "see." This resistance will usually be the largest of the three; however, where thin fins are used the resistance of the fin material may be significant.

Figure 51 demonstrates the effect of condensation heat-transfer coefficients on isothermal radiator area requirements. For heat-transfer coefficients above 500 Btu per hour per square foot per °F, heat transfer is controlled primarily by thermal radiation. Figure 52 shows condensation coefficients for mercury as presented by Misra and Bonilla (ref. 3). Although the experimentally measured coefficients are only about 5 to 15 percent of the Nusselt equation values for filmwise condensation, the lowest value recorded for mercury was 3000 Btu per hour per square foot per °F.

A zero-gravity environment exerts no appreciable effects on the forced-convection condensation process. For nonwetting fluids, drops

of condensate form on the condenser surface and moving drops or flowing vapor sweep the surface clean. The sweeping away of the condensate droplets in a forced convection condenser should improve the coefficients given by Misra and Bonilla.

A flat-plate mercury condenser consisting of two rectangular stainless steel plates 3 feet long and 1 foot wide with 1/8-inch spacing between the plate walls was tested to obtain condensing mercury heat-transfer coefficients, pressure drop, etc. Figure 53 is a photograph of the condenser with instrumentation taps installed. One side of the condenser was insulated and the other side cooled by forced air convection such that the radiant heat flux was simulated. Internal condenser temperatures were measured by 12 equally spaced thermocouples along the condenser length. Air temperature was measured by 17 radiation shielded thermocouples in the air duct adjacent to the condenser. A sight glass was installed between the inlet and the outlet lines to determine the approximate location of the condenser liquid level. Tests showed that the condensing coefficient was in the range of 500 to 1000 Btu per hour per square foot per ^{o}F. However, air was present in the condenser and was never completely removed. Hence, actual coefficients in a gas-free condenser are likely to be in the range measured by Misra and Bonilla.

A theoretical analysis to determine the effect of surface droplets on the condenser tube friction factor was also conducted. As part of this analysis, condensing heat-transfer coefficients were theoretically predicted for a vertical plate and for zero vapor velocity and found to be in the range of 1250 Btu per hour per square foot per ^{o}F. The theoretical equation for the condensing heat-transfer coefficient contains the entrainment drop size δ_c, which can be determined by flow and gravity.

NONCONDENSABLE GAS

The problem of noncondensable gas collection near the interface was first encountered in the flat-plate condenser tests mentioned in the last section. Figure 54 presents a temperature traverse made along the wall of the flat-plate condenser containing condensing temperature near the subcooler liquid-vapor interface and clearly shows that the gas-to-vapor concentration ratio increases very rapidly as the end of the condenser is approached.

The low velocities of the vapor-gas mixture near the interface produce an ideal situation for the formation of a gas plug. Figure 55 depicts the formation and transport of a gas plug. The flowing condensate droplets are slowed to a halt near the interface because of the relatively stagnant region of noncondensables. These droplets then grow by agglomeration until they fill the tube cross section and entrap a

volume of gas. A new subcooler liquid interface is thus formed downstream as the gas plug moves toward the condensate pump. Figure 54 shows that for low condenser pressures the region occupied by the gas before the subcooler interface is large, whereas at higher pressure this same region is compressed. During several condenser experiments it was observed that large gas plugs were formed at low condenser pressure and smaller plugs at higher pressures.

Equations for predicting the form of the temperature profile shown in figure 54 can be readily set up by applying the convection heat-transfer equation, and the equation of state for a mixture of saturated vapor and gas and by assuming that the mixture is always at the dewpoint and at a constant total pressure.

Several methods of gas removal were considered and experiments devised. Since there is a high concentration of gas upstream of the subcooler interface and in the plugs, separator-type devices are not contemplated because the gas is already in a separated state. Two methods of gas removal are possible: (1) removal of gas just upstream of the subcooler interface (this method is successfully used in test rig condensers); and (2) removal of gas when in plug form. Figure 56 shows both schemes. The removal of gas in the form of a plug can be accomplished by means of a porous tube wall having pore sizes sufficiently small to prevent the nonwetting mercury from flowing out. This phenomenon is presently being used in porous bed boiling experiments.

CONCLUSIONS

1. Pressure drop changes in mercury condensers can be expected when going from 1 to zero g if the Reynolds number is less than 10^4 and if the vapor specific volume is less than 10 cubic feet per pound. This applies to condensing downward.

2. At a Reynolds number of 5000 and specific volume of 5 cubic feet per pound, a pressure drop change amounting to 40 percent can be expected in going from 1 to zero g. This applies to condensing downward.

3. The mechanics of mercury condensing have been sufficiently well established so that confident predictions can be made as to zero-gravity condenser design and performance.

4. Surface tension, vapor drag, and gravity are the primary factors in establishing the two-phase flow patterns and resulting Φ values. The object is to minimize the influence of the gravity term on the design and performance of the prototype space condensers.

5. Stable water and mercury interfaces can be maintained in a zero-gravity environment against disturbance amounting to +0.055 and -0.02 g in glass tubes having inside diameters less than about 1/2 inch. Interfacial stability can be maintained against specified disturbance by proper selection of tube diameter.

6. As demonstrated by an upward condensing experiment and by an upward flowing (15° tilt) nitrogen-mercury test rig, the gravity effects will be much greater than when flowing downward.

7. Flow unbalance caused by improper vapor manifolding, unequal tube dimensions, and heat transfer will affect the position of the liquid interfaces in zero gravity. This applies when multiple liquid interfaces in parallel tubes are used.

8. Tapered tubes should be less sensitive to gravity from a pressure drop standpoint than tubes of constant diameter.

9. Tapered tubes show less sensitivity to liquid level differences produced by unbalances in heat transfer caused by solar or other sources of radiation.

10. A design procedure for a light-weight vapor manifold has been established by test and theory.

11. Two-phase flow, mercury-nitrogen pressure drop data can be used to approximate condenser pressure drop.

12. If noncondensable gases are present in a condenser, the greatest concentration will be at the condenser-subcooler interface. The gas will be carried along to the pump in the form of plugs and can unprime the pump if not removed.

13. A porous plug of a specified size will separate noncondensable gas plugs in the subcooler if they are of a given size and moving at a certain velocity.

RECOMMENDATIONS

A great deal of the research described in this report has been motivated by the need for early application to the design of specific prototype condensers. As a consequence, the results were judged on their adequacy to permit practical designs and to verify concepts. In some instances, approximate solutions have been sufficient for these purposes, so that additional refinements are necessary to complete the understanding of the phenomena involved in the condensation of mercury. To reduce the number of unknowns which still remain and to improve the accuracy of

correlations which will permit the minimization of design tolerances and prototype component weights, further research should be undertaken in the areas classified as follows:

(a) Development of mathematical analysis and physical understanding of the condensing process

(b) Condenser data

(c) Zero-gravity experiments

(d) Interfacial stability

(e) Associated problem areas for which a designer requires answers

It is recommended that further work be done in these areas. Specifically, the following experiments are still required:

1. Mathematical analysis and physical understanding:

Study experimentally the trajectory of mercury drops in various gravity flow fields. This would provide the necessary data for a more accurate computation of the slip ratio, a very important parameter in computing Φ for forced convection condensing with and without body forces. This can be done by high-speed photographic methods.

The effect of inserts (twisted ribbon or springs) on the trajectory and dynamics of the liquid drops should be extended.

Entrainment drop sizes in a mercury-vapor environment are needed. A stainless-steel heat-transfer surface should be used. Most of the data now available were obtained in glass tubes with nitrogen gas under adiabatic conditions.

Refinement of mathematical treatment is required to include the integrated effect of drops of various sizes moving through different paths toward the interface. Evaluate E_σ for mercury drops for forced convection condensation in the presence of body forces by the mathematical techniques of Bashforth and Adams (ref. 2). Measure drop deformation optically in the above-mentioned conditions for determining E_σ.

2. Condenser data:

More condensing pressure drop data are required for a greater range of tube geometries.

Condenser data for Reynolds numbers greater than 15×10^3 are necessary in order to close the gap between the nitrogen-mercury data and available condenser data and to establish the trend in Φ for these higher Reynolds numbers.

If possible, the transition to fog flow should be determined. This is the region where the two-phase flow is homogenized and where it behaves as a single-phase fluid.

Measure local Φ values during condensing by using multiple-pressure taps along the condenser tube.

Determine effect of spring insert on condenser performance. A spring insert in conjunction with a lower flow rate may be comparable to a bare tube condenser with a higher flow rate insofar as gravity effects and pressure drop are concerned.

3. Zero-gravity experiment:

A larger OFFBACE condenser should be tested in zero gravity in order to improve accuracy of measurement of the gravity effects. Evaluate by experiment the gravity effects in a tapered tube condenser. Establish interfacial stability limits in zero gravity with controlled disturbances (vibrations of known amplitude and frequency).

4. Interfacial stability:

Stability limits are required for mercury in a steel tube at condensing temperatures (600° F) with controlled disturbances (known frequency and amplitudes). Determine stability limits of mercury interface during controlled internal disturbances in which mercury droplets are sprayed onto the interface. Drop sizes, number, and velocity should be controlled, thereby identifying the magnitude of the internal interface disturbance. This should be done in conjunction with external disturbances (vibration of test setup).

5. Associated problems areas:

Further develop optimum degassing technique. This applies to (1) degassing procedure during initial fillup, (2) intermittent degassing, (3) continuous degassing.

Experimentally determine startup performance of condensers. Study flow pattern, interface position, and thermal transients.

Analytically and experimentally determine a more complete stability criteria for parallel tube operation where flow is opposite body forces which have a powerful destabilizing effect.

REFERENCES

1. Griffith, P., and Kulinski, E.: Water Condensing Tests. ER-4200 Thompson Ramo Wooldridge, Inc.

2. Bashforth, F., and Adams, C.: An Attempt to Test the Theories of Capillary Action. Cambridge Univ. Press, 1883.

3. Misra, B., and Bonilla, C. F.: Heat Transfer Vapors Mercury and Sodium up to Atmospheric Pressure. Am. Inst. Chem. Eng., vol. 52, no. 18, 1956.

4. Kiraly, R. J., and Koestel, A.: The SNAP II Power Conversion System Topical Report No. 8 Mercury Condensing Research Studies. ER-4104, Thompson Ramo Wooldridge, Inc.

5. Sunflower Power Conversion System Quarterly Report. ER-4384, Thompson Ramo Wooldridge, Inc., Dec.-Feb. 1961.

6. Kiraly, R. J., and Reemsnyder, D. C.: SNAP I Power Conversion System Condenser-Radiator Development. ER-4056, Thompson Ramo Wooldridge, Inc.

7. Koestel, A.: Hydrodynamic Problem Areas in Zero Gravity. TM-1488, Thompson Ramo Wooldridge, Inc.

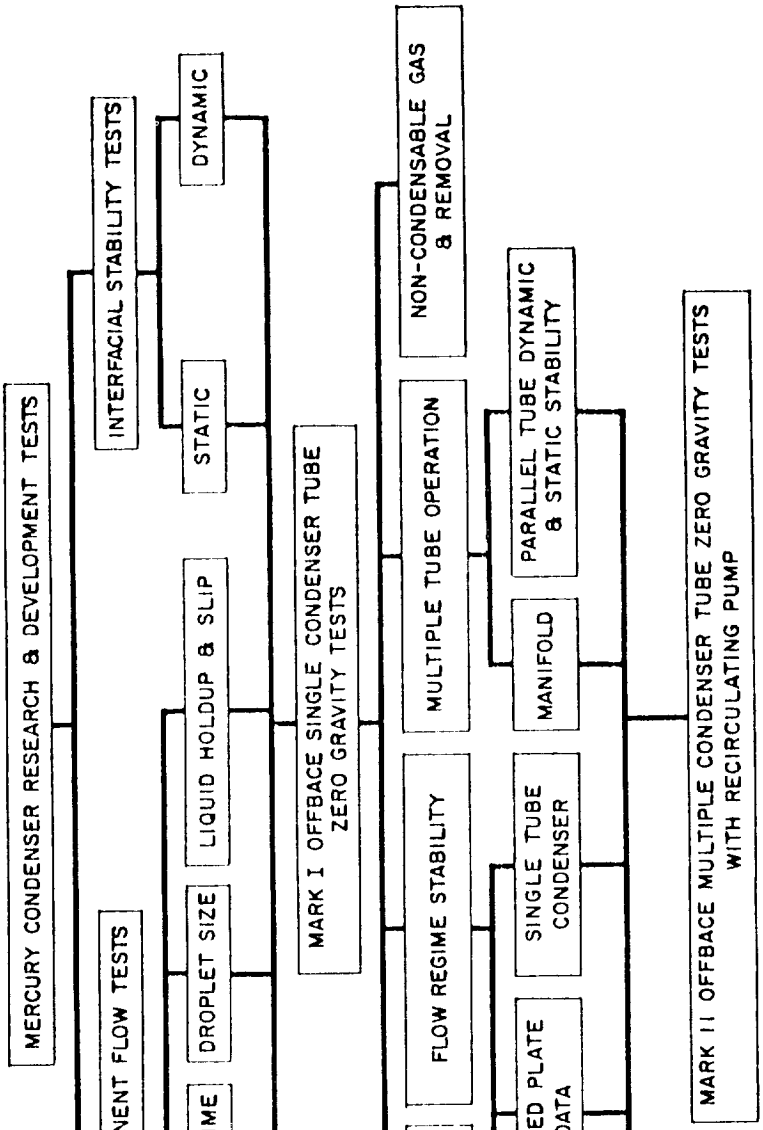

Figure 1. - Activity chart.

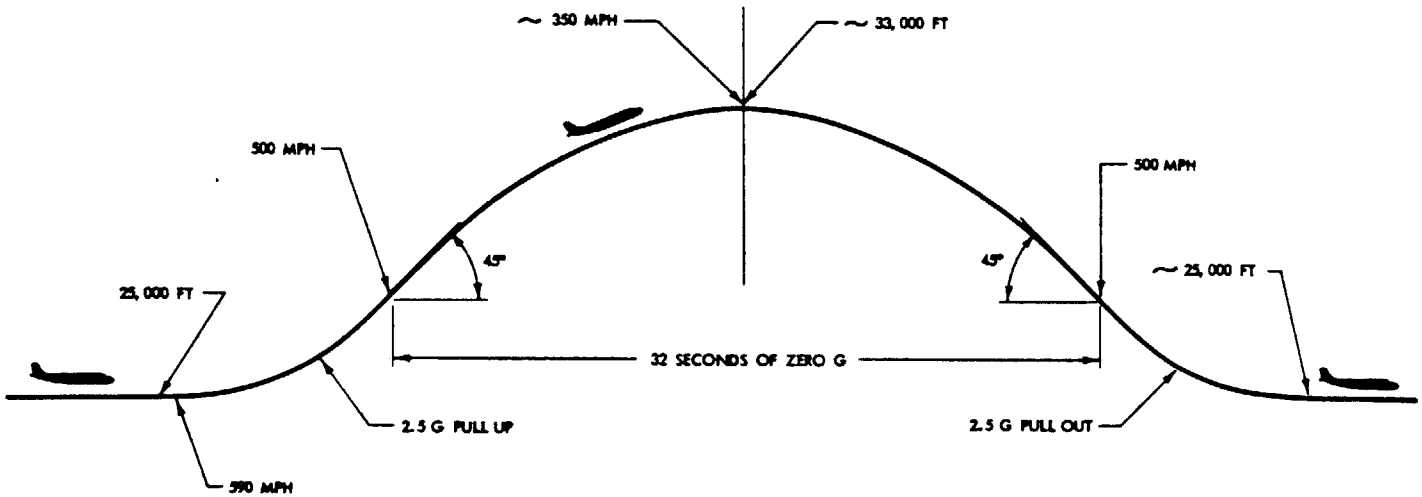

Figure 2. - KC-135 zero-gravity maneuver.

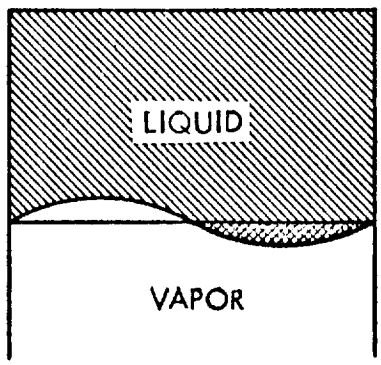

Figure 3. - Inverted two-dimensional tube for interfacial stability analysis.

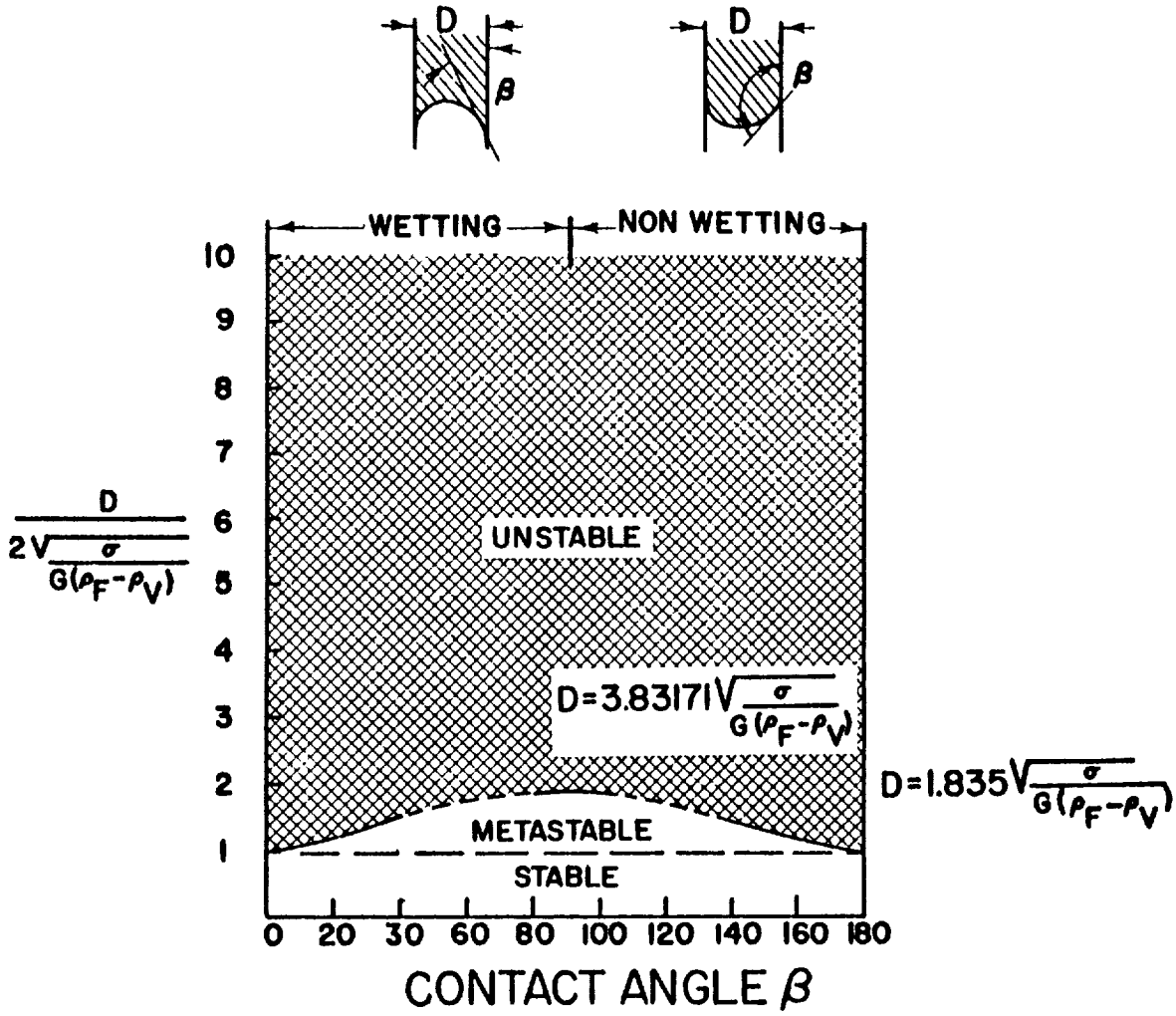

Figure 4. - Regions of instability, metastability, and stability for liquid contained in a tube of diameter D.

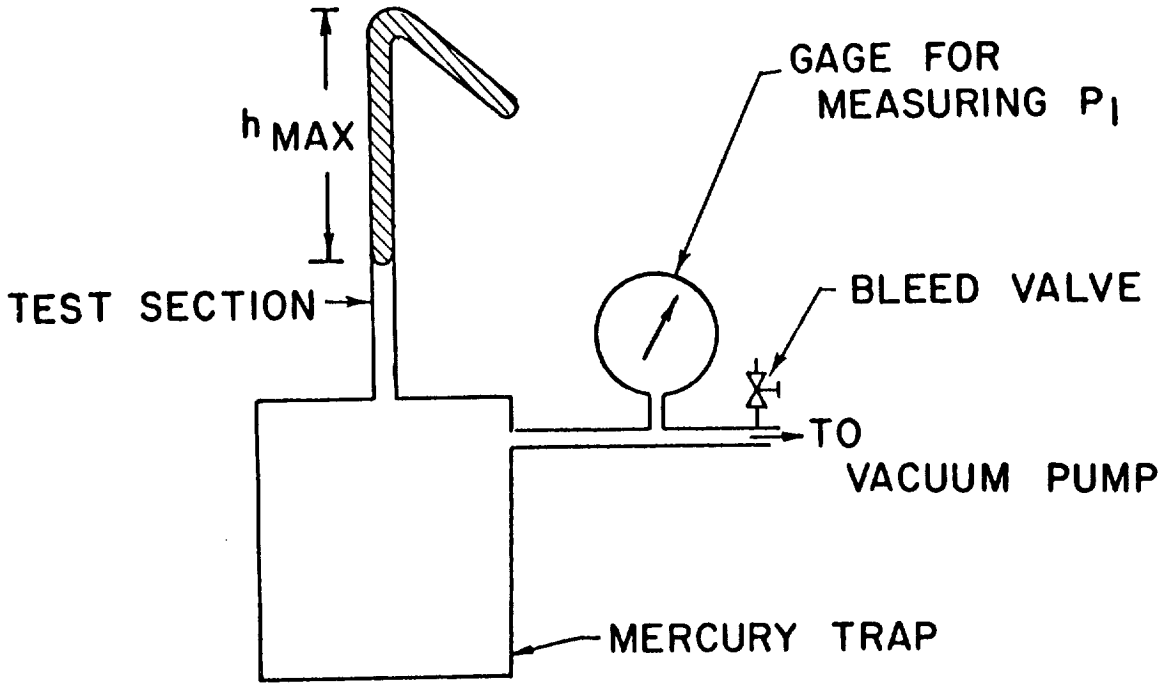

Figure 5. - Test apparatus for static tests on mercury columns.

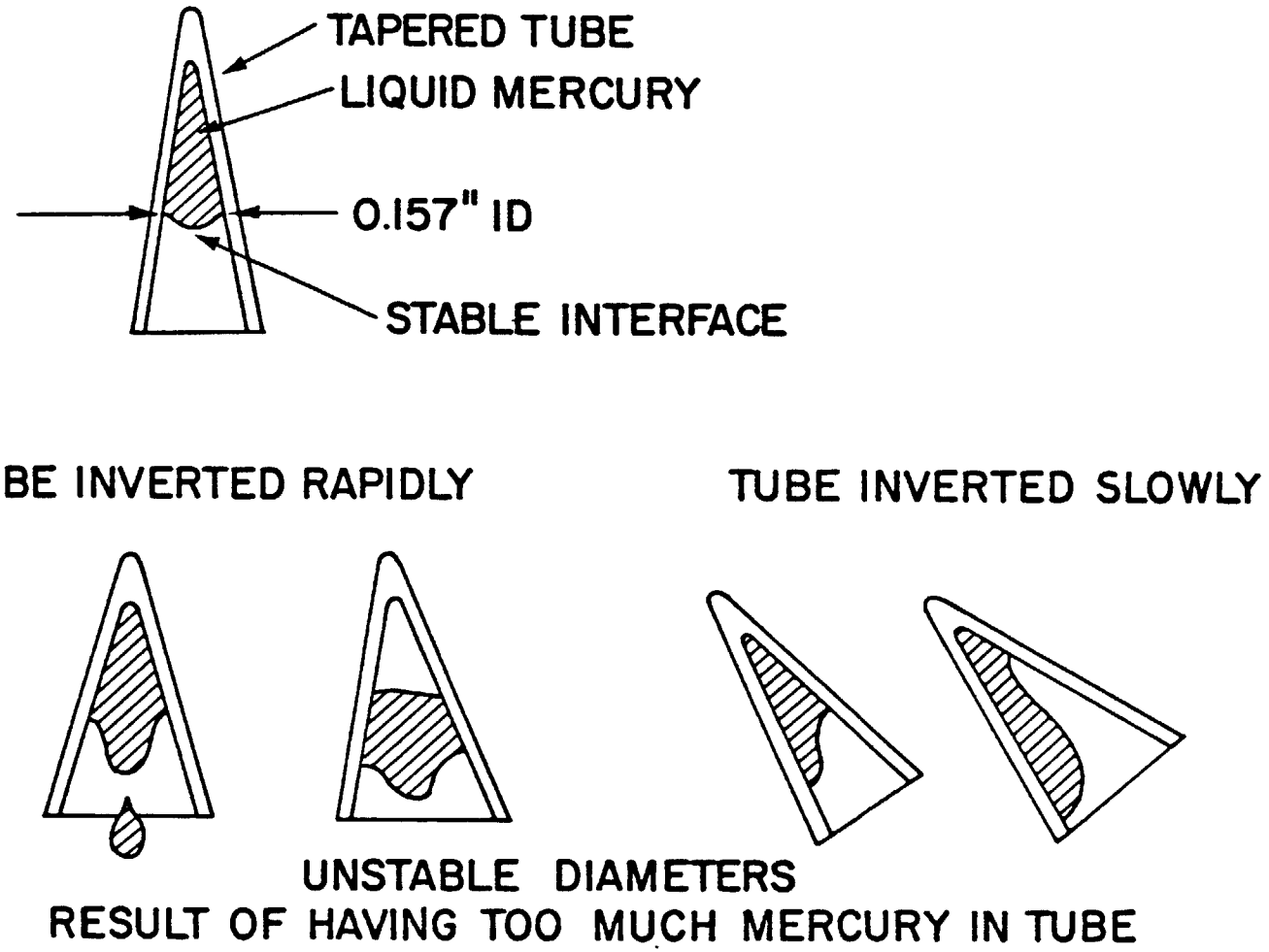

Figure 6. - Interfacial stability in tapered glass tube.

E-1501

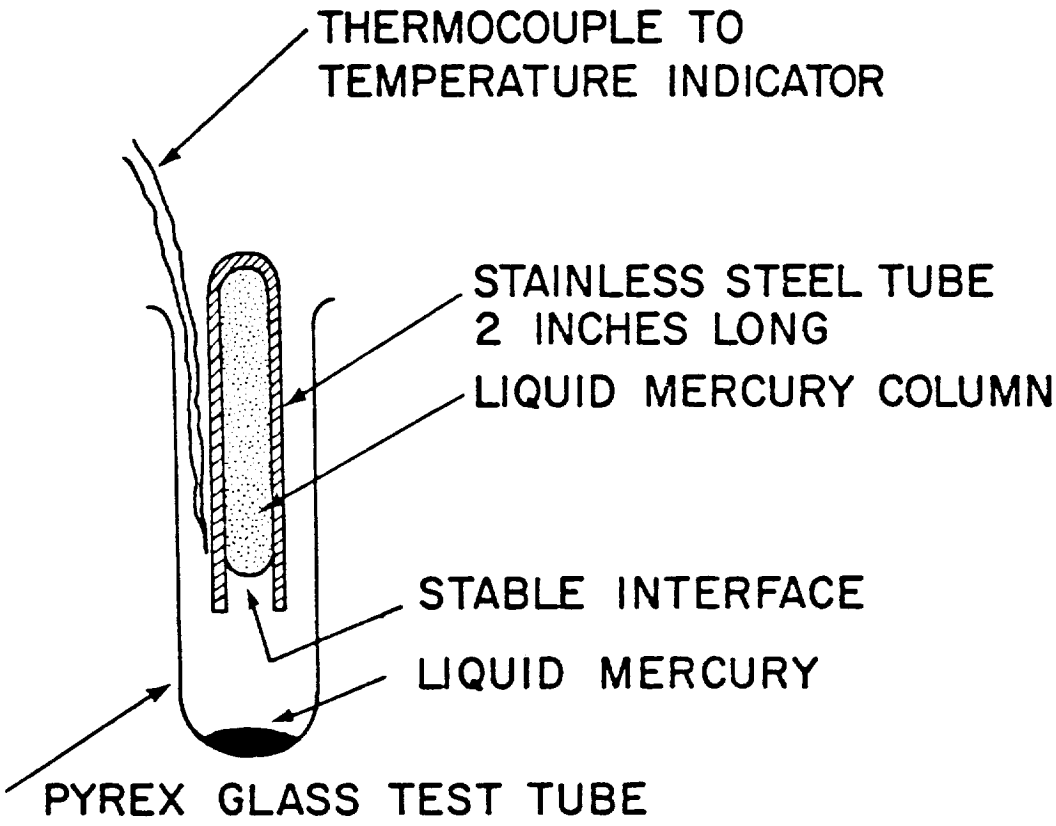

Figure 7. - Interfacial stability with temperature.

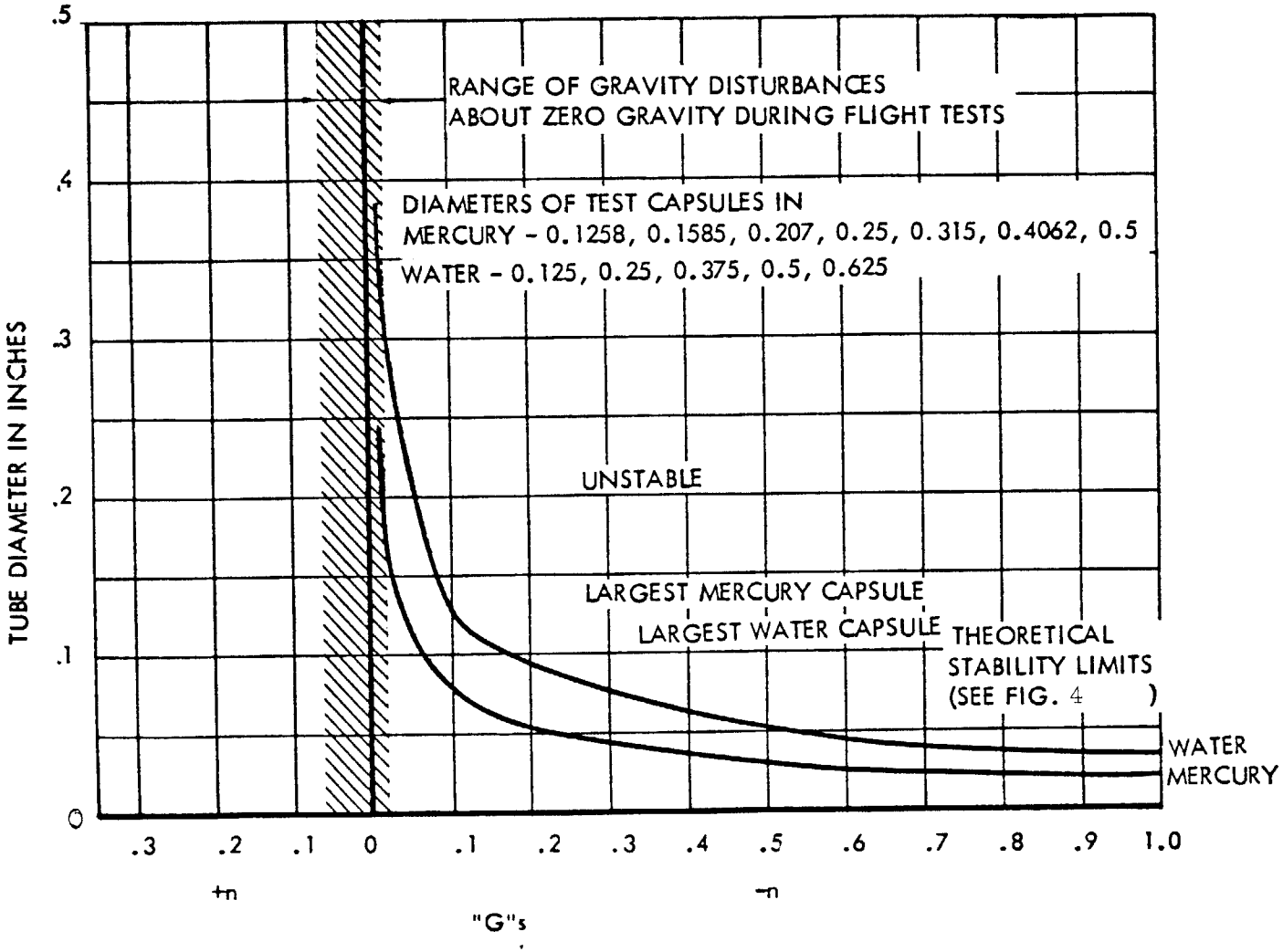

Figure 8. - Disturbances observed during zero-gravity maneuvers and the diameters of the test capsules for demonstration of interfacial stability.

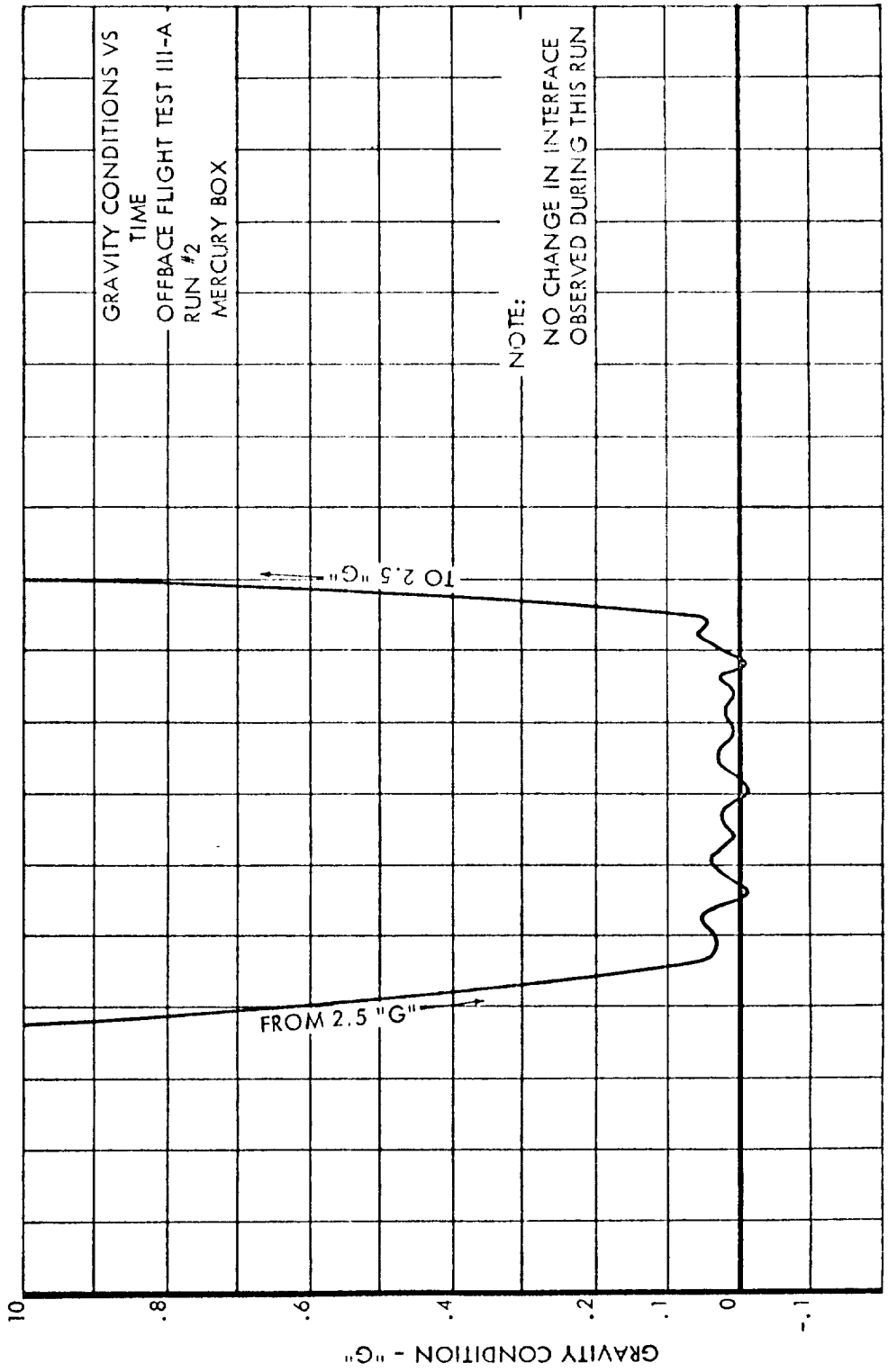

Figure 9. - Gravity fluctuations during zero-gravity run.

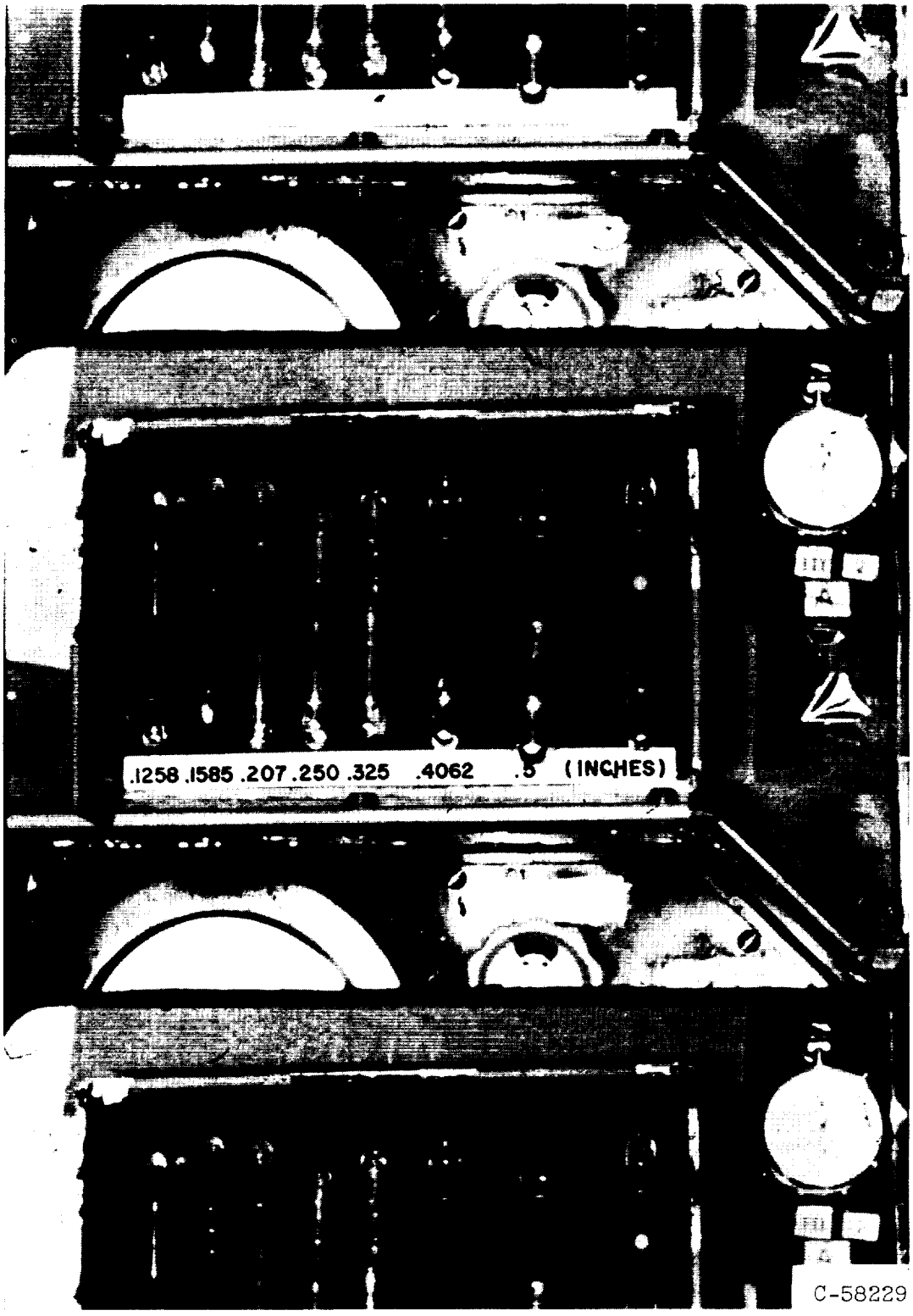

Figure 10. - Interfacial stability mercury test rig during zero gravity.

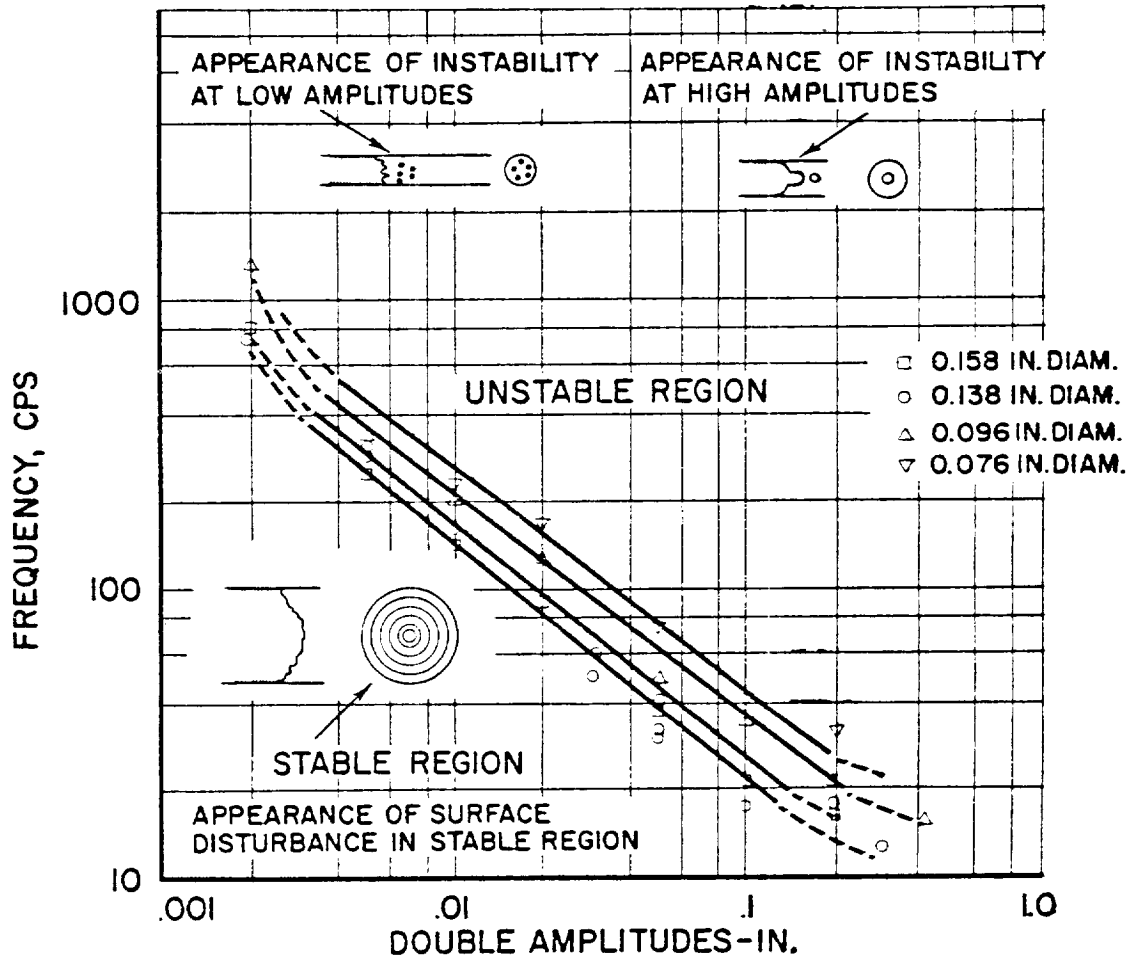

Figure 11. - Stability with external disturbances. Liquid mercury in horizontal glass tubes, vertical displacement.

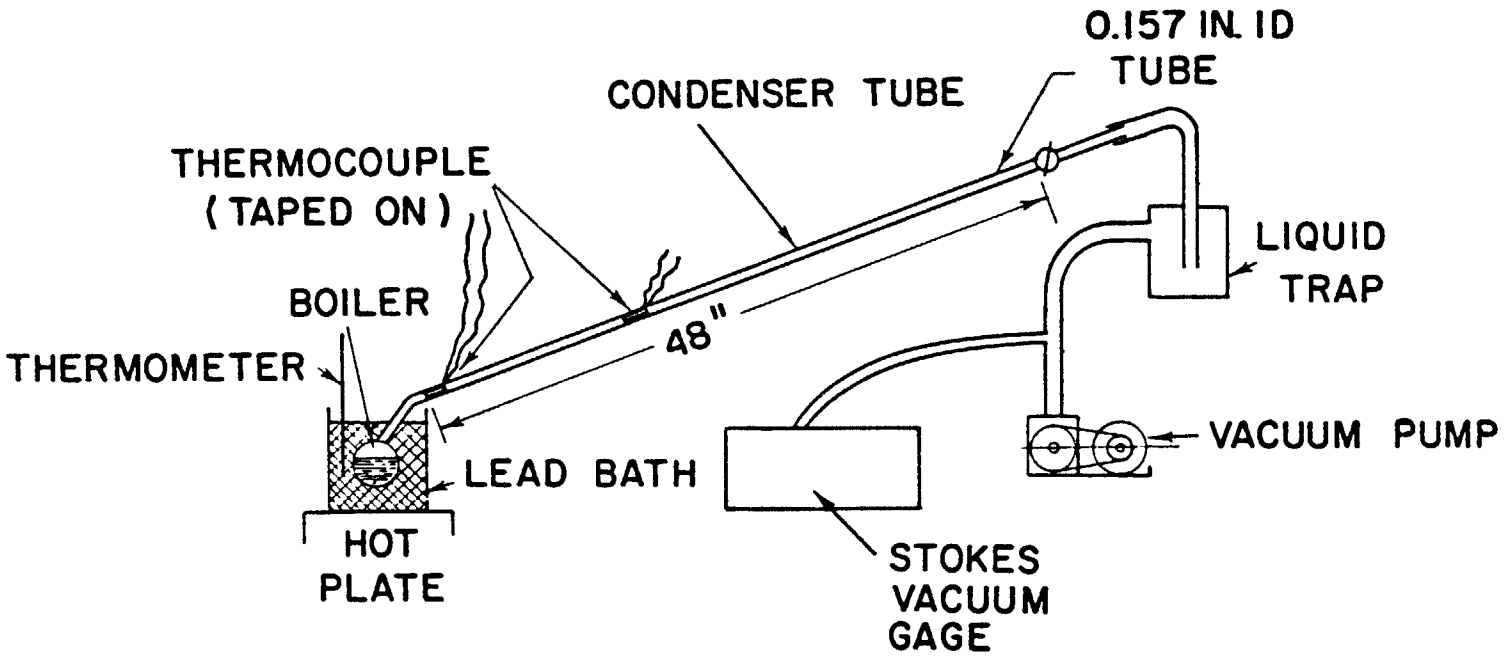

Figure 12. - Test setup for interfacial stability with internal disturbances.

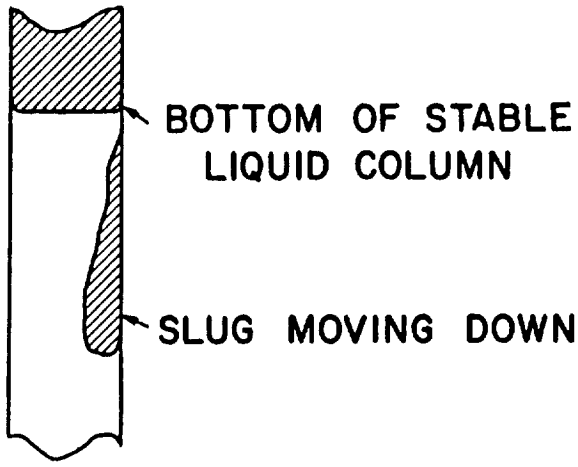

Figure 13(a). - Slugging in mercury vertical condenser tube.

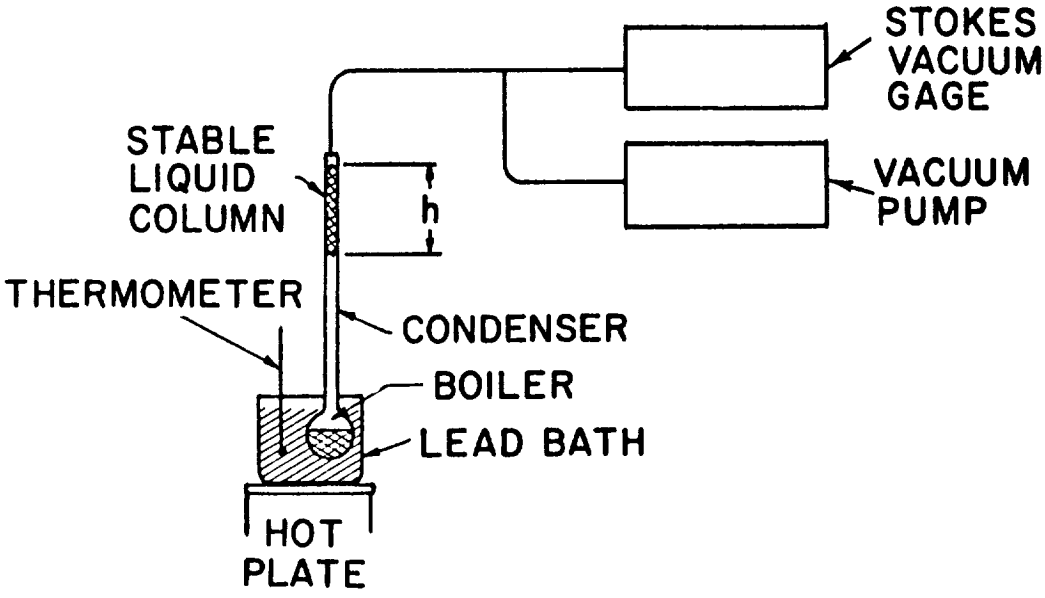

Figure 13(b). - Interfacial-stability test setup.

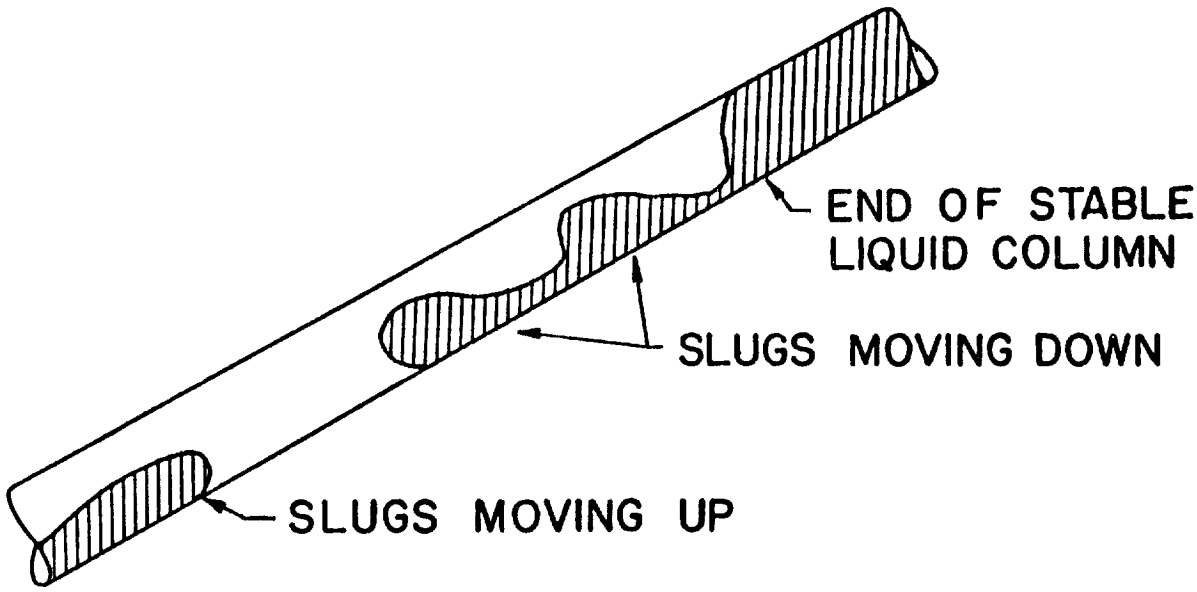

Figure 14. - Slugging in inclined mercury condenser tube.

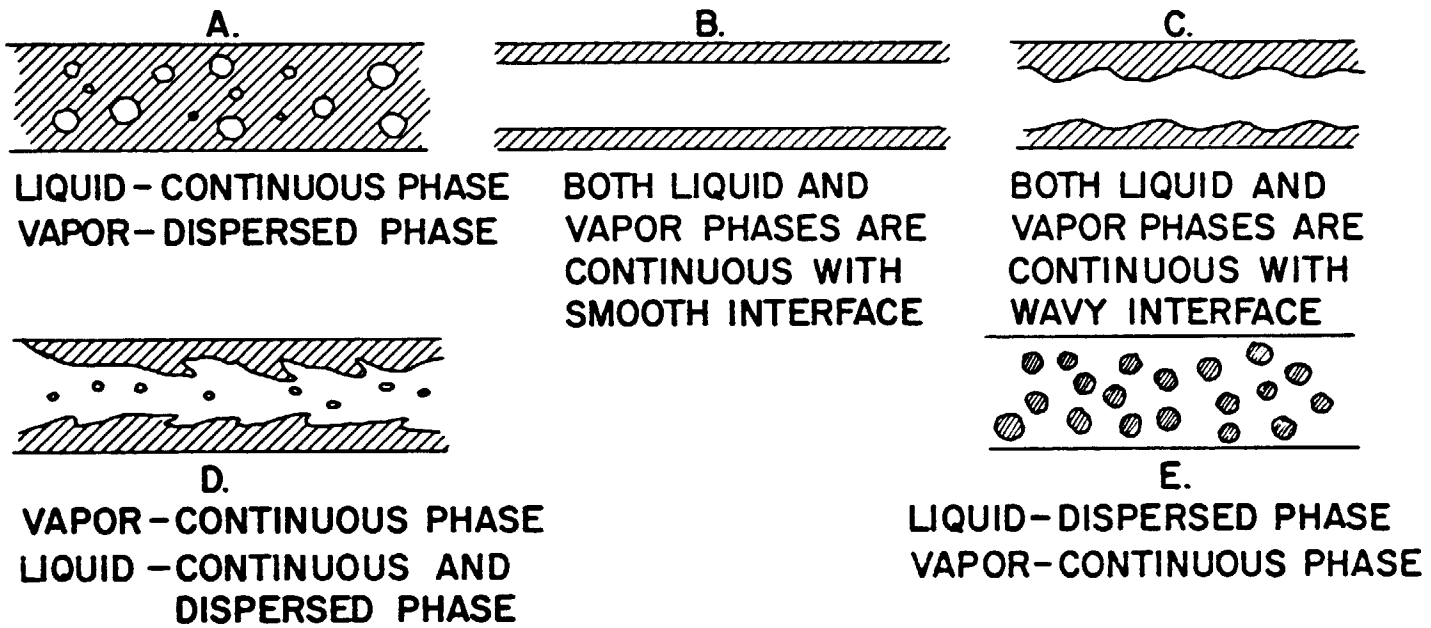

Figure 15. - Two-phase flow regimes.

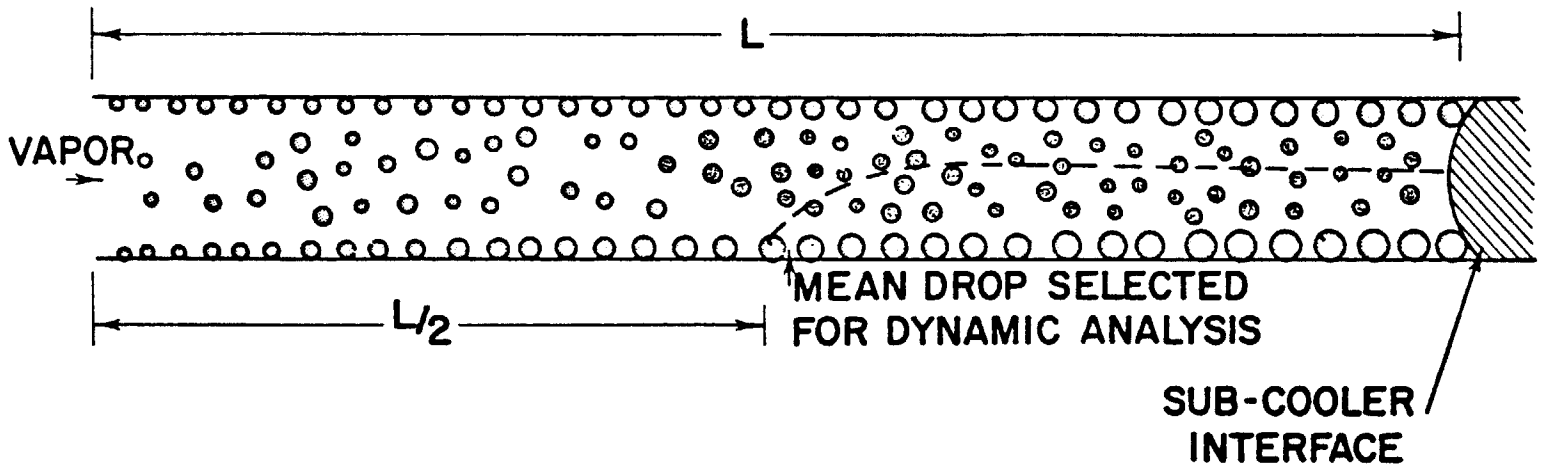

Figure 16. - Mercury condenser flow pattern.

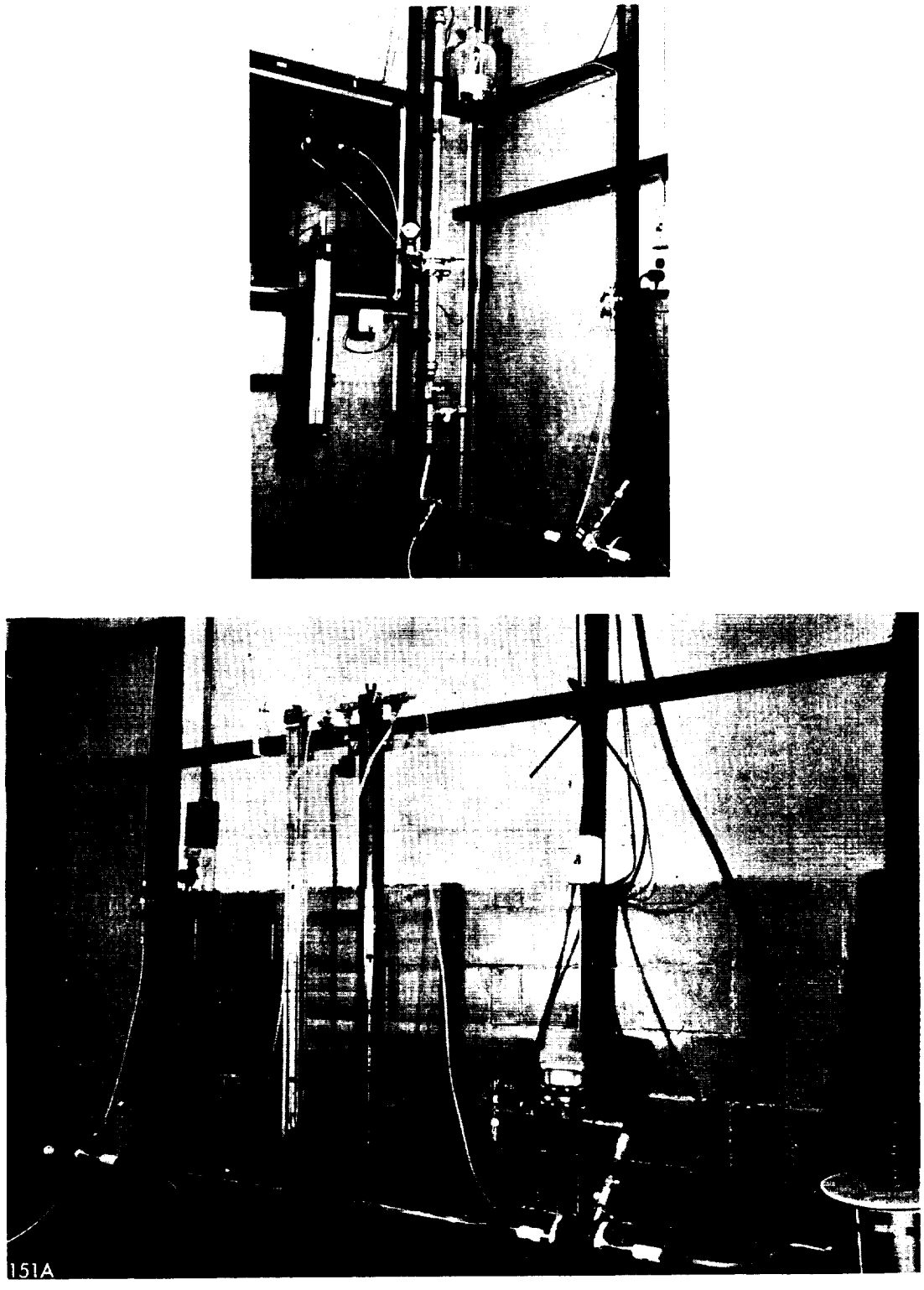

C-58230

Figure 17. - Two-phase flow rig.

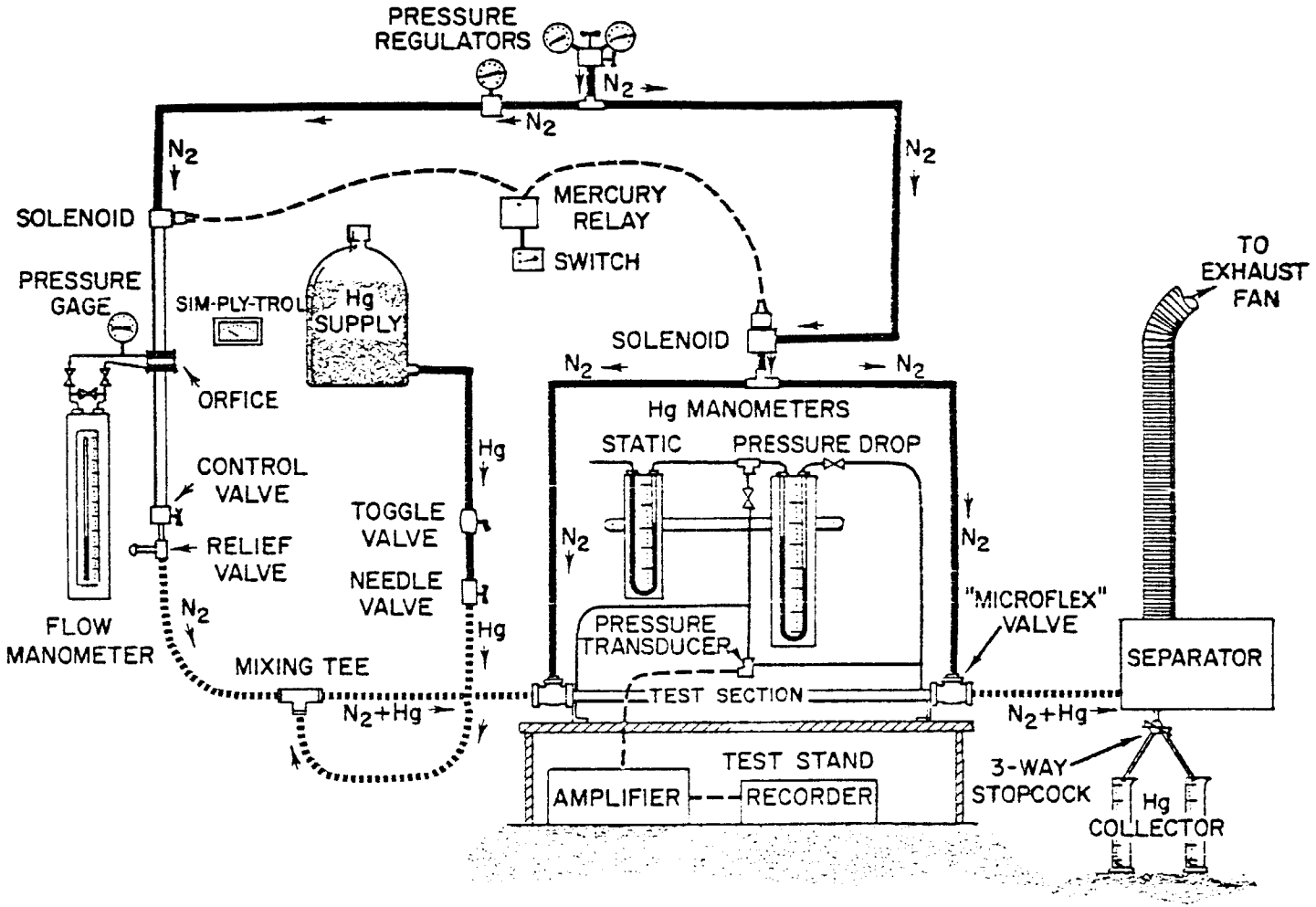

Figure 18. - Schematic diagram of two-phase flow test rig.

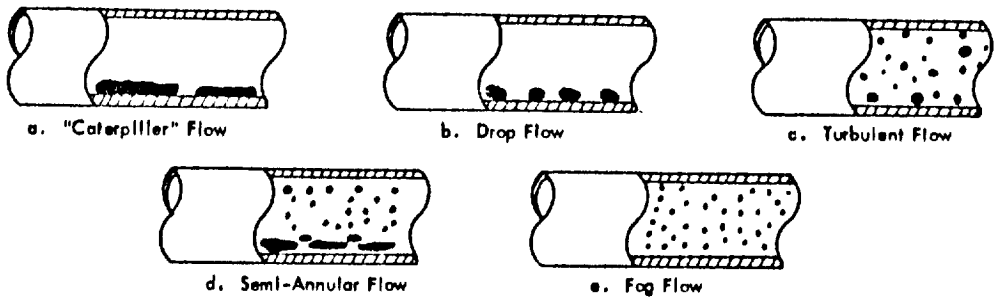

Figure 19. - Observed two-phase flow regimes for liquid mercury and nitrogen gas in a horizontal tube.

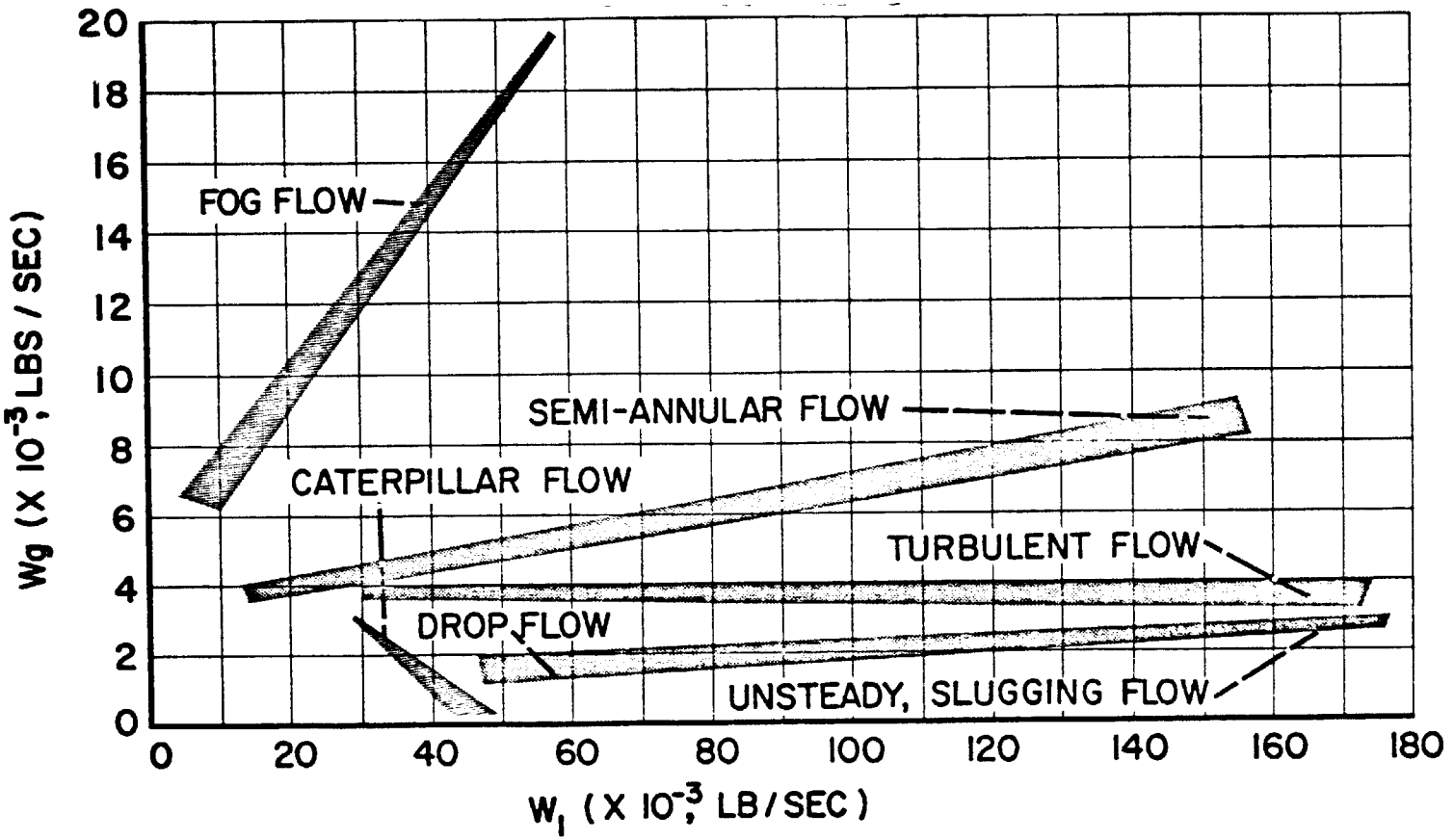

Figure 20. - Flow regimes for nitrogen - liquid mercury two-phase flow. Horizontal tube inside diameter, 0.394 inch.

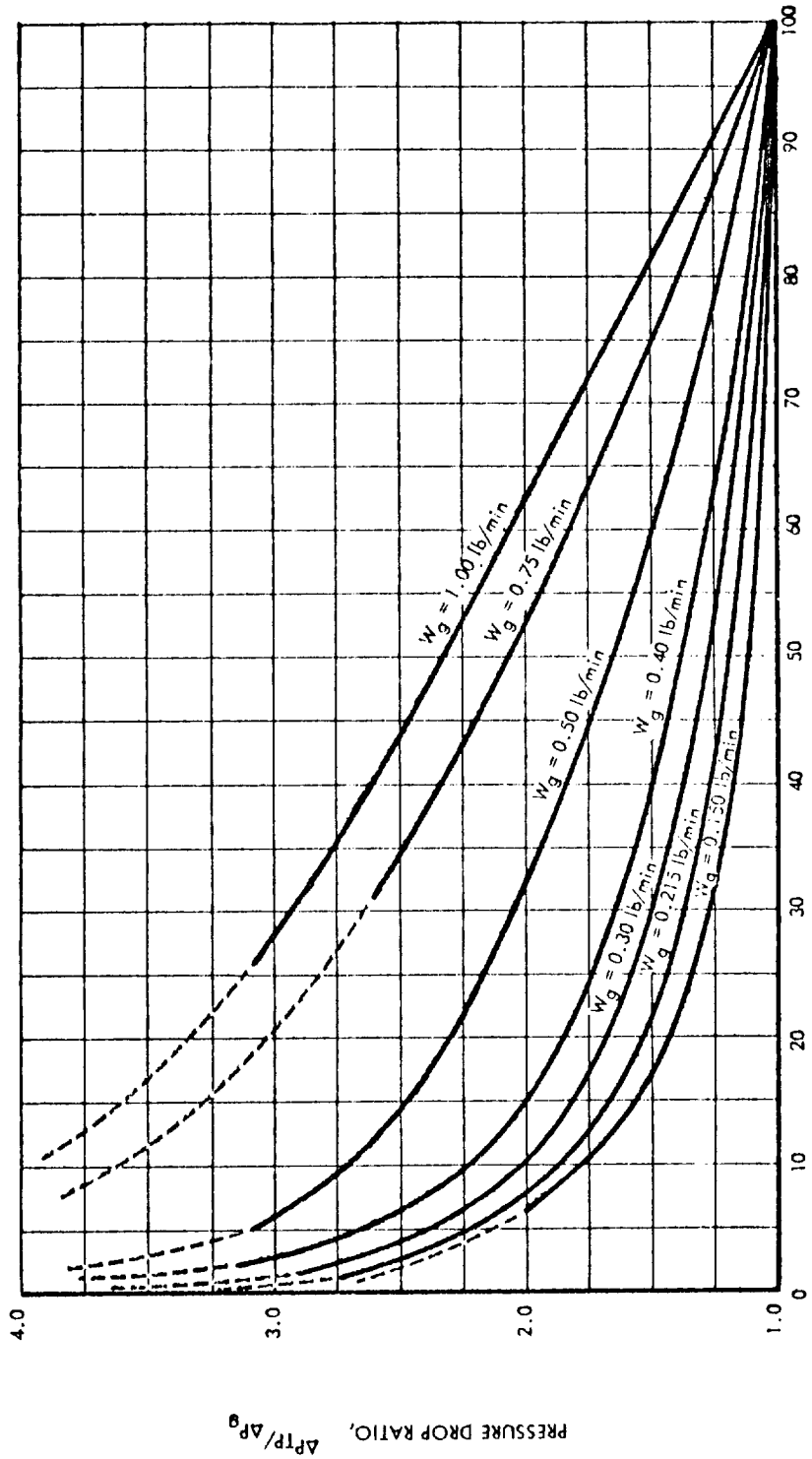

Figure 21. - Pressure drop ratio against flowing quality. Concurrent flow of nitrogen and mercury. Pyrex glass tube diameter, 0.394 inch; length, 4.3125 feet.

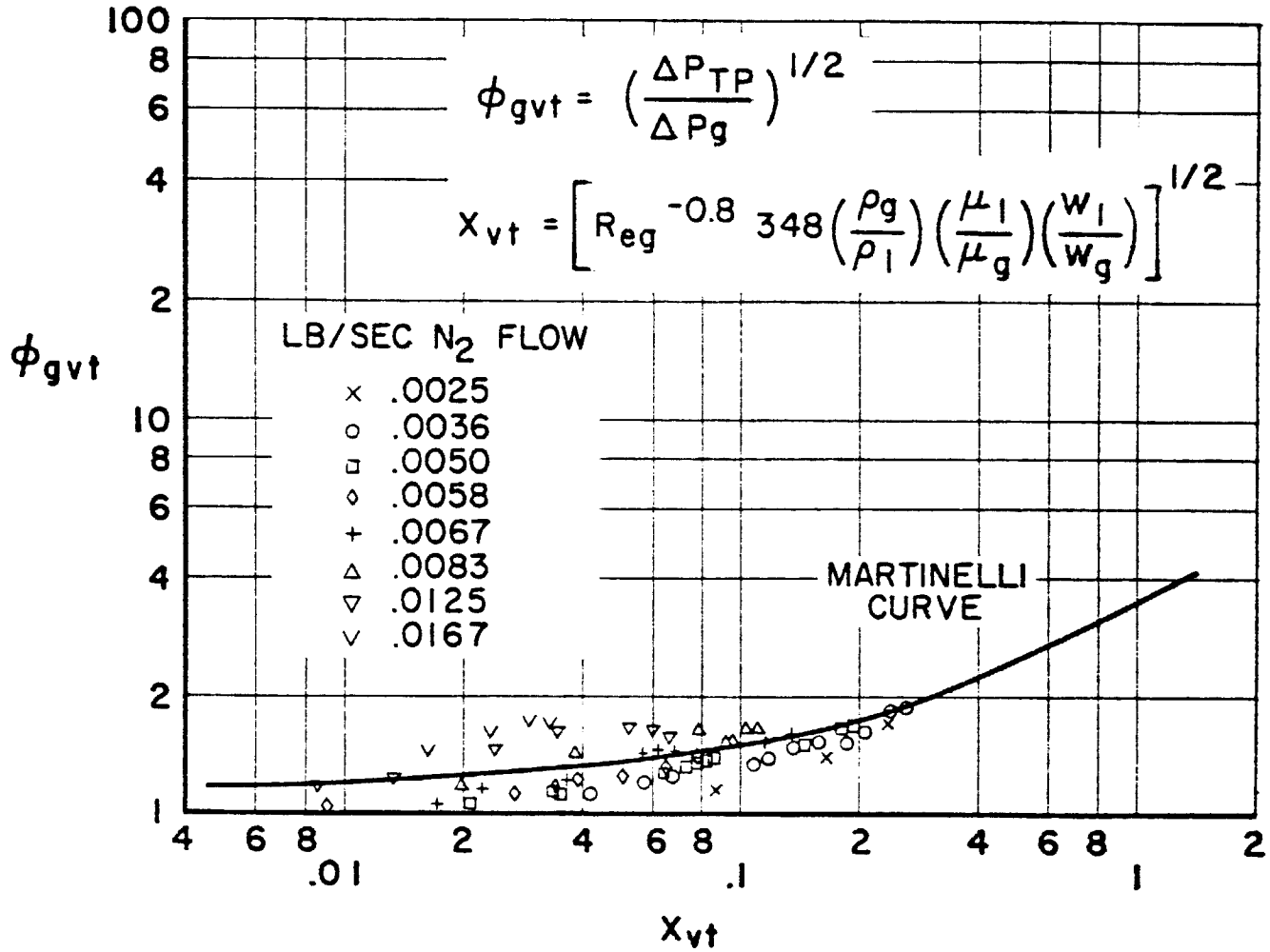

Figure 22. - Comparison of two-phase liquid mercury - nitrogen gas pressure drop with Martinelli correlation for viscous-turbulent flow. Horizontal tube inside diameter, 0.394 inch; length, 4 feet.

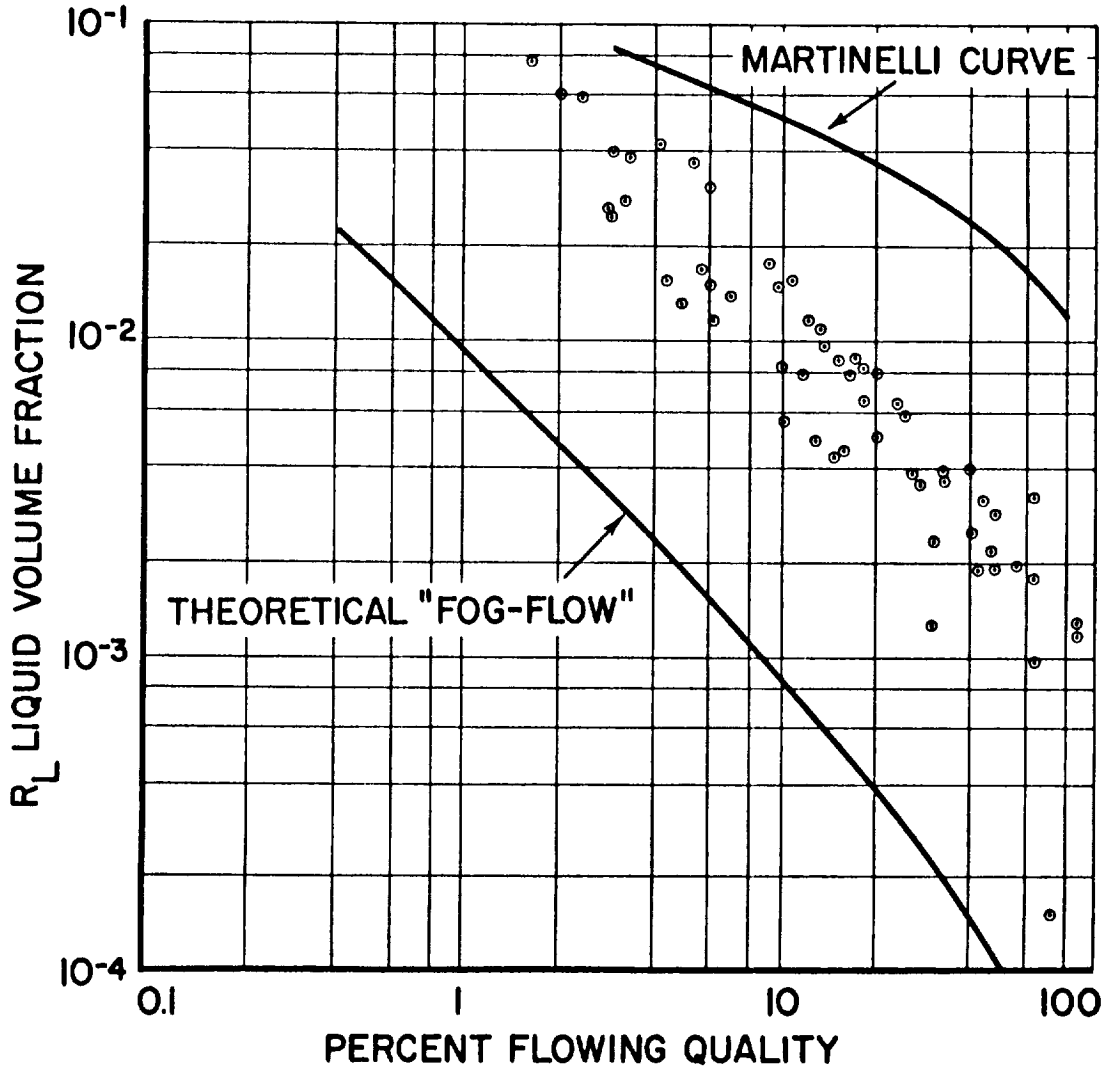

Figure 23. - Liquid hold-up two-phase flow. Test results for liquid mercury - nitrogen gas. Horizontal 0.394 inch inside diameter tube, 4 feet long.

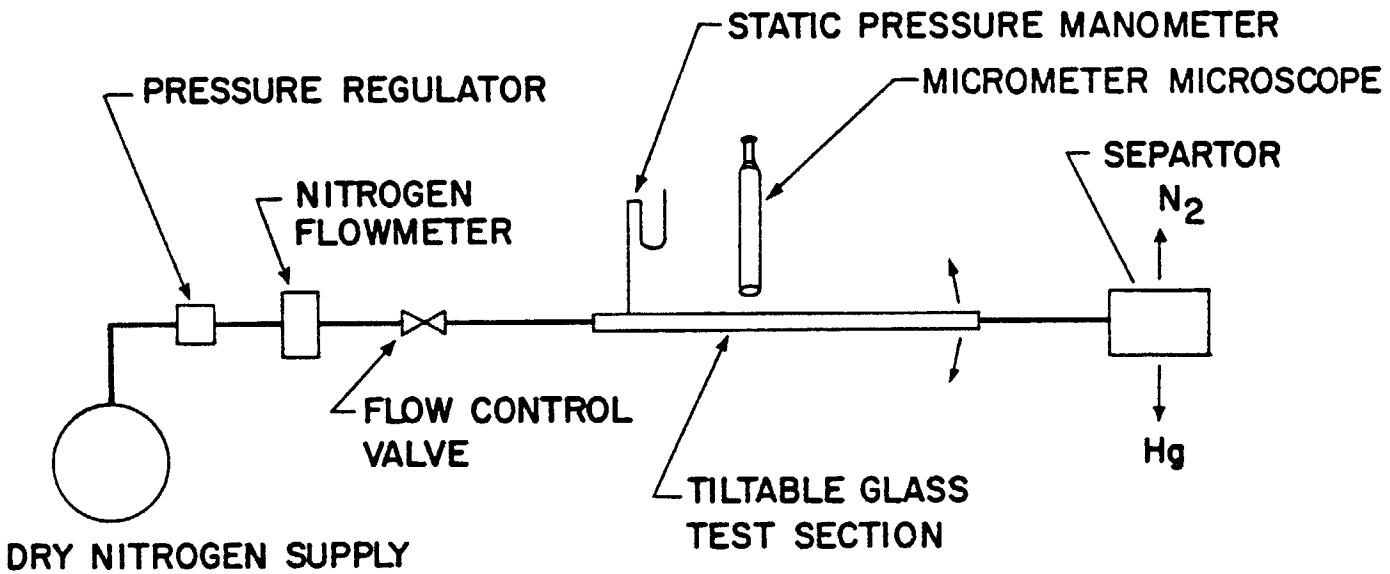

Figure 24. - Schematic of test apparatus to determine critical mercury drop size.

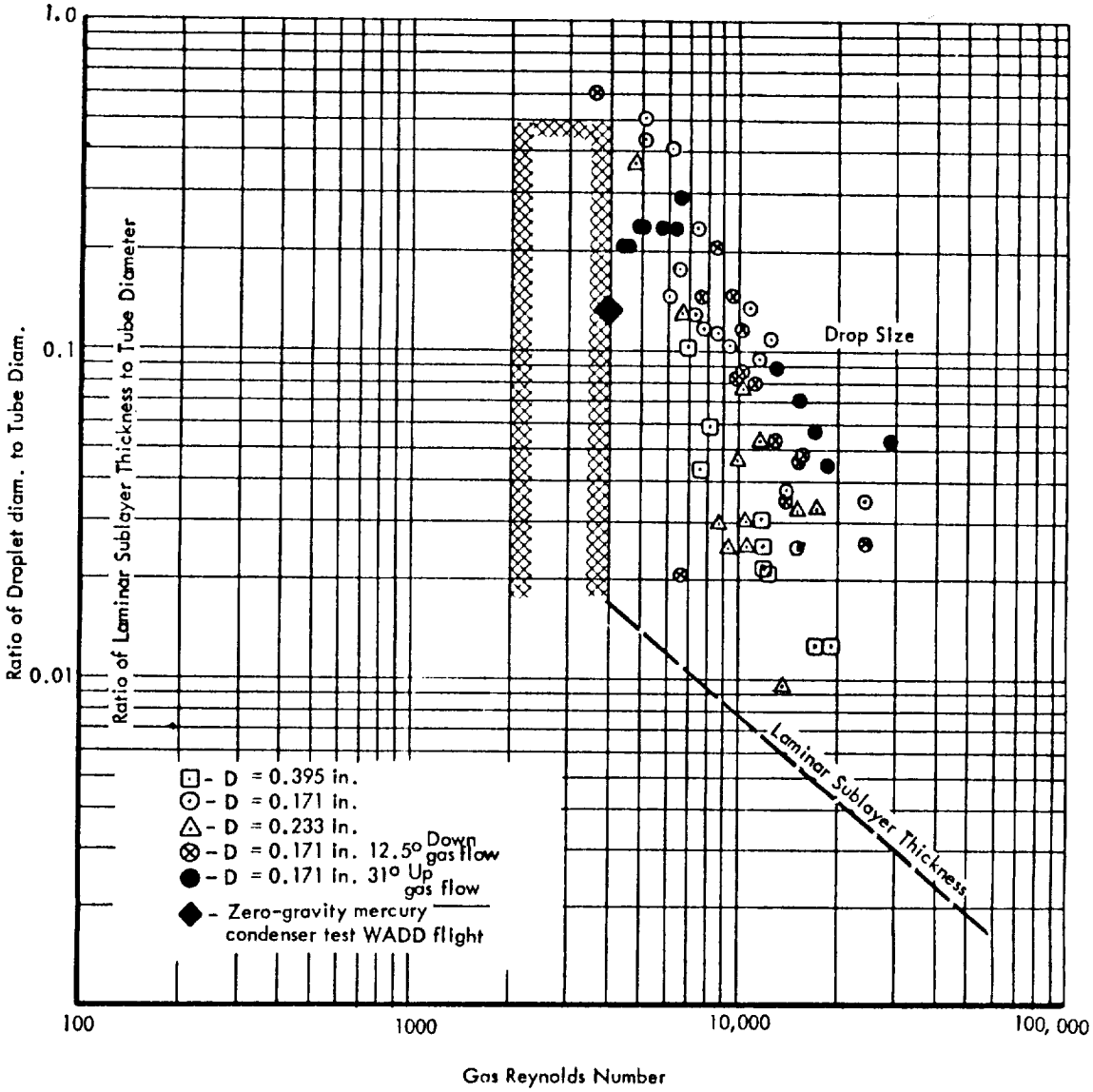

Figure 25. - Drop diameter against critical gas Reynolds number for entrainment.

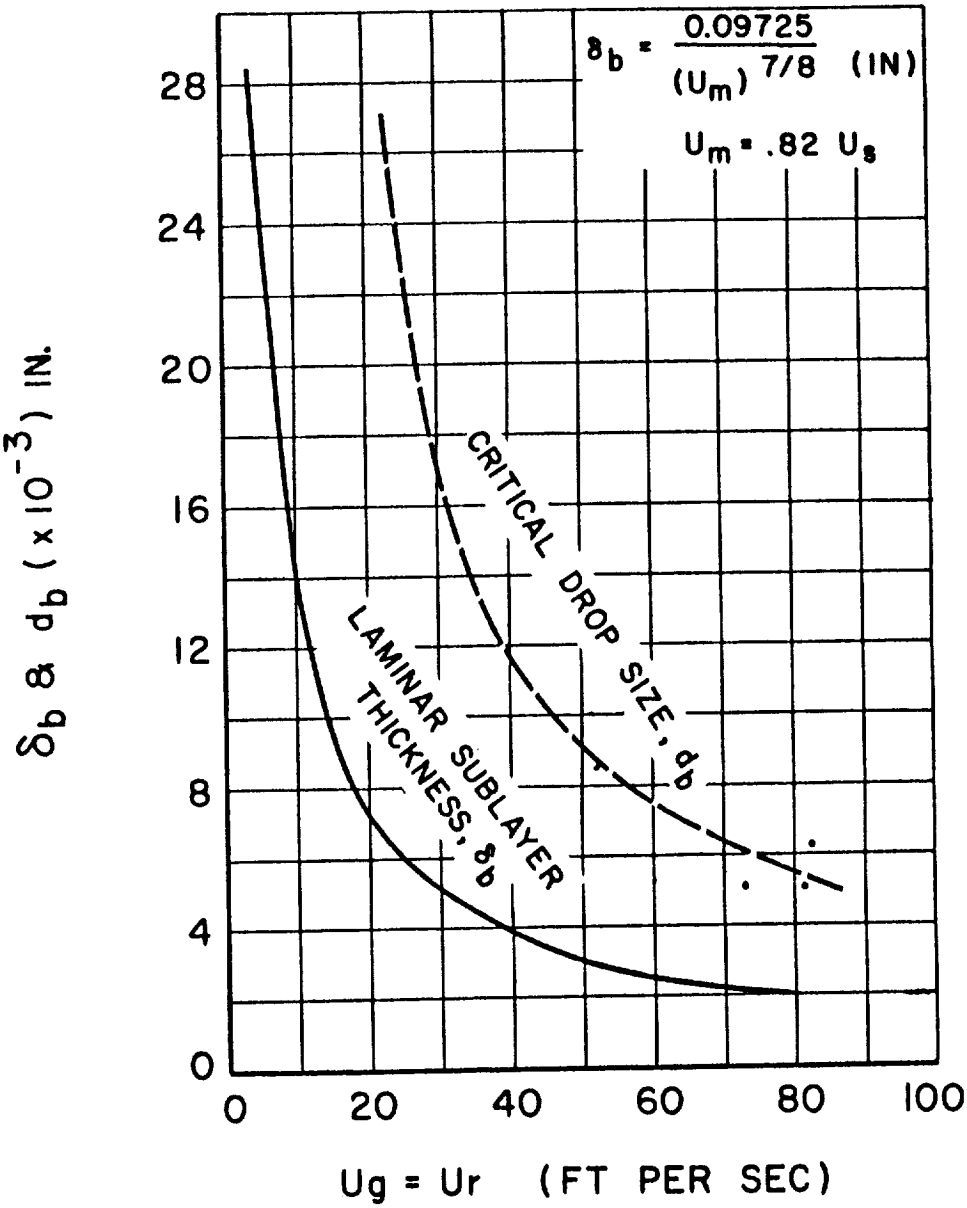

Figure 26. - Critical drop size d_b and laminar boundary-layer thickness δ_b against critical velocity.

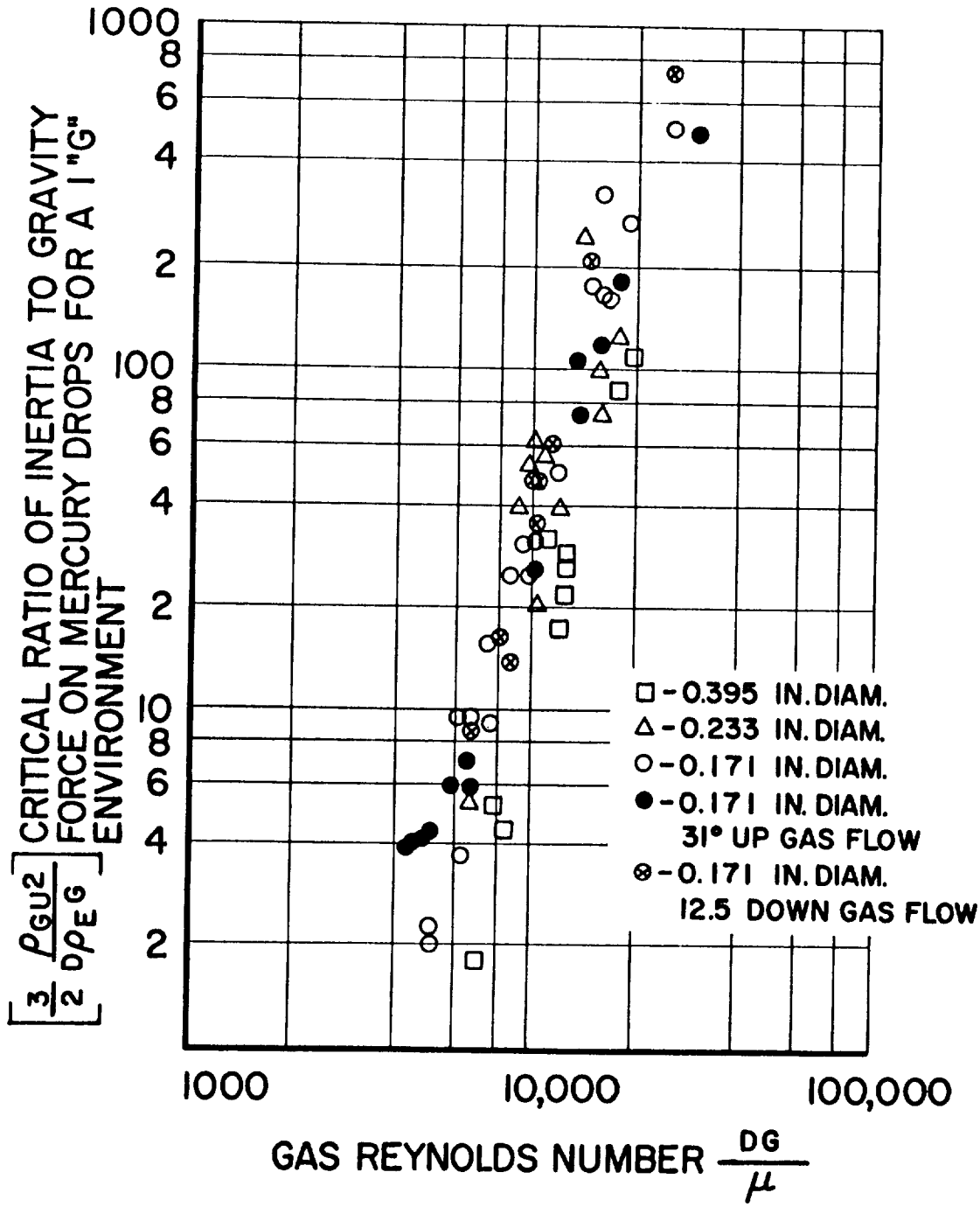

Figure 27. - Froude number of mercury droplets against gas Reynolds number of pipe.

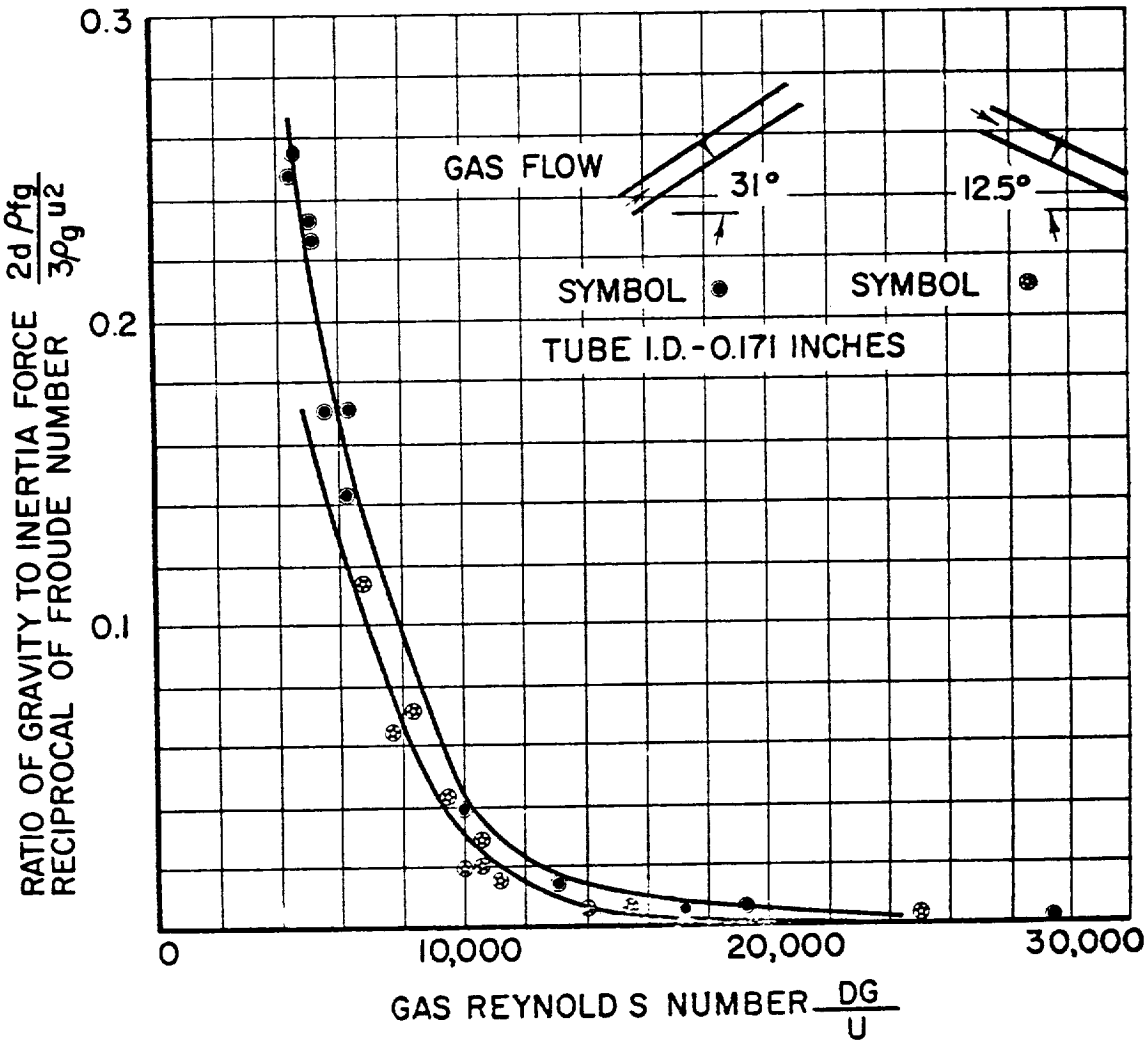

Figure 28. - Effect of gravity on critical drop size.

INLET REYNOLDS NUMBER = 1950
2.55 "G"

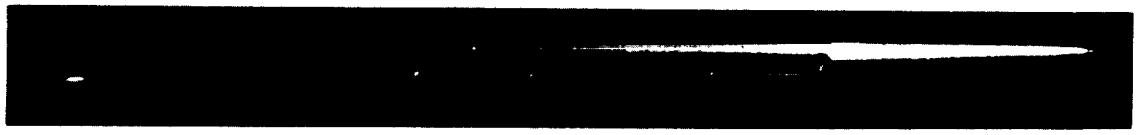

INLET REYNOLDS NUMBER = 3440
1.0 "G"

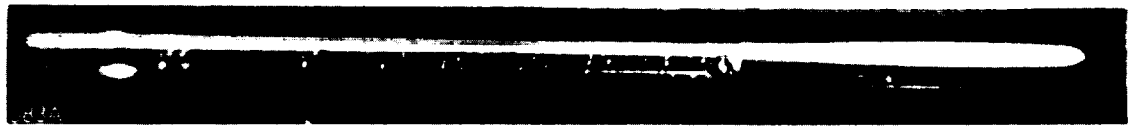

INLET REYNOLDS NUMBER = 3860
0 "G"

C-58231

Figure 29. - Mercury condensing in a 0.136-inch inside-diameter tube, 12-inch effective condenser length. Flow from left to right. Photographs from TRW apparatus aboard C-131-B aircraft flying zero-gravity maneuvers at WADD, March 18, 1960.

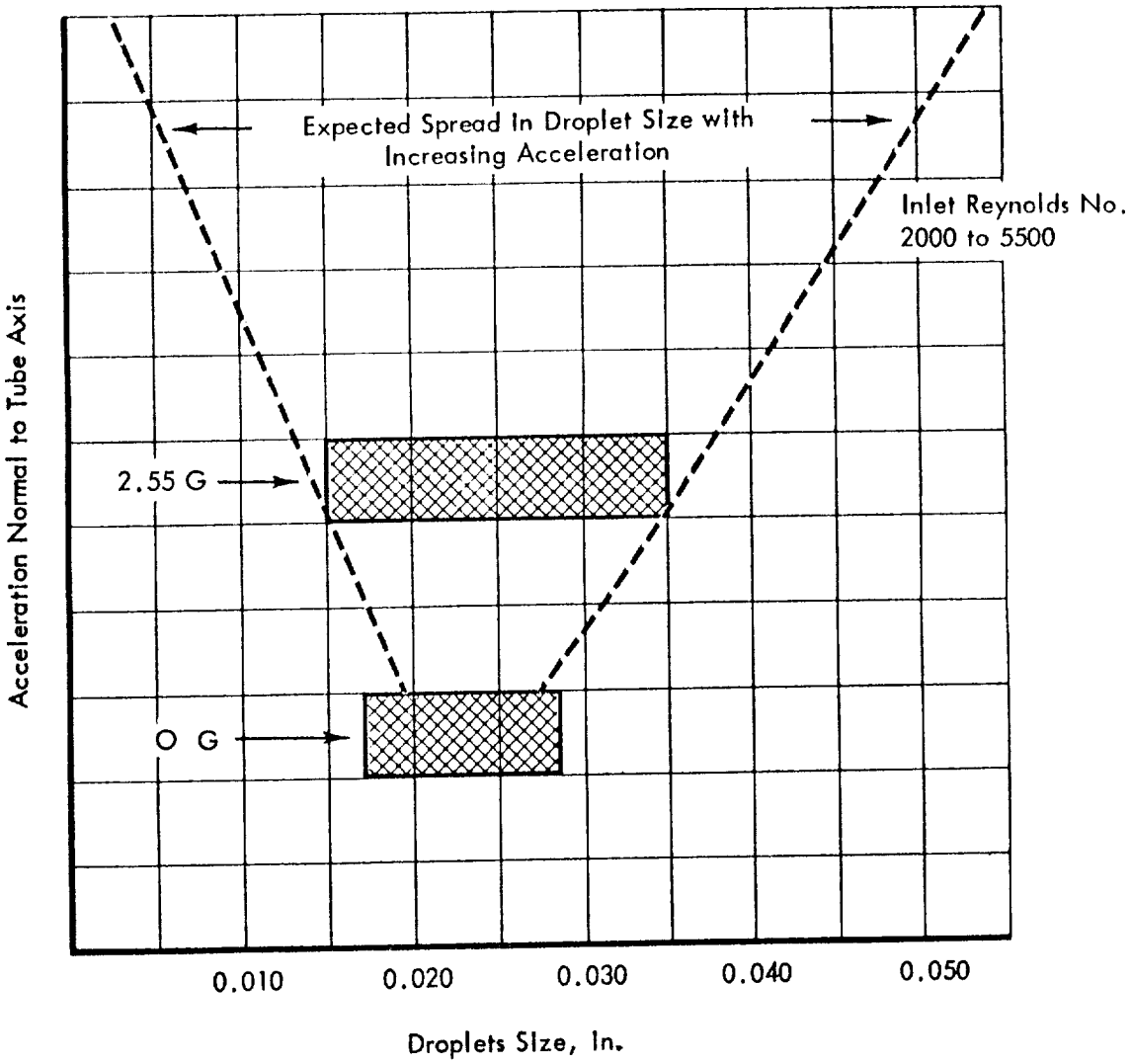

Figure 30. - Spread in droplet size of visible moving droplets in midsection of condenser tube with acceleration.

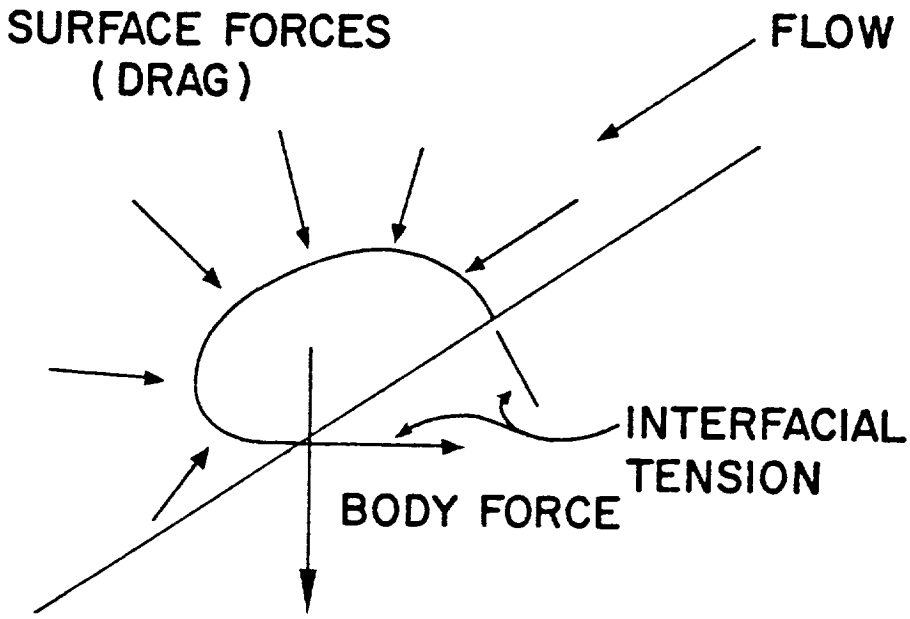

Figure 31. - Drop resting on surface under the influence of drag, body forces, and interfacial tension.

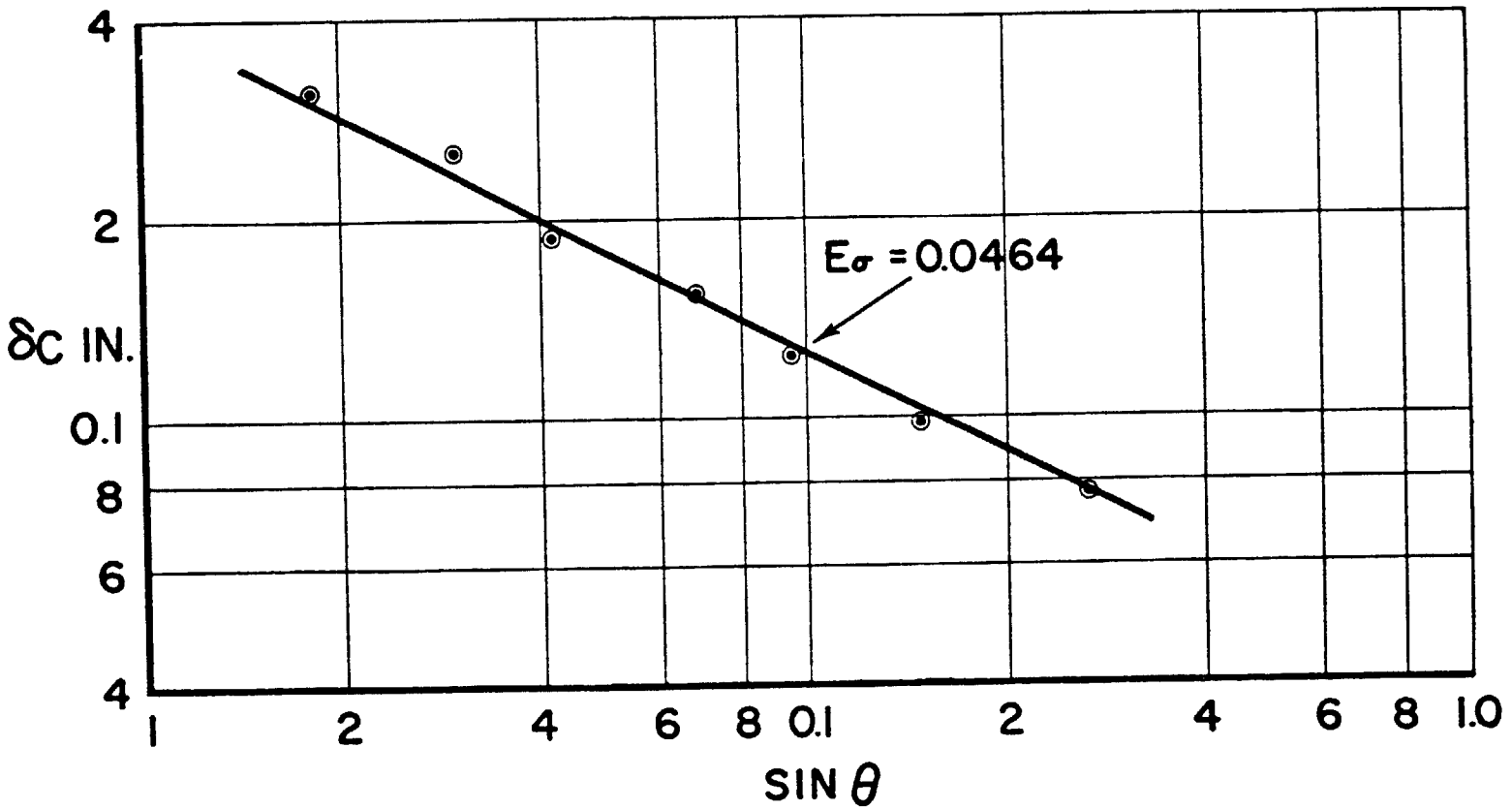

Figure 32. - Critical drop size measurements in a gravity field.

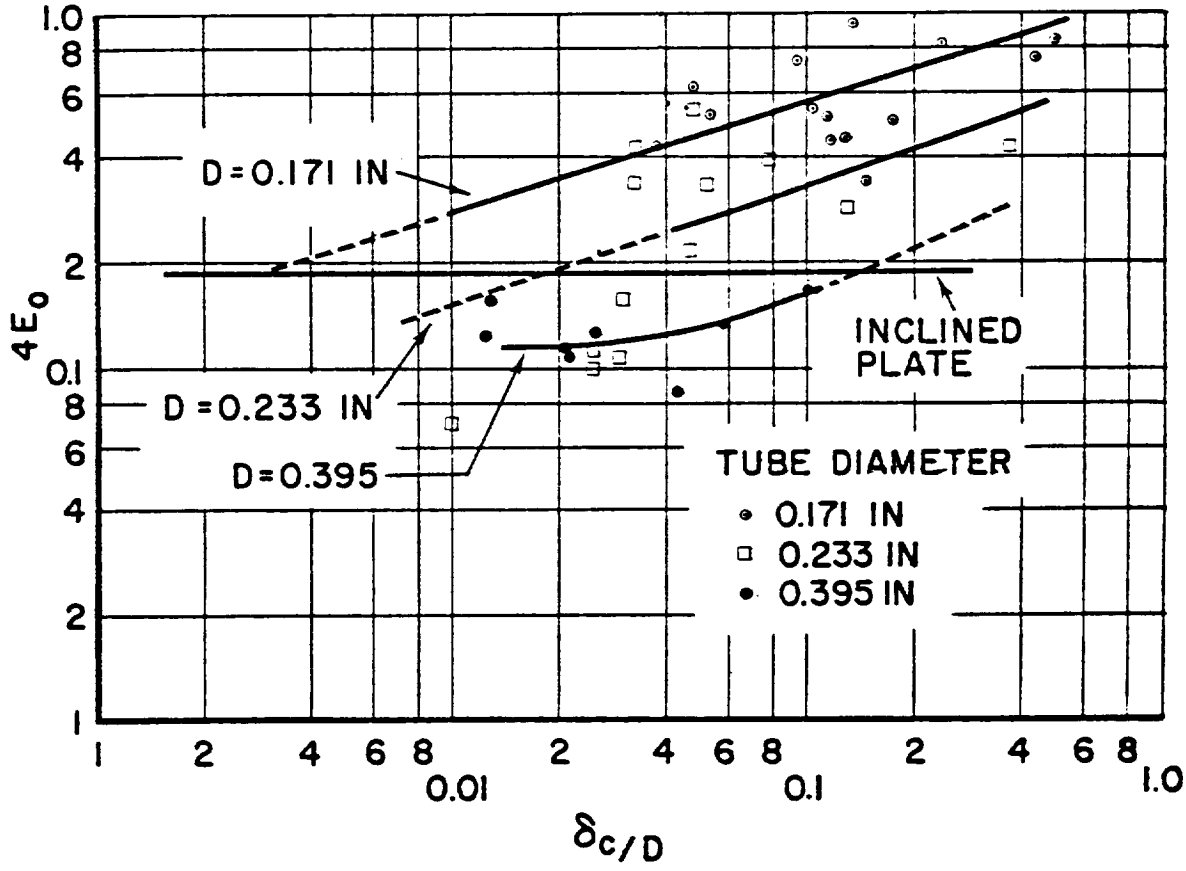

Figure 33. - Critical drop size measurements in a flow field with horizontal tubes.

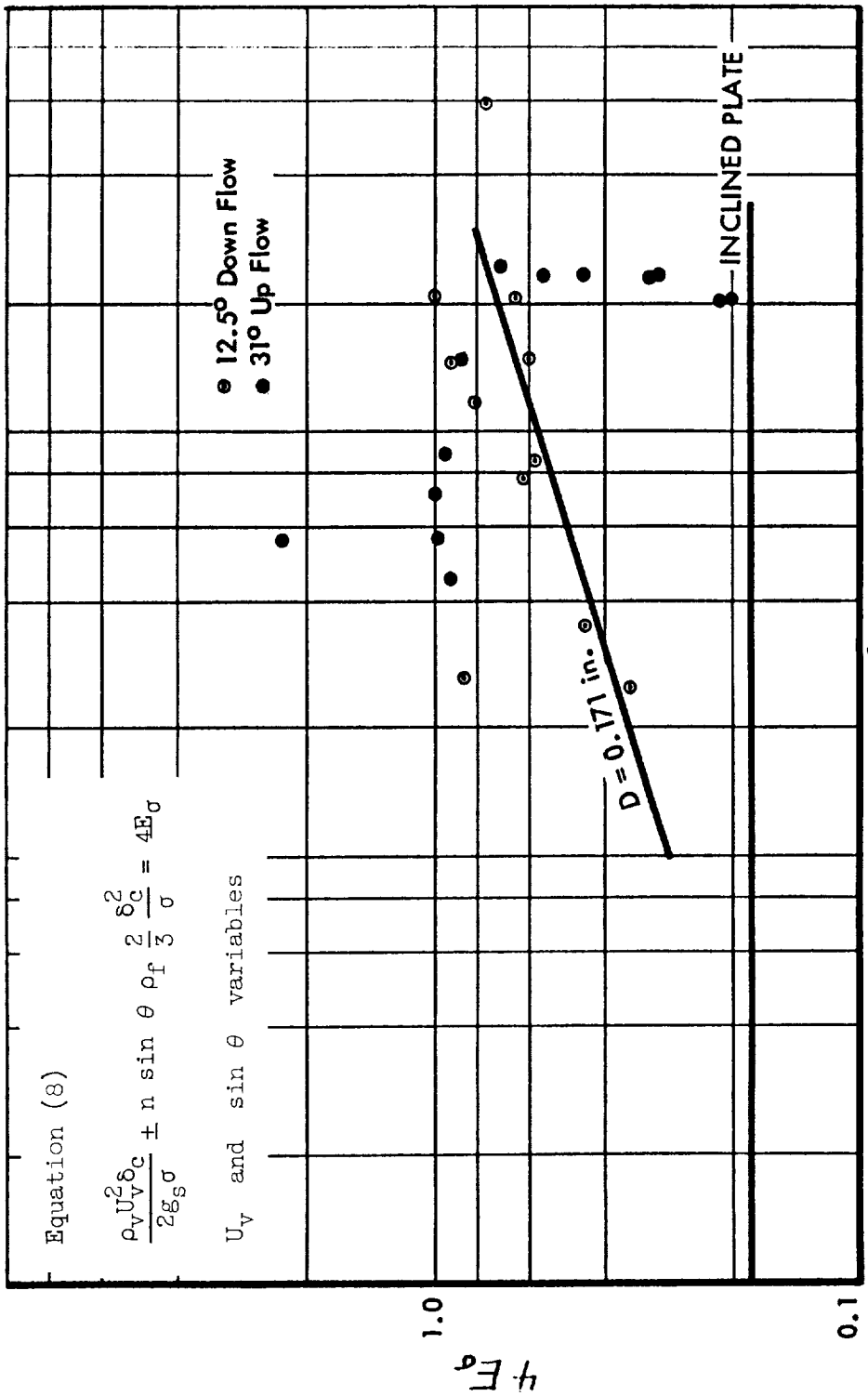

Figure 34. - Gas flow rate required to cause movement of a mercury drop in inclined glass tubes.

E-1501

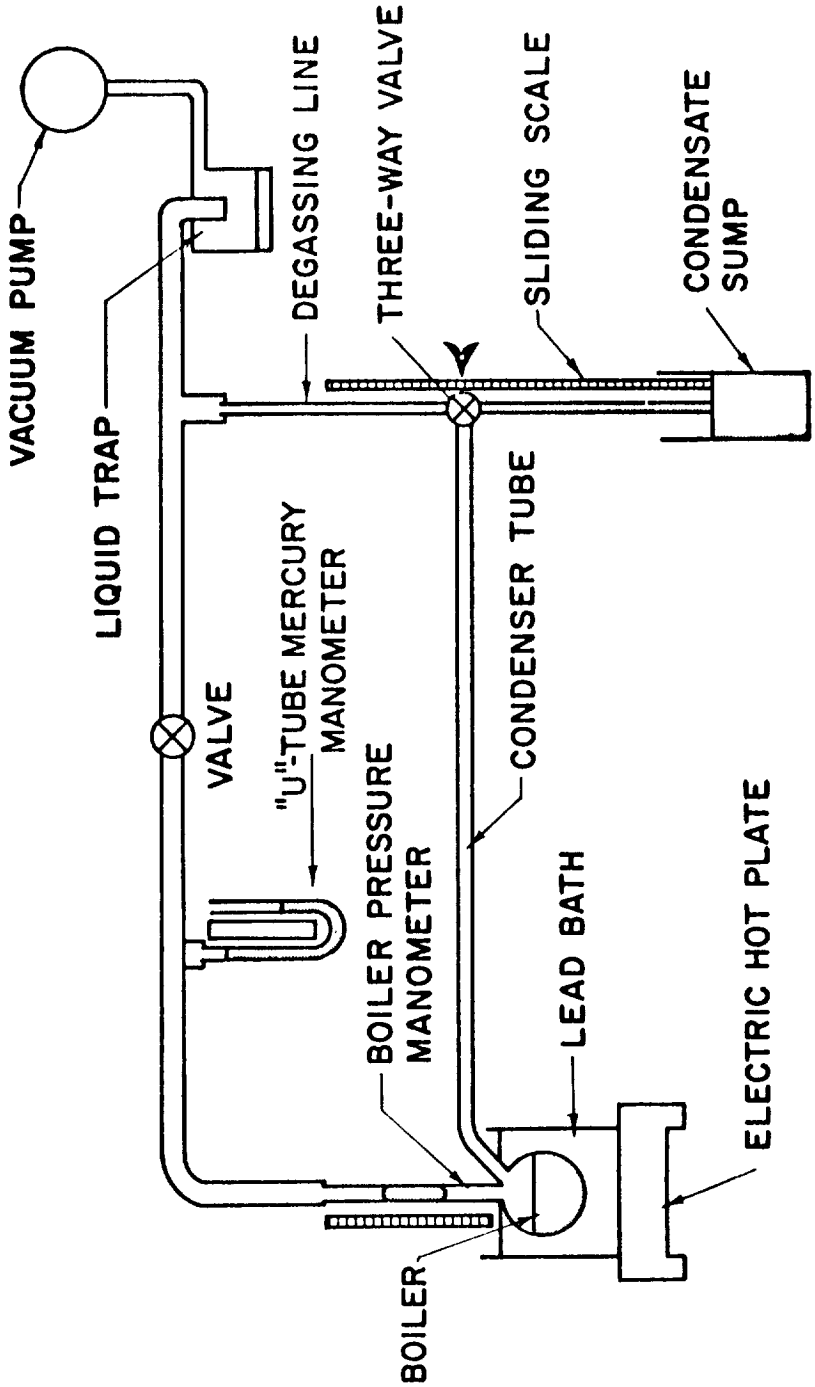

Figure 35. - Typical mercury condenser test setup.

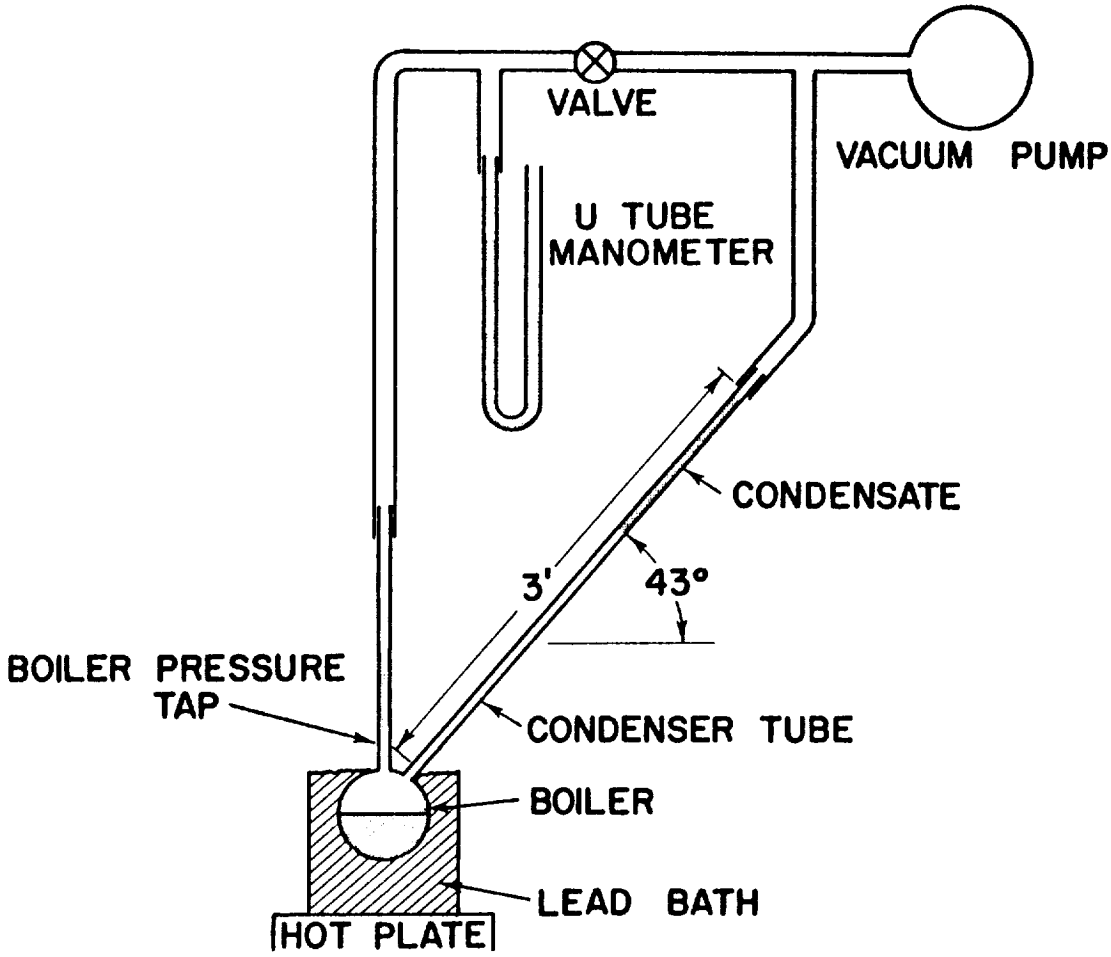

Figure 36. - Inclined tapered tube test setup.

E-1501

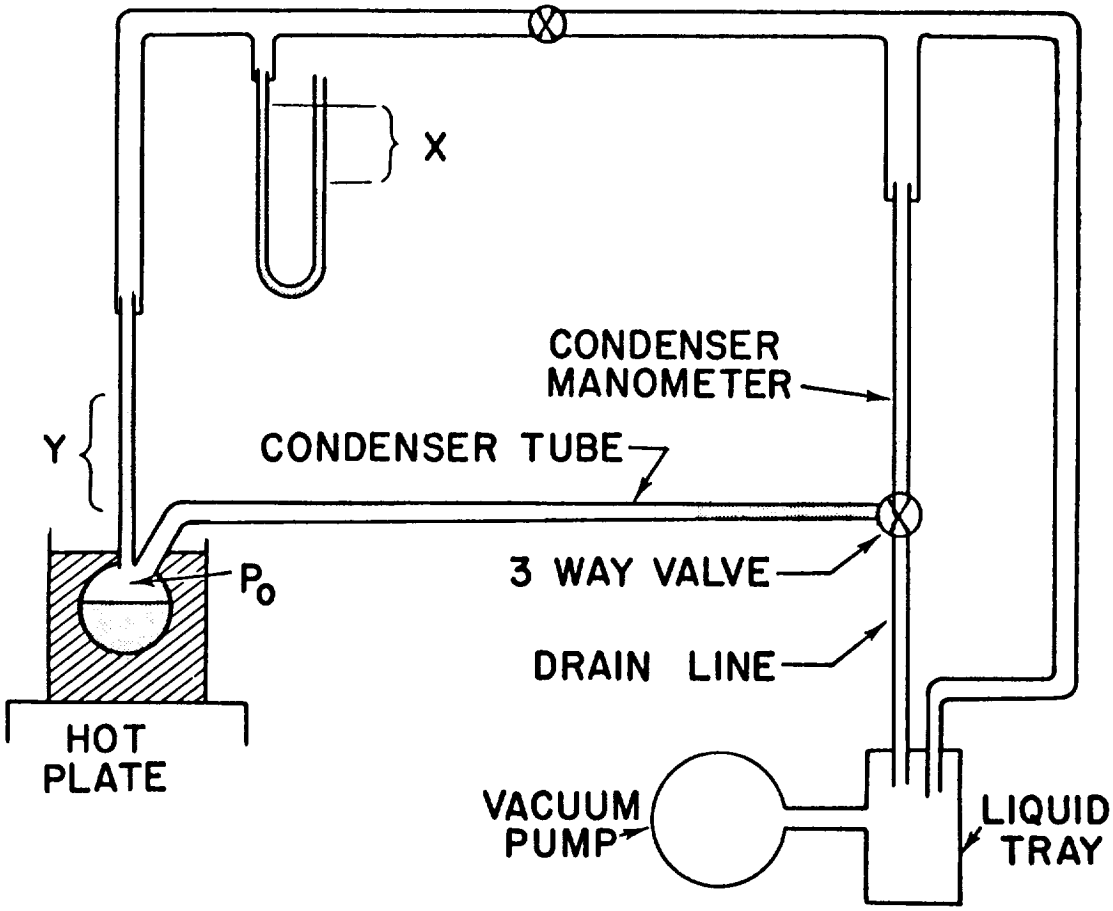

Figure 37. - Horizontal tapered tube test setup.

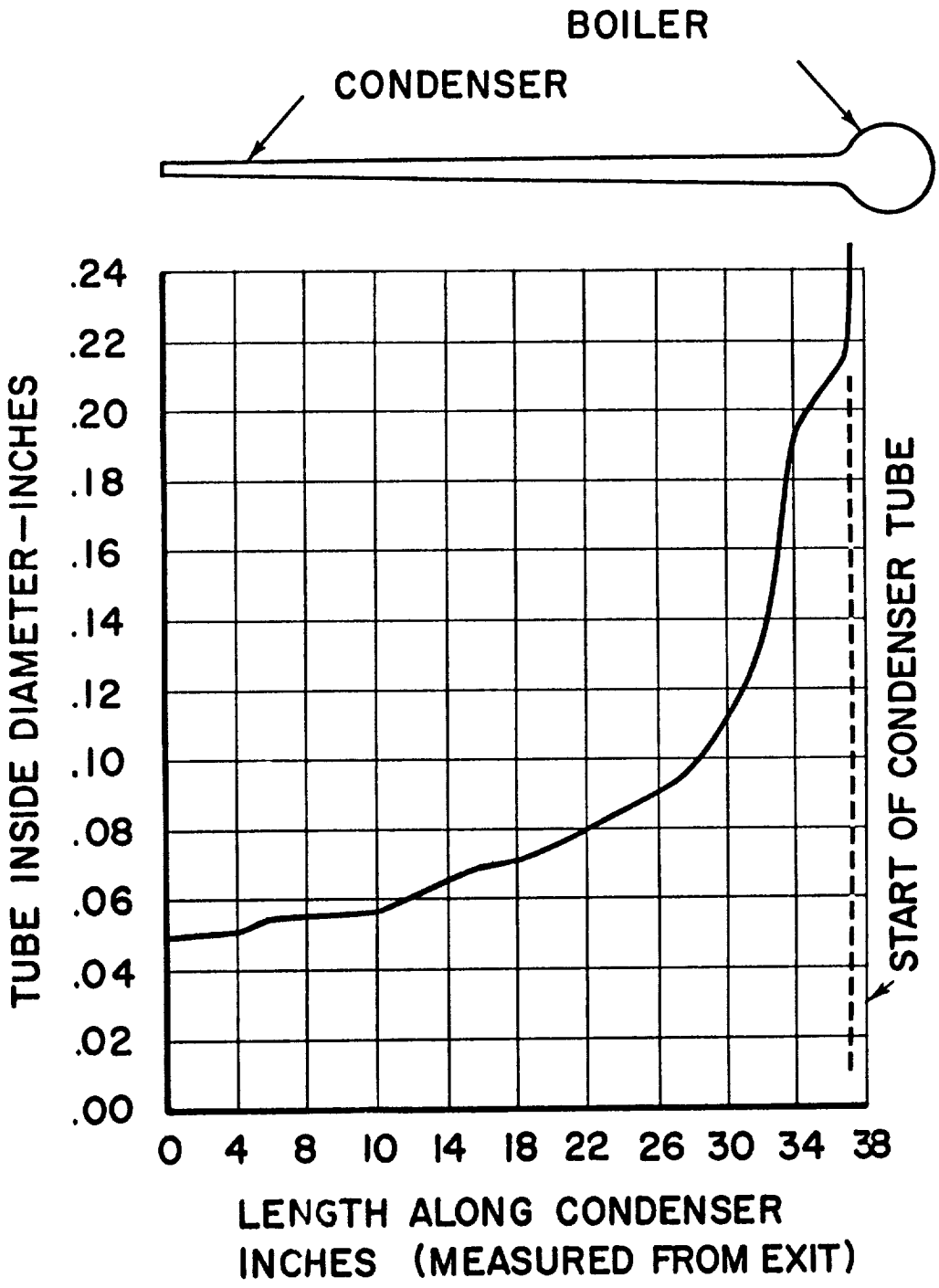

Figure 38. - Measured tapered tube inside diameter.

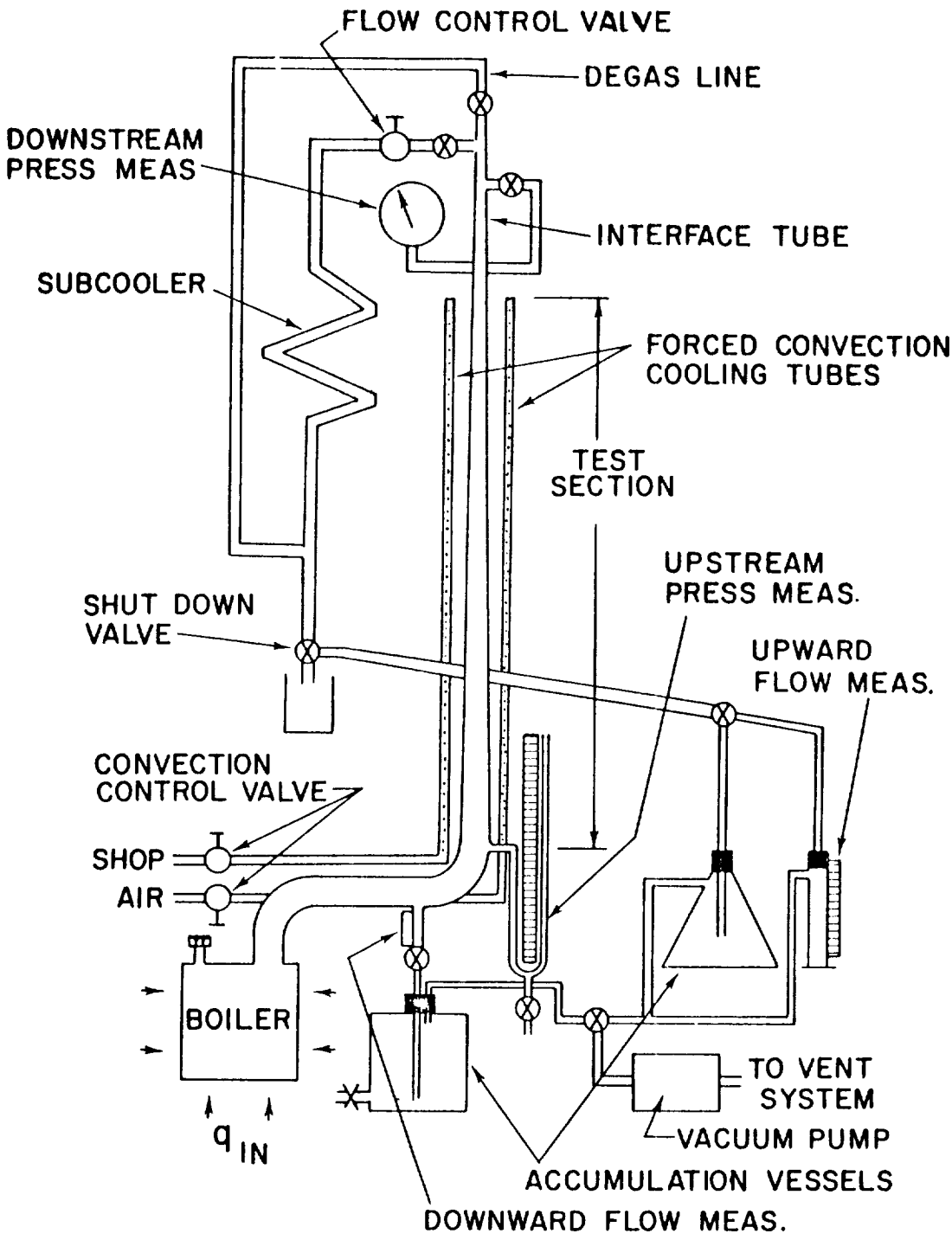

Figure 39. - Test apparatus for 8-feet stepped tapered tube with upward flow.

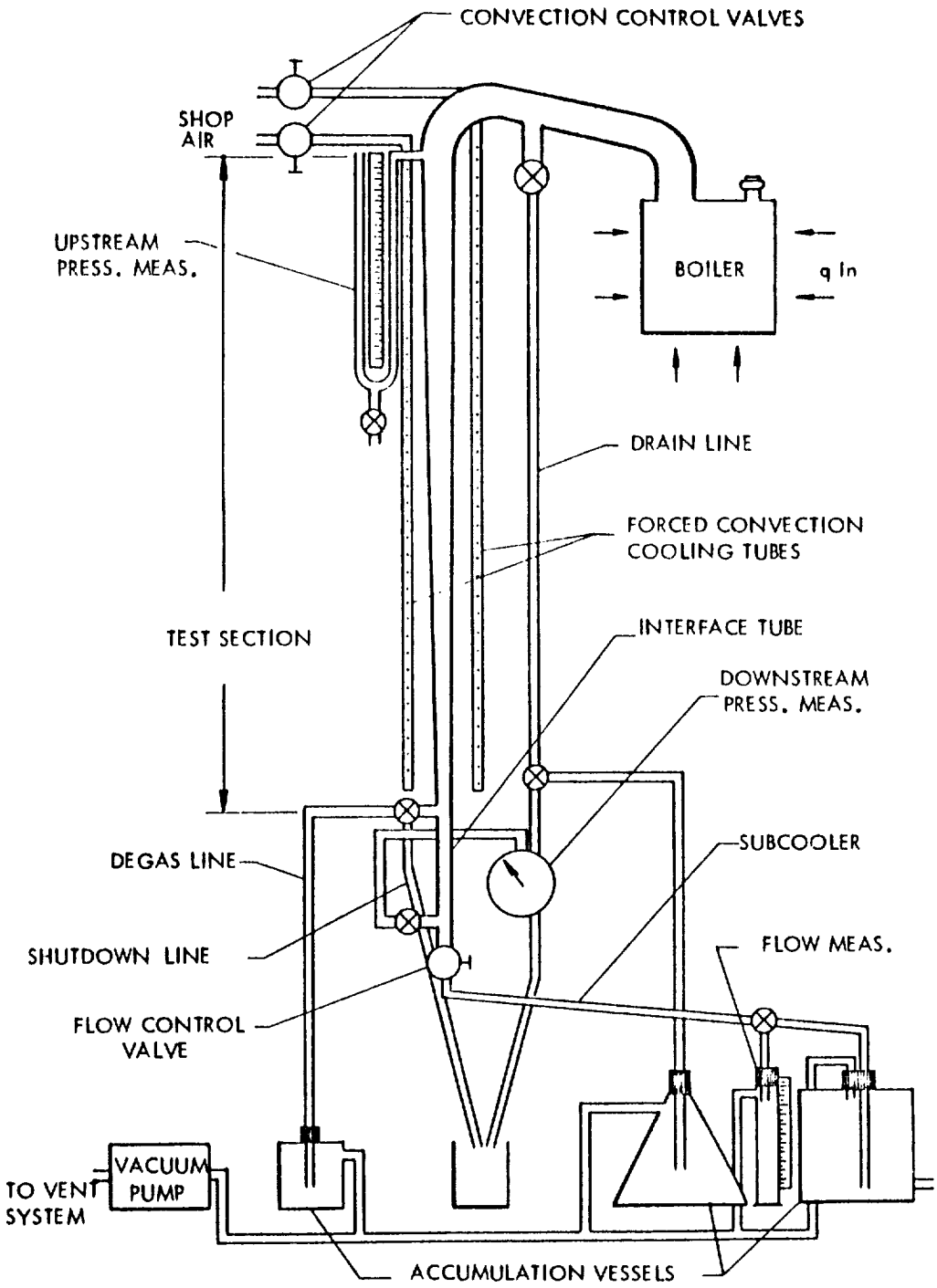

Figure 40. - Mercury condenser test setup for vertical downflow in a stepped tapered tube.

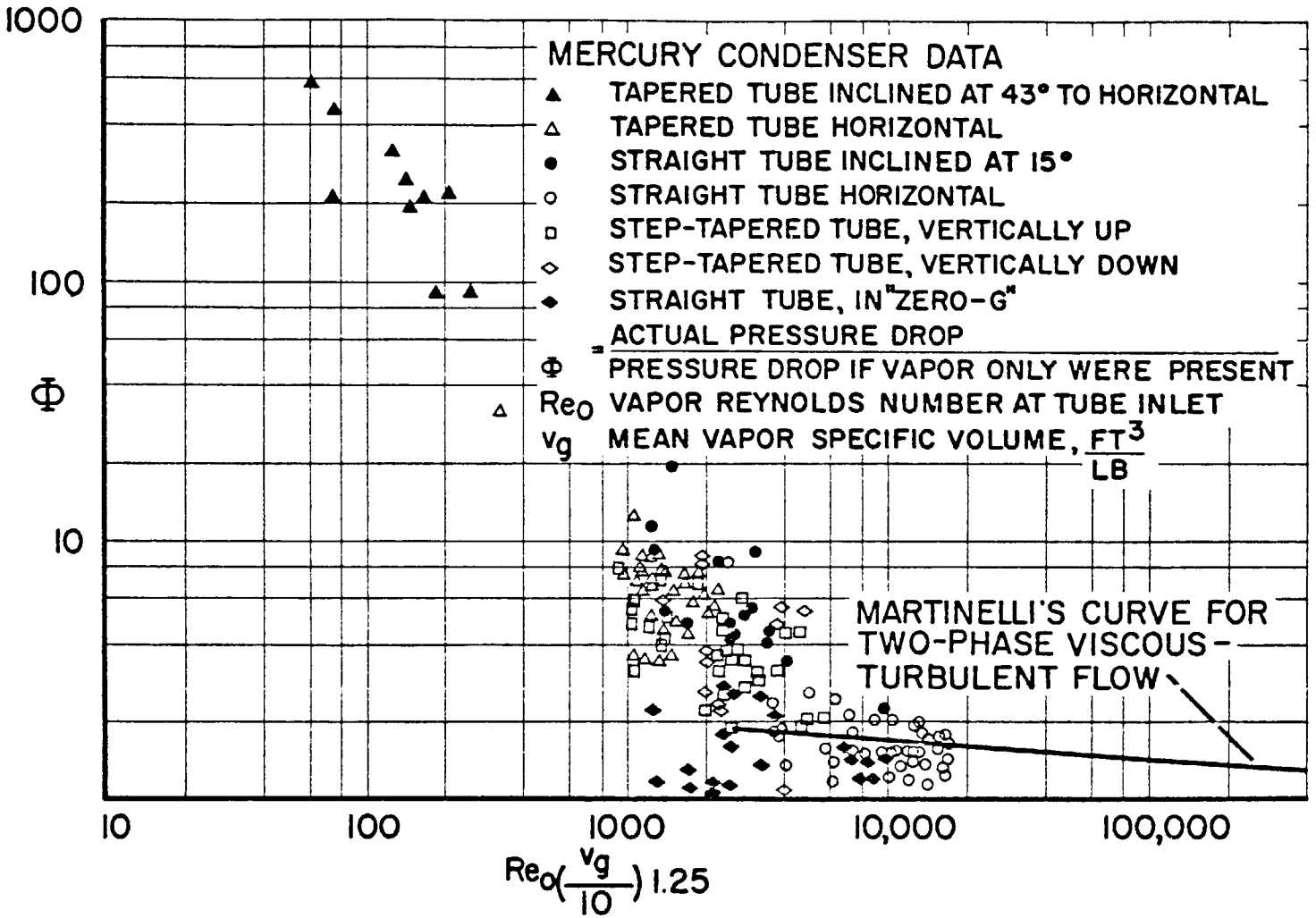

Figure 41. - Pressure drop test results for mercury condensing in glass tubes.

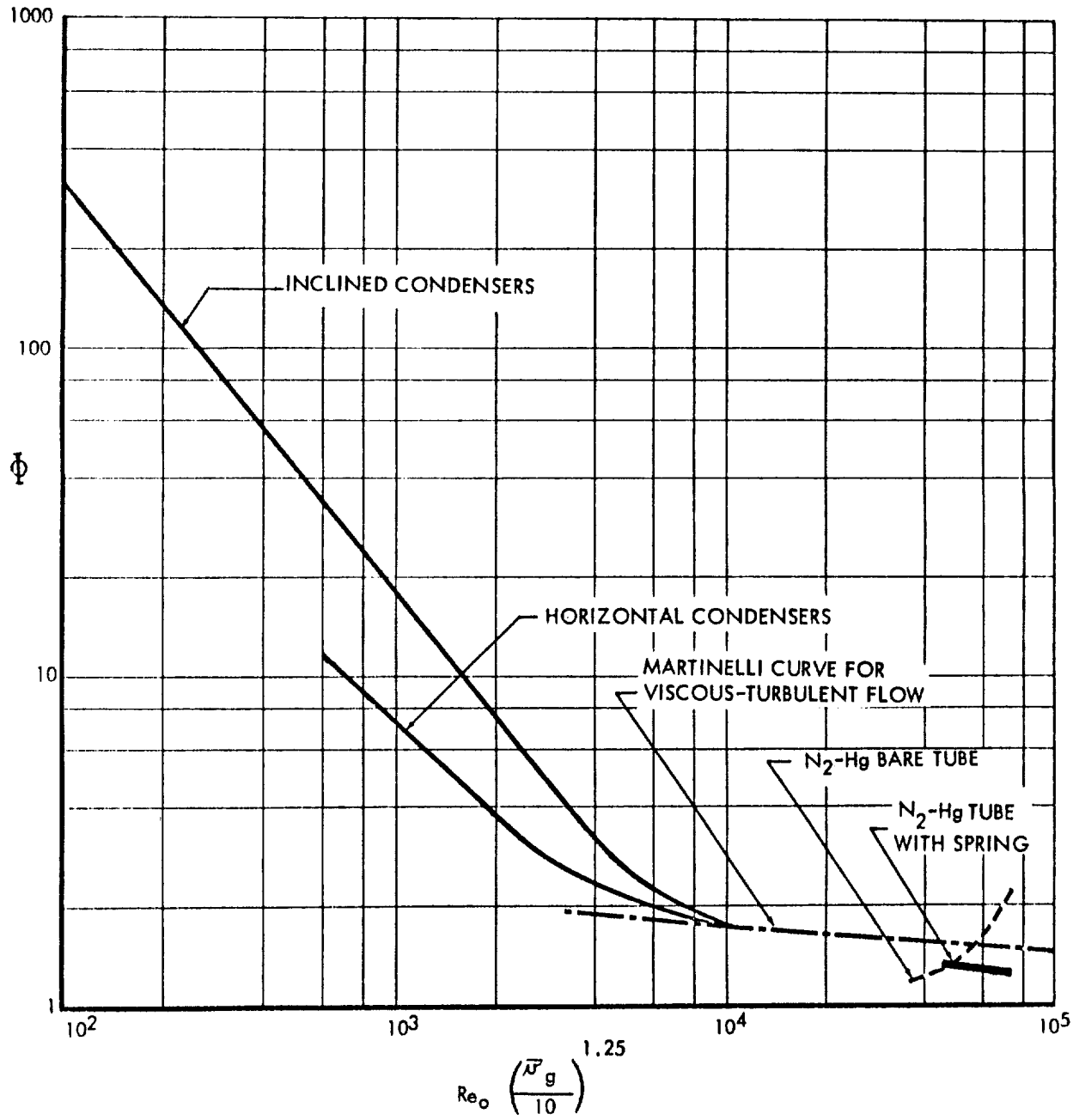

Figure 42. - Comparison of mercury pressure drop data.

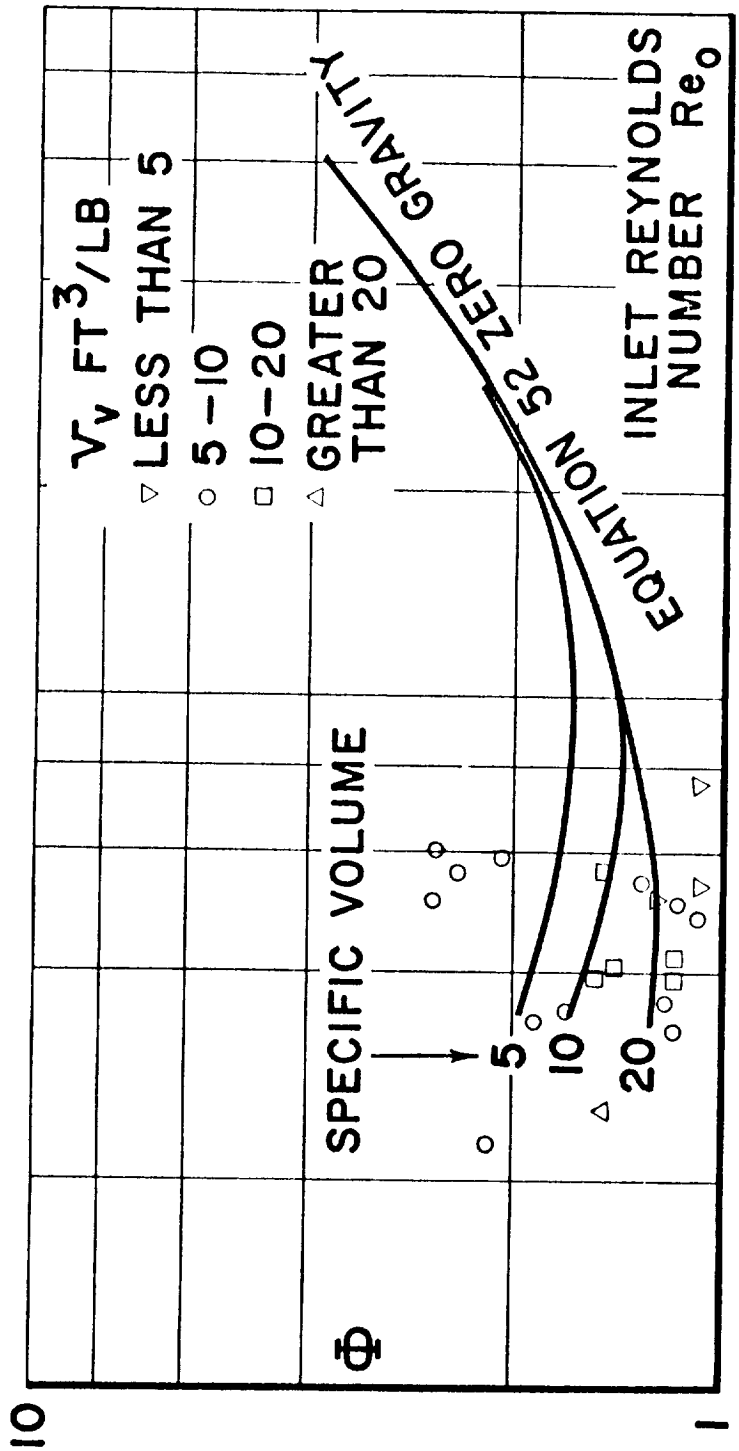

Figure 43. - Comparison of zero-gravity test results with theoretical equation.

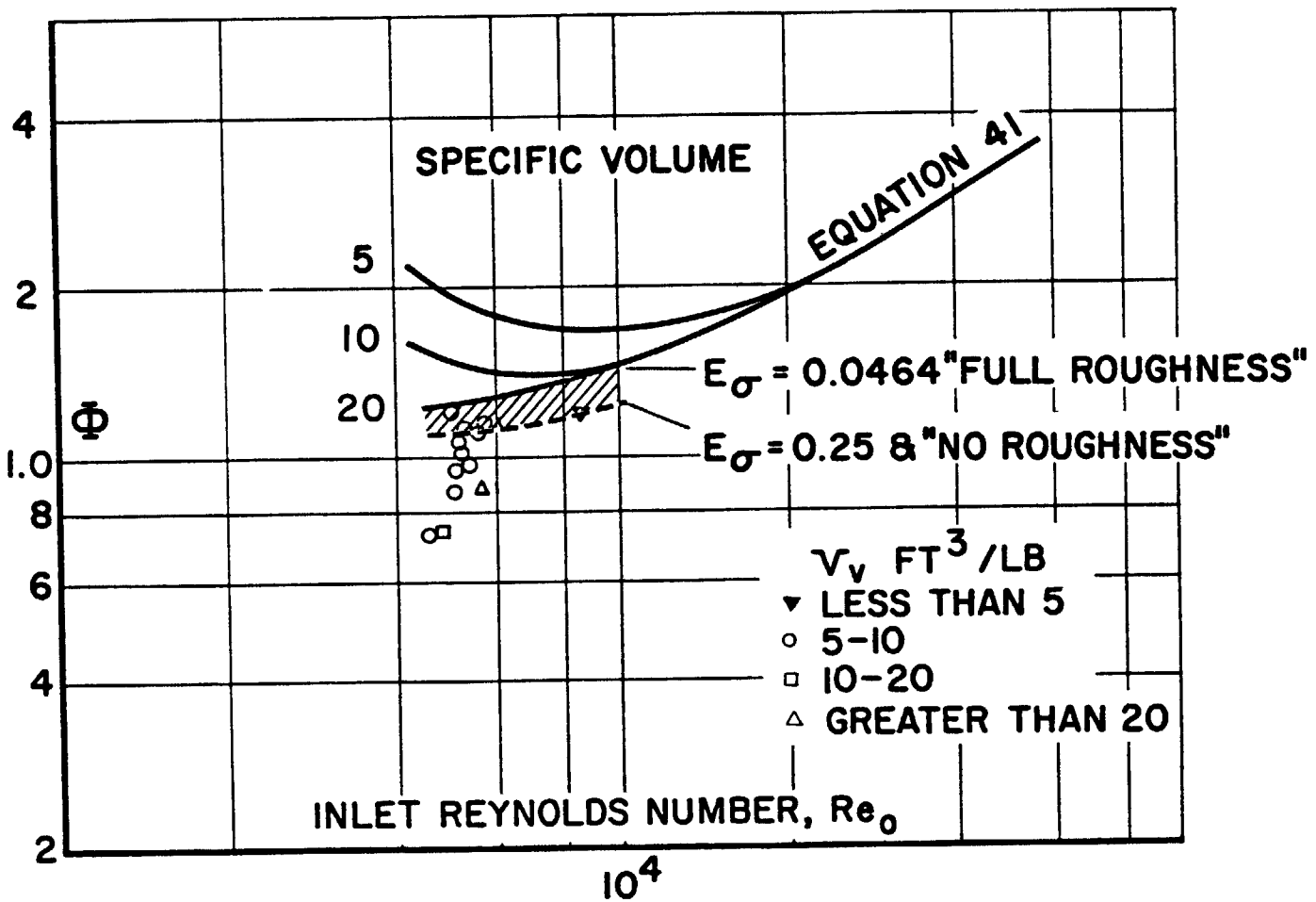

Figure 44. - Comparison of ground test results with theoretical equation for condensing downward.

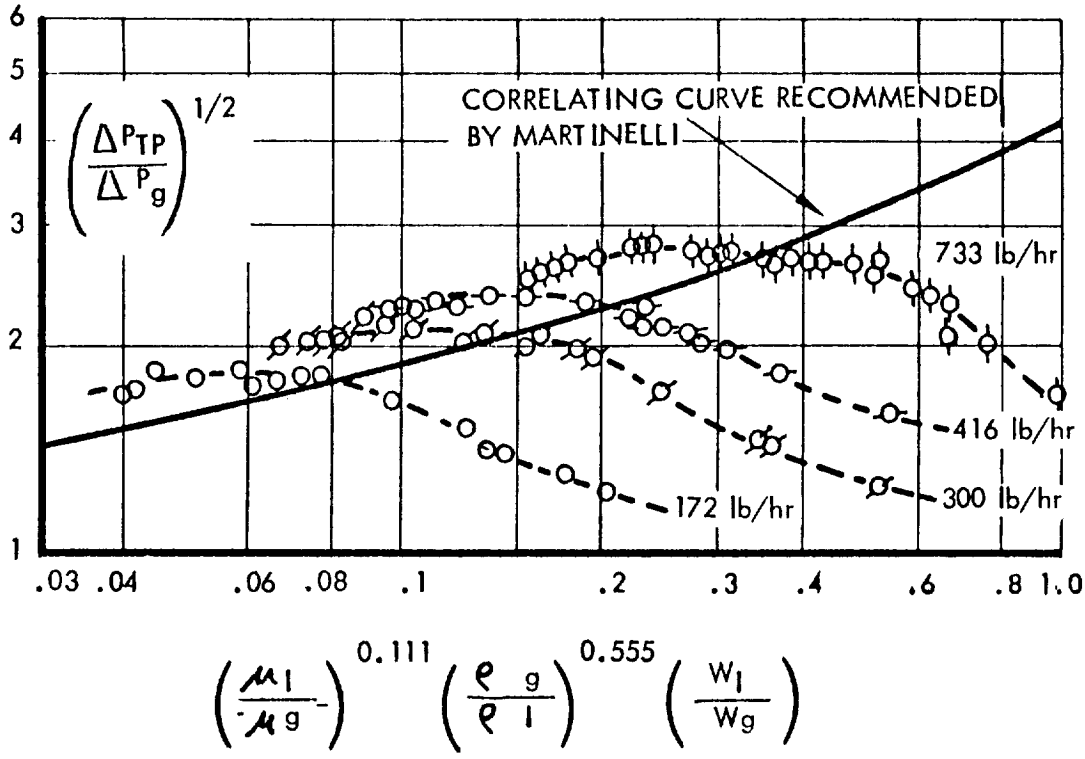

Figure 45. - Experimental data of Dukler from "Review Of The Literature On Two-Phase Fluid Flow In Pipes," WADC Technical Report 55-422.

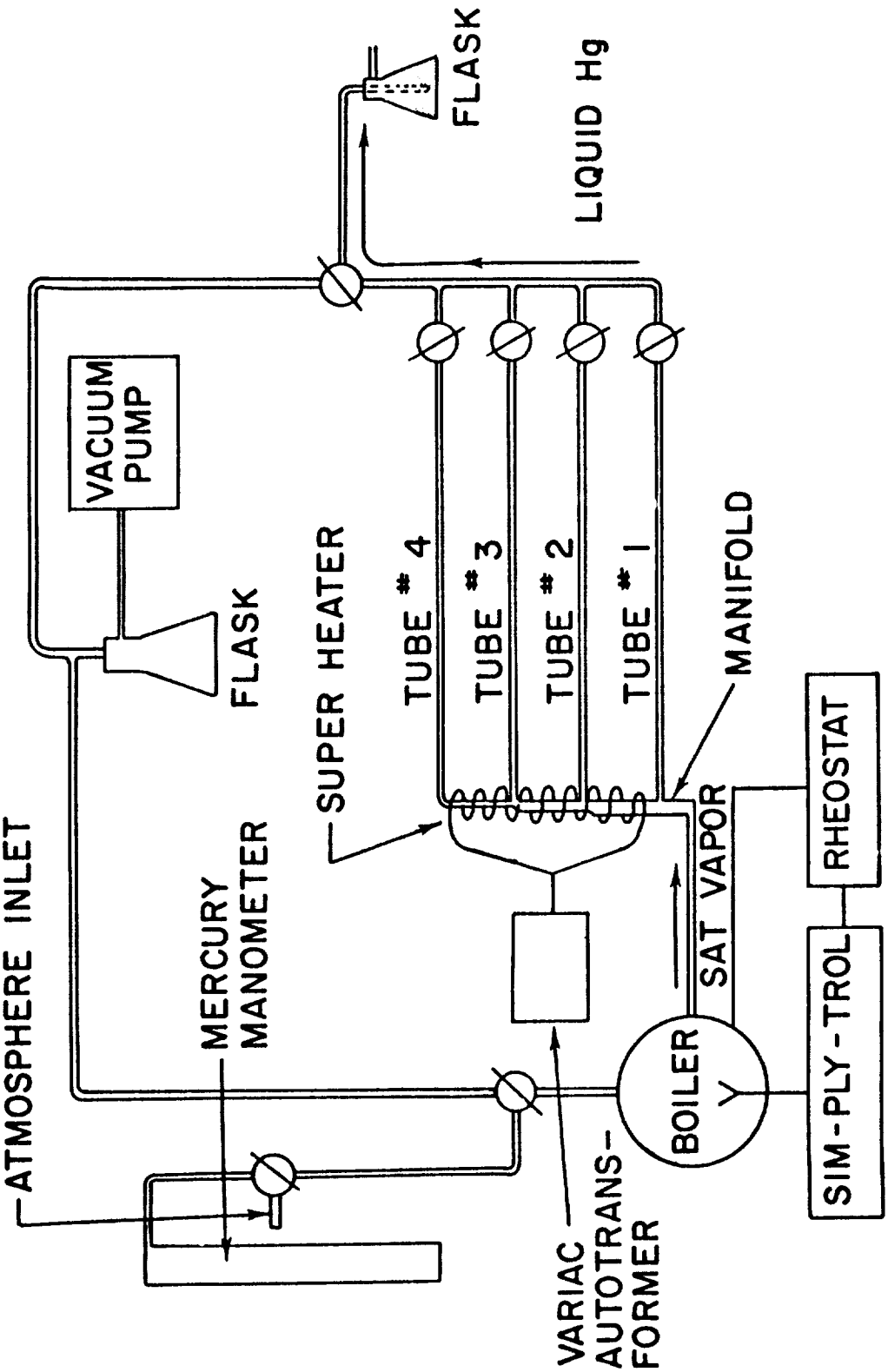

Figure 46. - Manifold test rig.

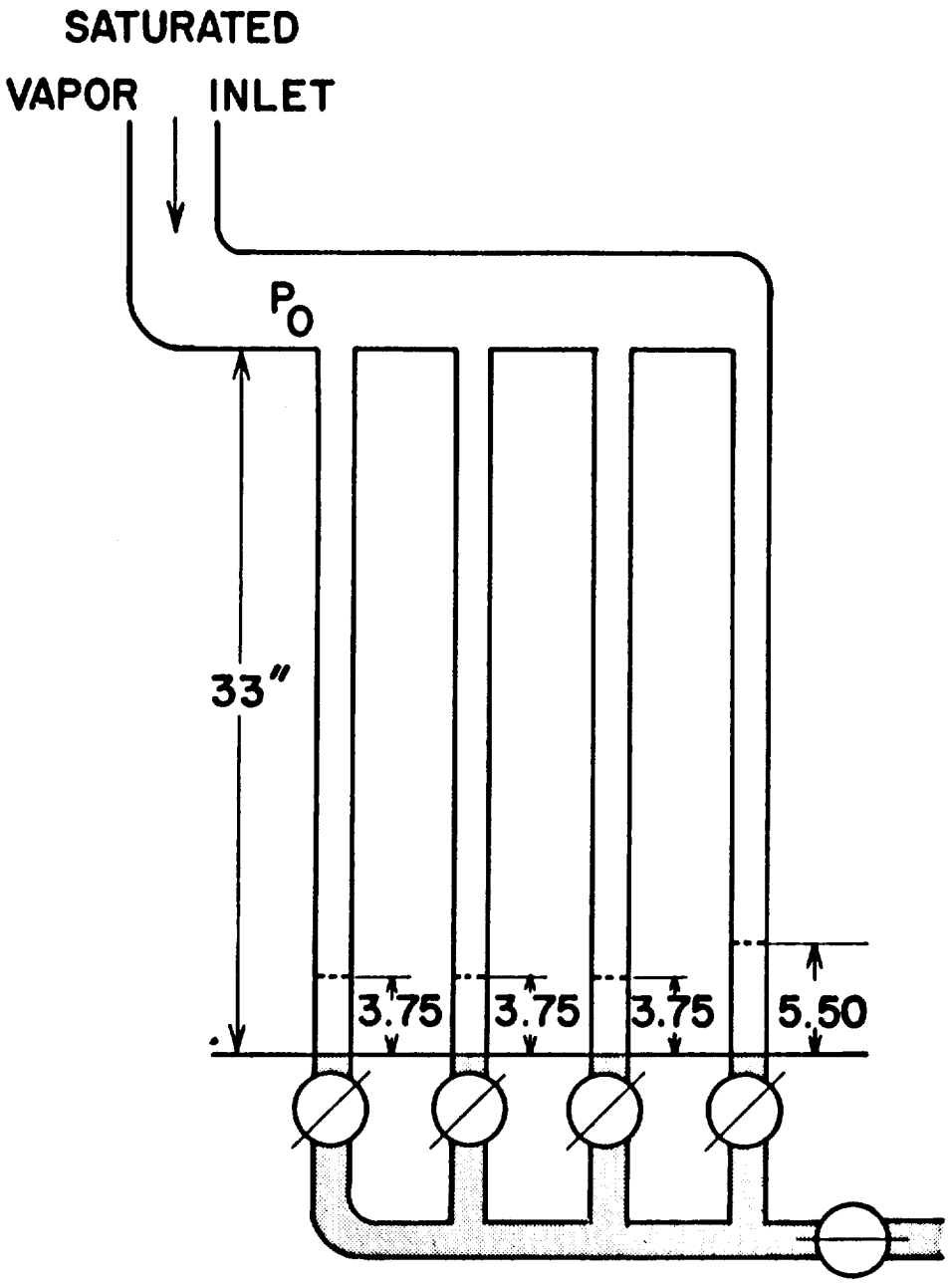

Figure 48. - Straight manifold. Valves closed.

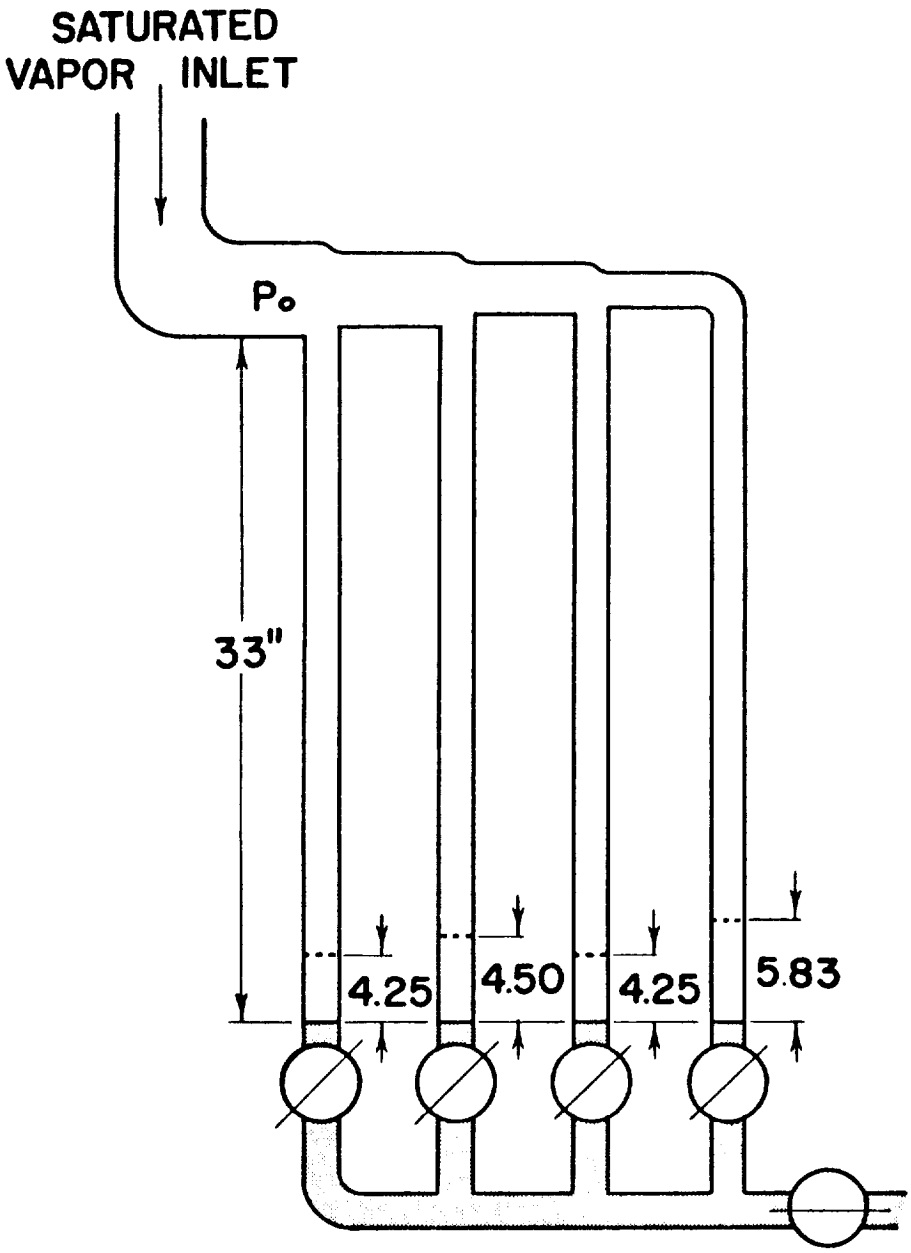

Figure 47. - Tapered manifold. Valves closed No. 42. Typical run.

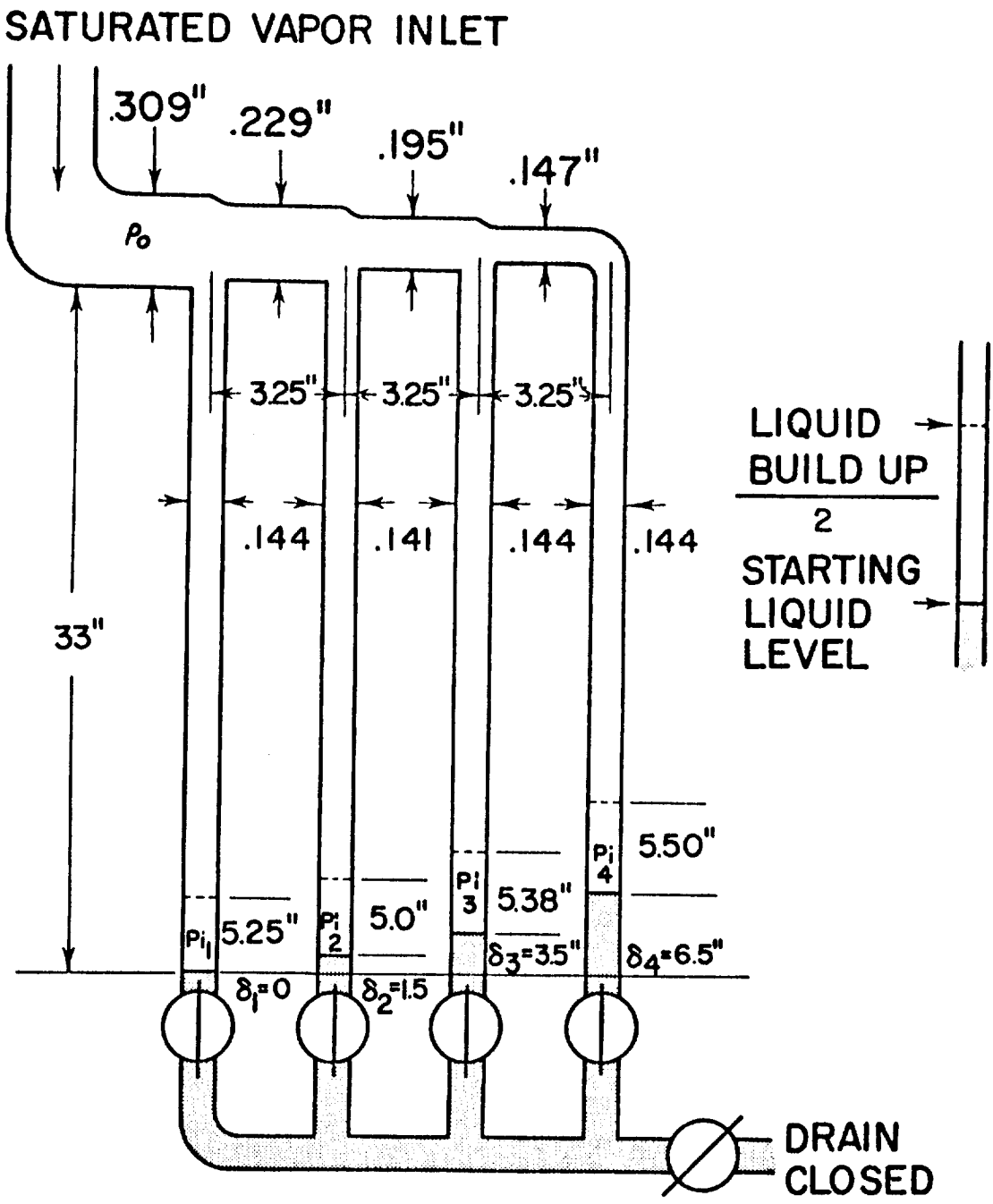

Figure 49. - Tapered manifold. Valves open.

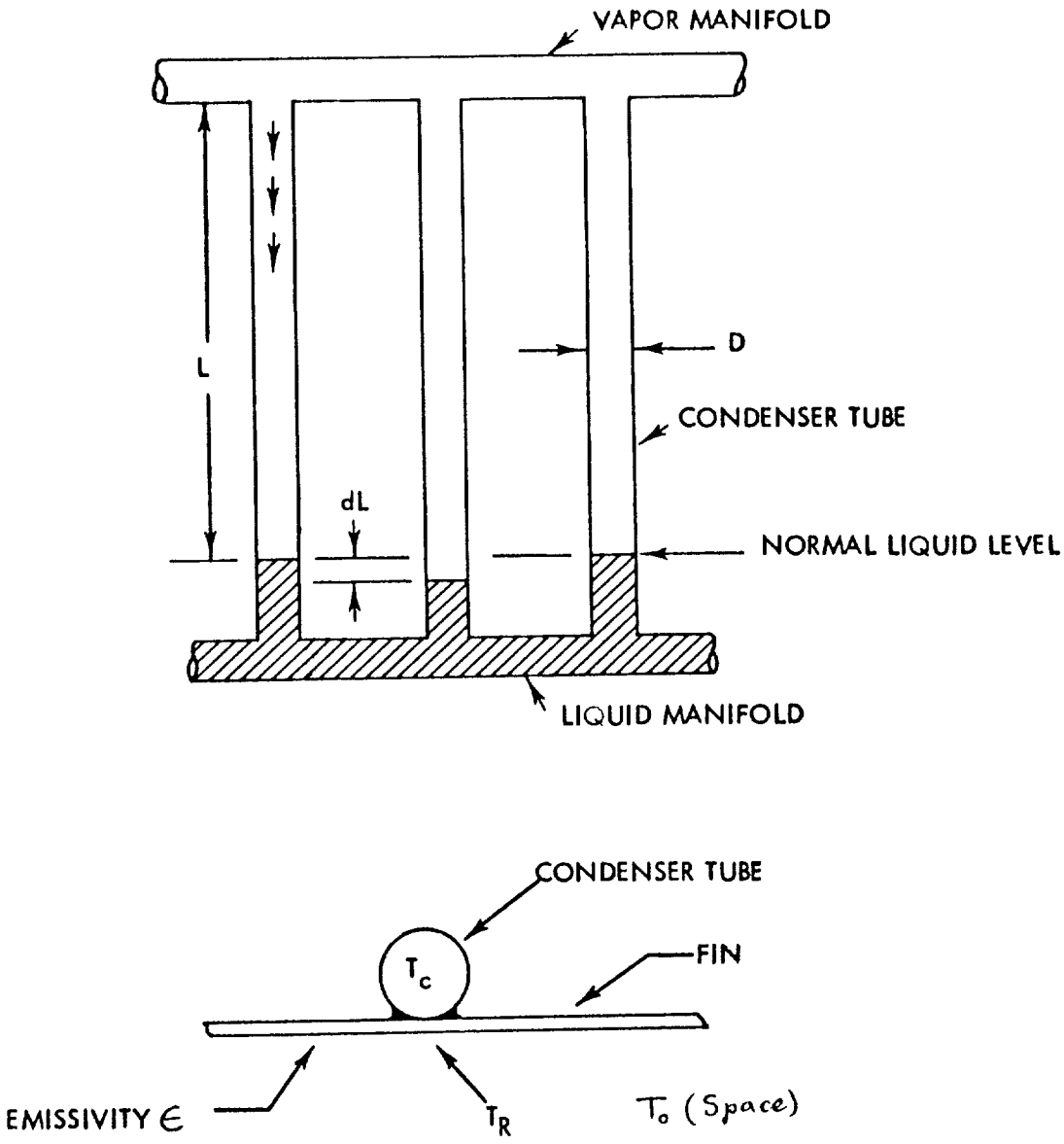

Figure 50. - Radiator schematic for stability analysis.

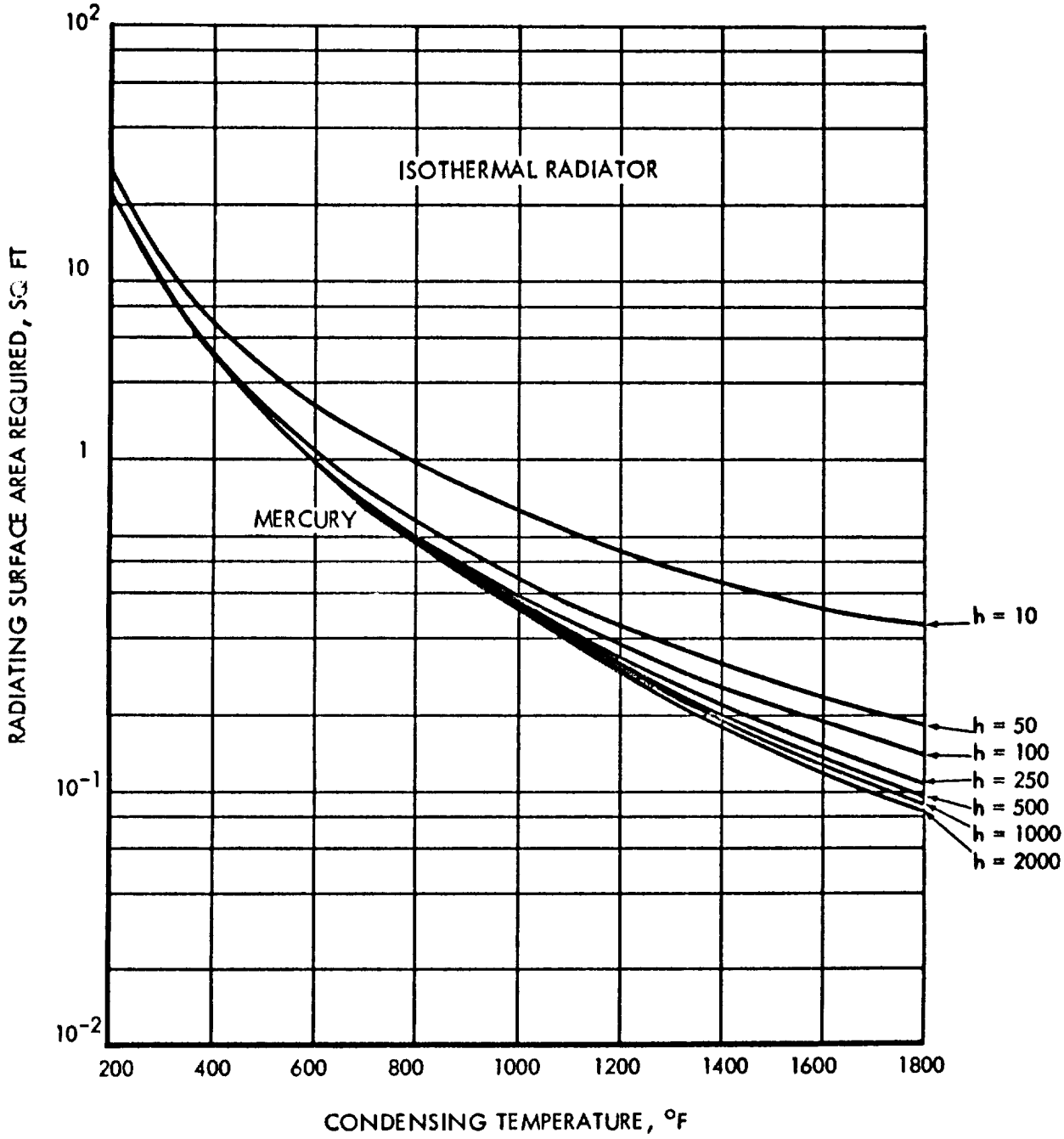

Figure 51. - Radiating area required to reject 1 kilowatt.

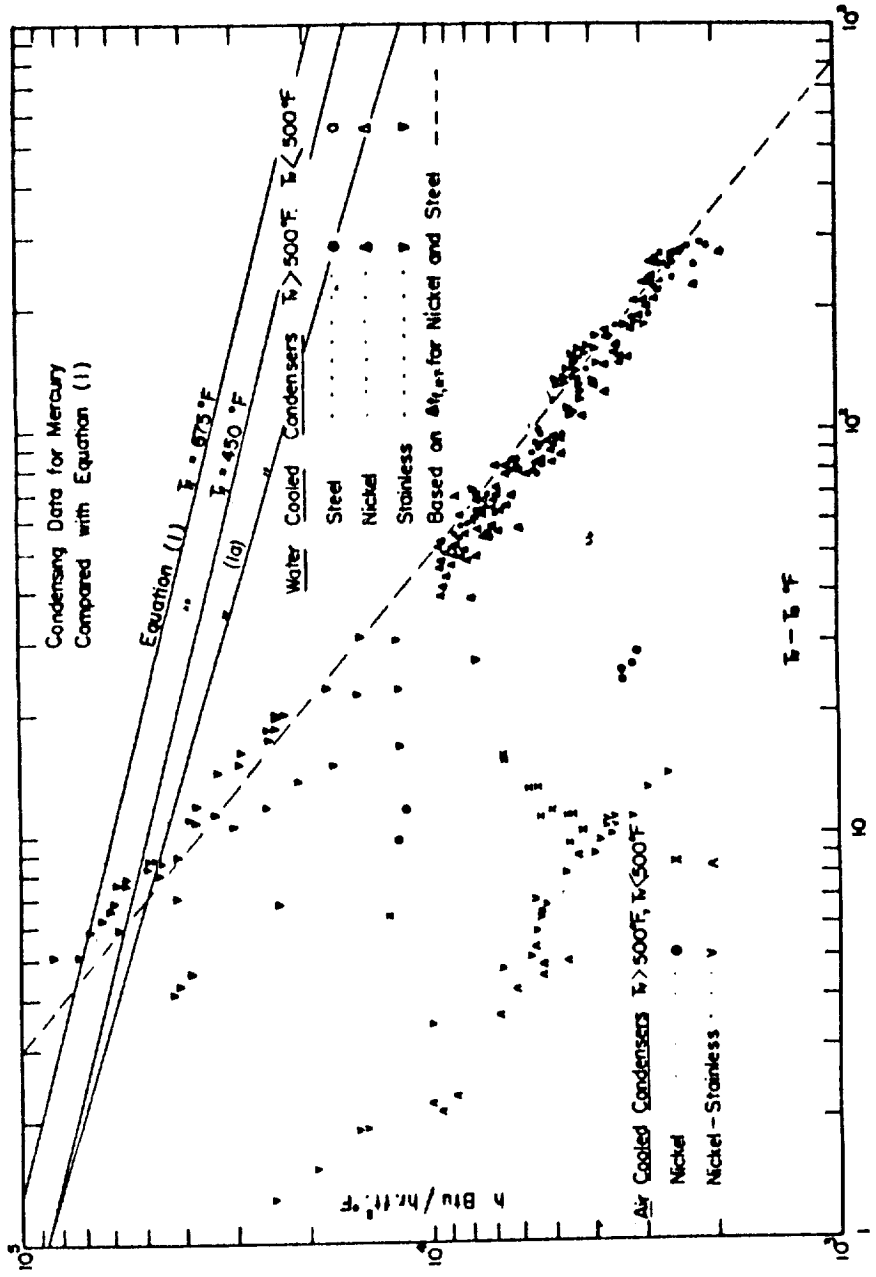

Figure 52. - Experimental mercury condensing coefficient compared with equation (1).

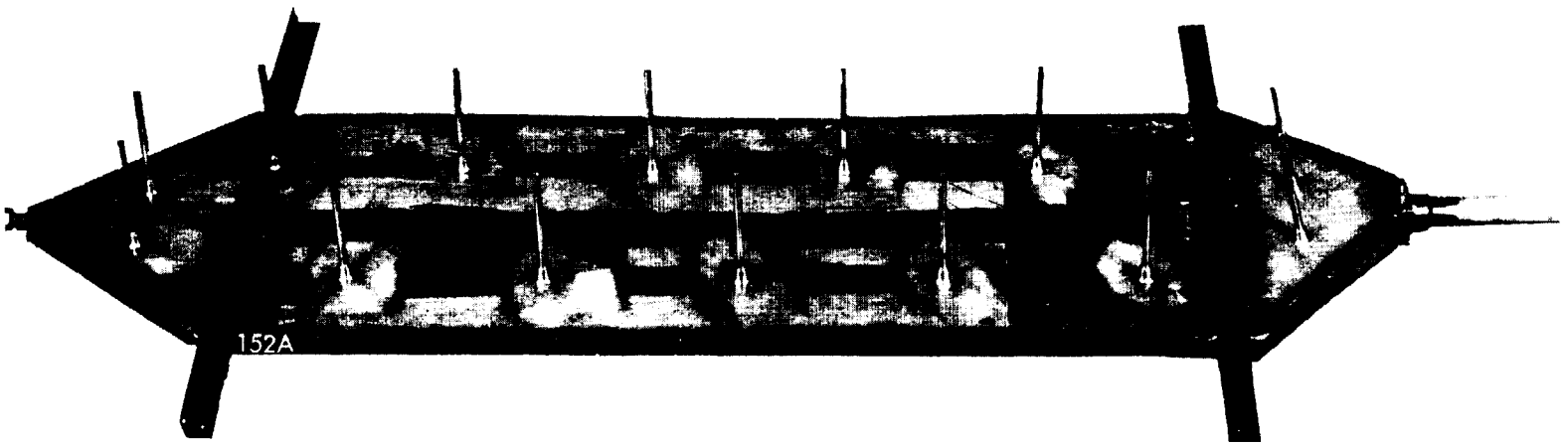

C-58232

Figure 53. - Flat plate mercury condenser.

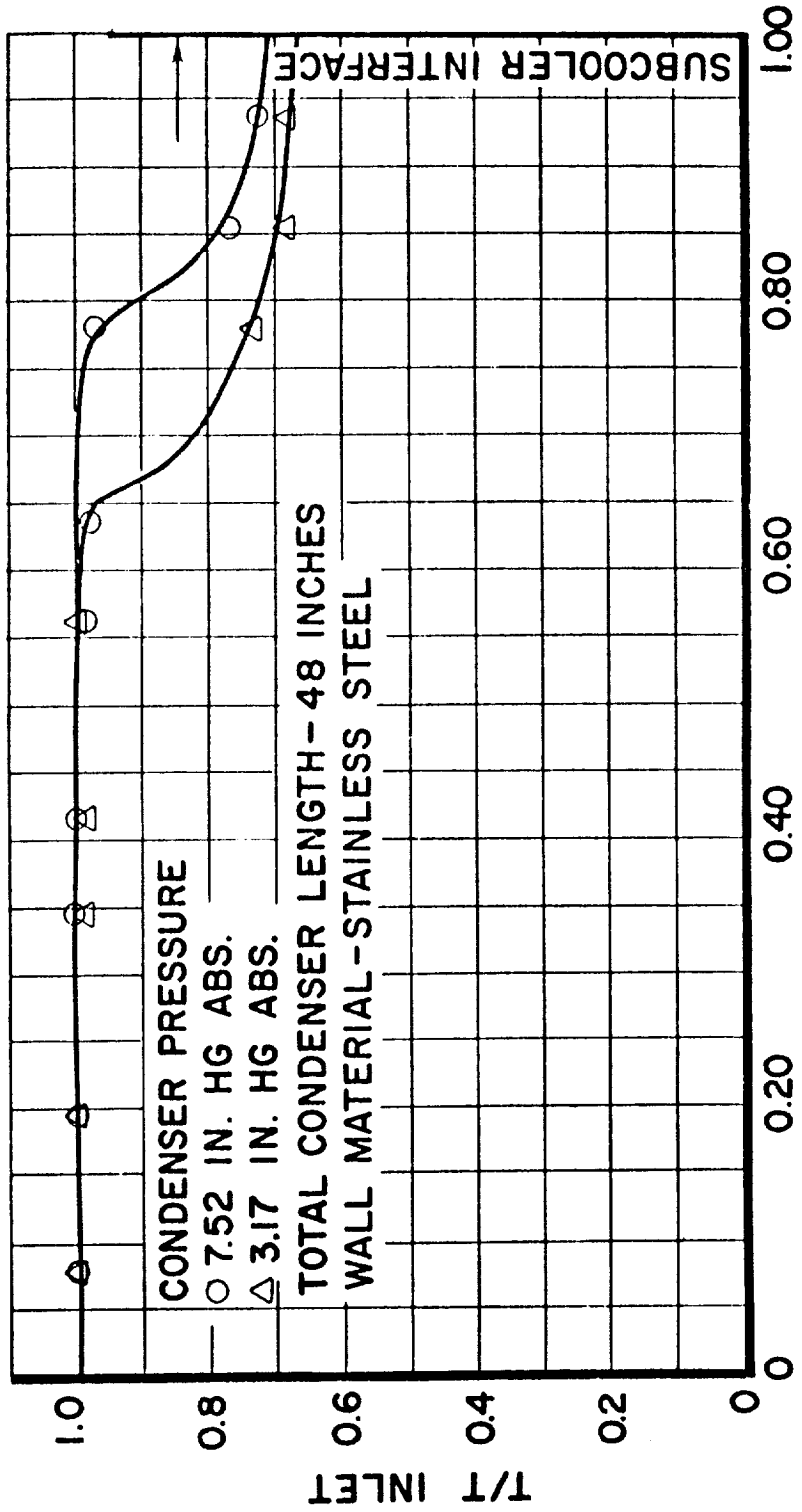

Figure 54. - Effect of noncondensable gas on condenser wall temperature. T/T, inlet ratio of absolute temperatures.

E-1501

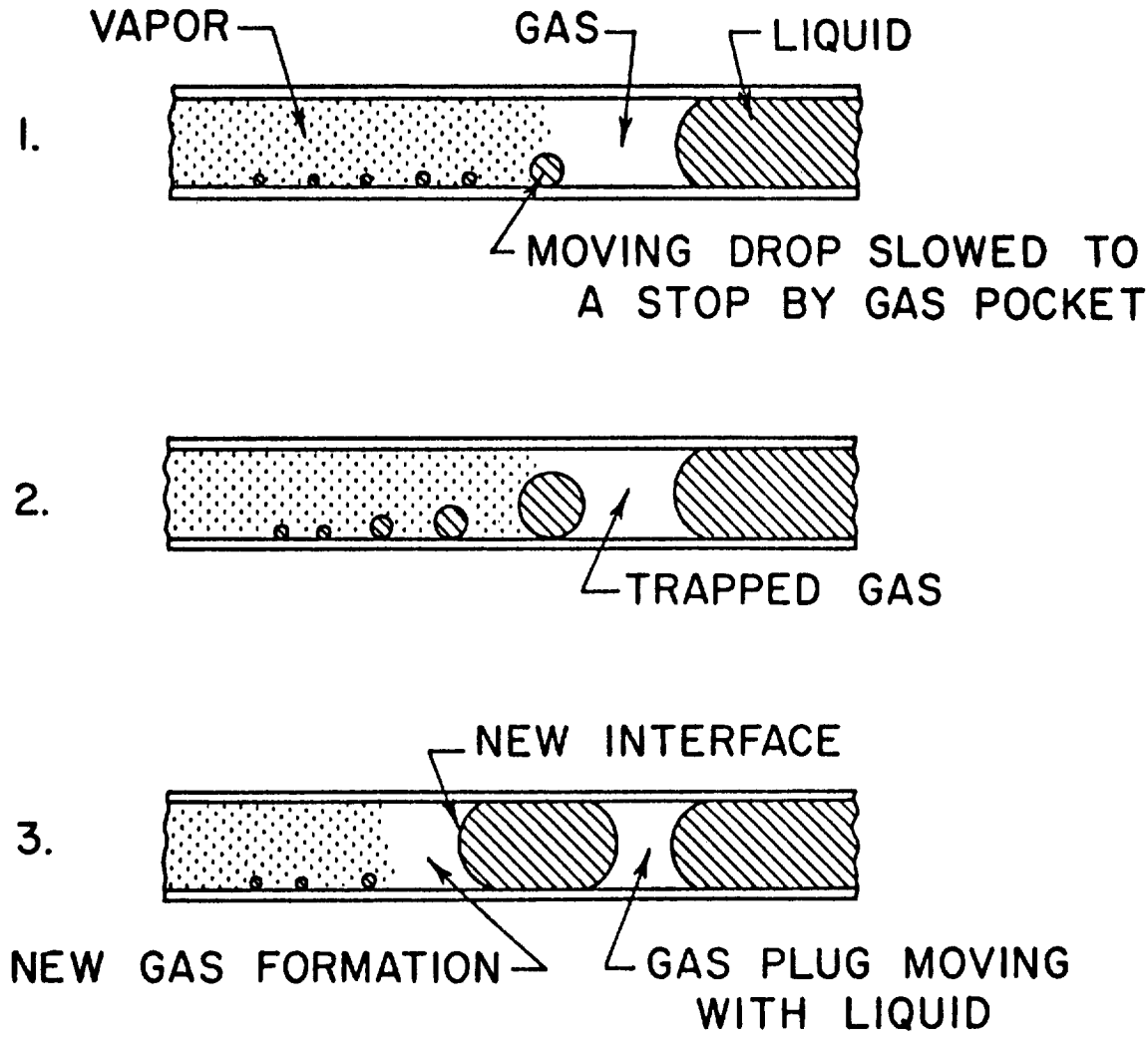

Figure 55. - Sequence of the formation and transport of a gas plug.

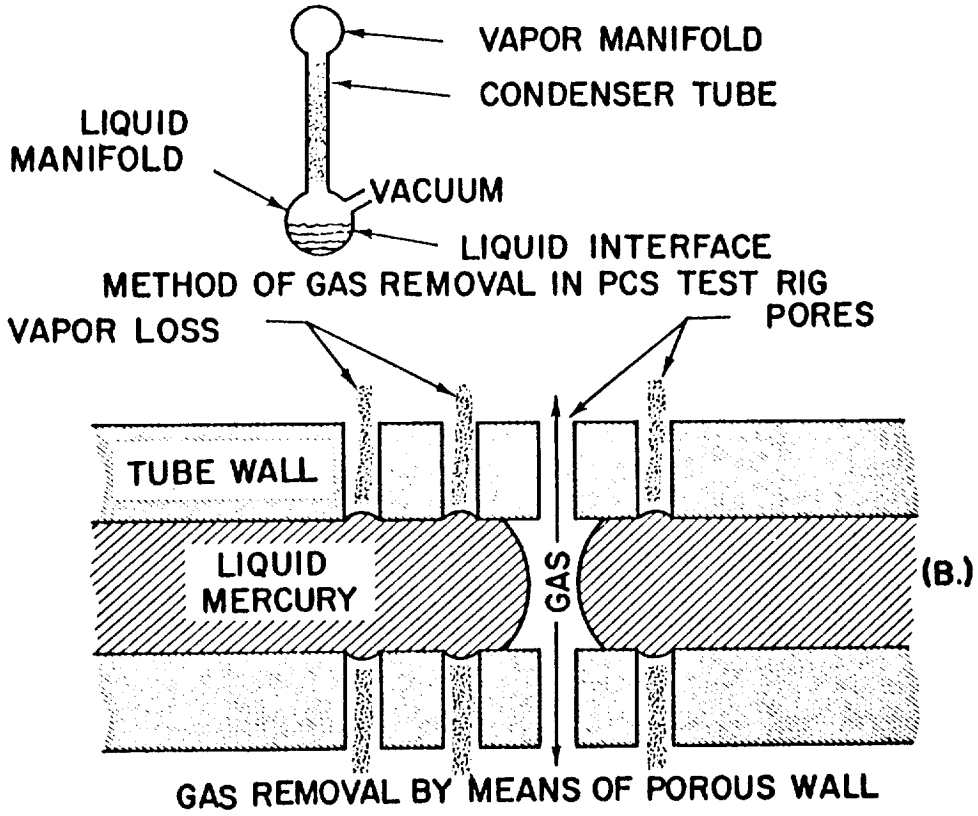

Figure 56. - Noncondensable gas removal methods.

ATOMICS INTERNATIONAL DIVISION

NORTH AMERICAN AVIATION, INC.

PRESSURE DROP IN TWO-PHASE FLOW

Presented by C. Baroczy and J. Sells

Interest in condensing mercury at Atomics International is centered around the SNAP 2 power system. Early work in condensing mercury research for the SNAP 2 program was conducted by Thompson Ramo Wooldridge. The work at Atomics International has been an extension of this effort along two major lines. The first is an attempt to determine a better method of correlation of the pressure drop data. The second activity that is currently being undertaken is to obtain additional condensing pressure drop data of greater accuracy. (As indicated earlier, difficulty had been experienced in making accurate pressure drop measurements.) These test data will be obtained in a radiator-condenser test loop that has been designed mainly for acceptance and performance testing of radiators. However, it will be a good facility for making pressure drop measurements.

The results of the attempt to obtain an improved pressure drop correlation are contained in a report (ref. 1), which has just recently been published as an AEC research and development report entitled "Pressure Drop for Flowing Vapors Condensing in a Straight Horizontal Tube." The work is an outgrowth of the two-phase two-component pressure drop data obtained by TRW for liquid mercury and nitrogen. This improved correlation came about from the use of the well-known Lockhart-Martinelli two-phase two-component correlation. In this correlation, the ratio of the two-phase pressure drop to the gas-phase pressure drop is made a function of X, which is the Martinelli two-phase flow modulus. Figure 1 illustrates the data variations and the correlation for the viscous-liquid - turbulent-gas flow regime.

Originally, the liquid mercury - nitrogen two-phase two-component data (fig. 1) were correlated by this method, and it was found that about 77 percent of the points fell below the Martinelli line. Close inspection of the data revealed that there was a definite trend with gas Reynolds number (fig. 2). The high gas Reynolds number data tended to form a line similar to the Lockhart-Martinelli curve but well above it, and very low Reynolds numbers data fell well below it. On this basis, a striking improvement was made possible in the correlation of the experimental data. The order of this improvement can be seen in figure 3. Now, 80 percent of the points fall into the band of ±10 percent within prediction compared with about 20 percent for the original Martinelli correlation.

It was also reasoned that if the turbulent gas Reynolds number gave a definite correlation, the same condition should hold for constant liquid Reynolds number lines. If so, this would indicate that the data are consistent. In this respect, it was found that a constant liquid Reynolds number line produced a variation with increasing Reynolds number, as indicated in figure 2. This trend is similar to that obtained by other investigators. One of the reasons given to support the argument that the Martinelli correlation does not fully describe the true two-phase two-component condition is that constant liquid lines give curves that cross the Martinelli curve or are quite flat at low values of X. In the higher X regions, the data generally follow the Martinelli curve. The current constant liquid mercury Reynolds number data gave a similar shape except that they started high, reached a minimum, and then increased. In general, however, the data revealed liquid lines similar in shape to what has been observed by Gazley and Bergelin (ref. 2).

On the basis of these results it is proposed that the Martinelli-type correlation be modified to include the turbulent gas Reynolds number as an additional parameter. The gas Reynolds number parameter explains some of the previous deviations from the original Lockhart-Martinelli correlation. It appears now that the Lockhart-Martinelli line is an average line through a wide range of points. The introduction of the gas Reynolds number produces a grid that is formed about the Martinelli line. The grid is in the low X regions and becomes narrower at the high values. In the high X regions, for example, greater than 10 or so, the band becomes quite narrow and the Martinelli line will fit the wide range of Reynolds numbers very well. In the lower regions of X below about 0.2, the data spread can be considerable. Preliminary correlation of the available Lockhart-Martinelli data using air and water, air and oil, and some other fluids confirmed the gas Reynolds number effect. A similar correlation was obtained except that the lines appeared to be somewhat lower for liquids other than mercury.

On this basis, the same procedure used by Martinelli-Nelson in computing boiling pressure drop was applied to determine condensing pressure drop. In this process, the two-phase two-component relations are used in a step-by-step process that takes into account the liquid and gas weight flows at each point to compute the two-phase pressure drop. Integration of the two-phase pressure drop and correction for momentum then yields the overall pressure drop. Considering the varying liquid to gas weight flow throughout the tube made it possible locally to predict the process to some extent. This correlation does not purport to show a complete understanding of the process. It does represent an improvement, however, in making available for design purposes a method that will more closely approach actual conditions than has been possible heretofore.

The method was checked against some limited data obtained by the Rocketdyne Division of North American Aviation. These tests consisted of condensing steam in a steel tube with condensing length varying from 6 to 13 feet and with six to eight pressure taps along the length of the tube. From this experiment, it was possible to plot the pressure drop gradient along the tube. Using the procedure previously described and assuming saturated vapor entering yielded a calculated pressure drop gradient that was reasonably close to the experimental data. The calculated magnitude was about 15 percent high, however. Assuming 90 percent vapor quality entering the tube (there was no way to measure the inlet quality, so that it was entirely possible that other than saturated vapor was entering the test section) resulted in calculations that gave a close approximation of the actual measured pressure drop gradient. On this basis it is felt that the improved correlation and attendant condensing pressure drop calculation method offer some hope for improved checks between experimental and calculated results. It is expected that this will aid in a more accurate design for the SNAP 2 condenser.

REFERENCES

1. Baroczy, C. J. and Sanders, V. D.: Pressure Drop for Flowing Vapors Condensing in a Straight Horizontal Tube. Atomics International Report NAA-SR-6333, June 1961.[1]

2. Gazley, C. and Bergelin, O. P.: A Preliminary Investigation of Two-Phase Flow. University of Delaware Report No. TPF-1, May 1947.

---

[1]Abstract of report: This report presents a method for calculating condensing static-pressure drop of a saturated vapor flowing in a straight round tube on which there is a prescribed heat flux. The method postulates that this system is equivalent to a quasi-static two-phase two-component fluid flow system in which no condensation takes place. The effect of condensation is accounted for by a variable liquid- to vapor-flow weight ratio, which is a function of the condensation rate. The method utilizes an improved Lockhart-Martinelli type of two-phase two-component pressure drop correlation that was devised especially for it and is proposed for general use. The pressure drop is obtained by a point-by-point calculation and numerical integration over the range of condensation.

The results of the method are compared with measured pressure drops for condensing steam and the agreement is favorable. Some numerical examples are given.

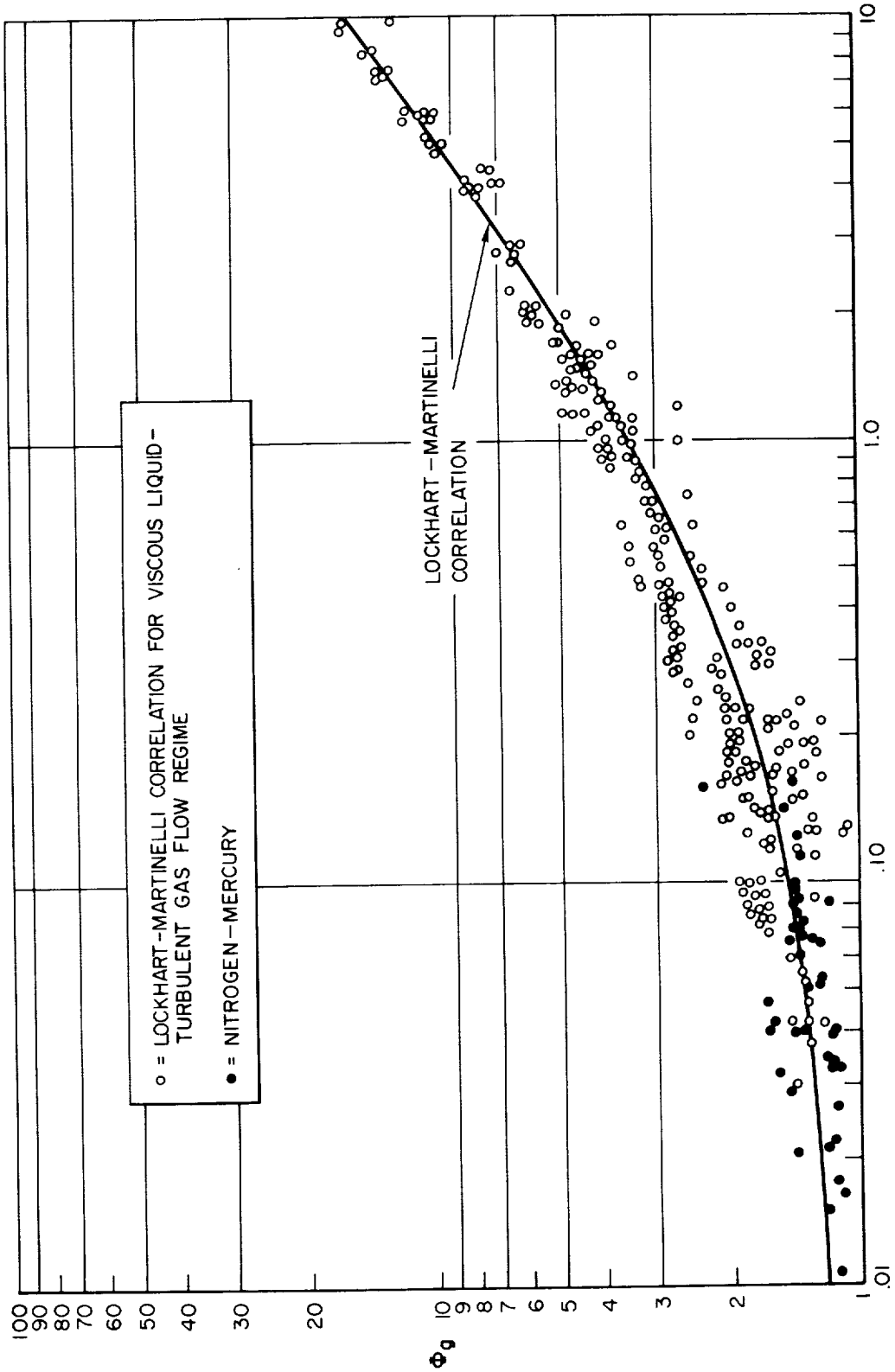

Figure 1. - Lockhart-Martinelli correlation for two-phase two-component pressure drop.

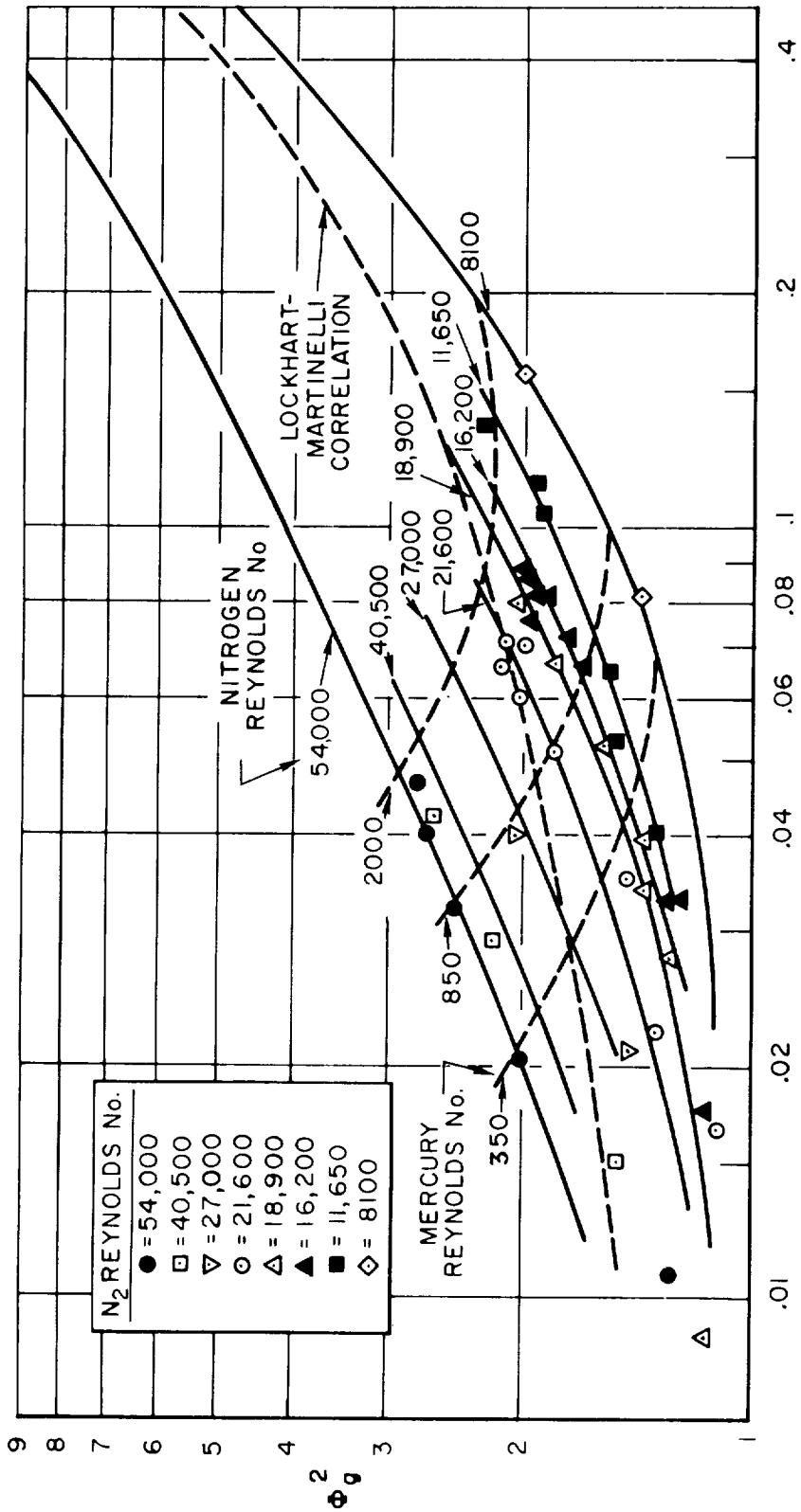

Figure 2. - Correlation of pressure-drop data for liquid mercury and nitrogen (viscous mercury, turbulent nitrogen).

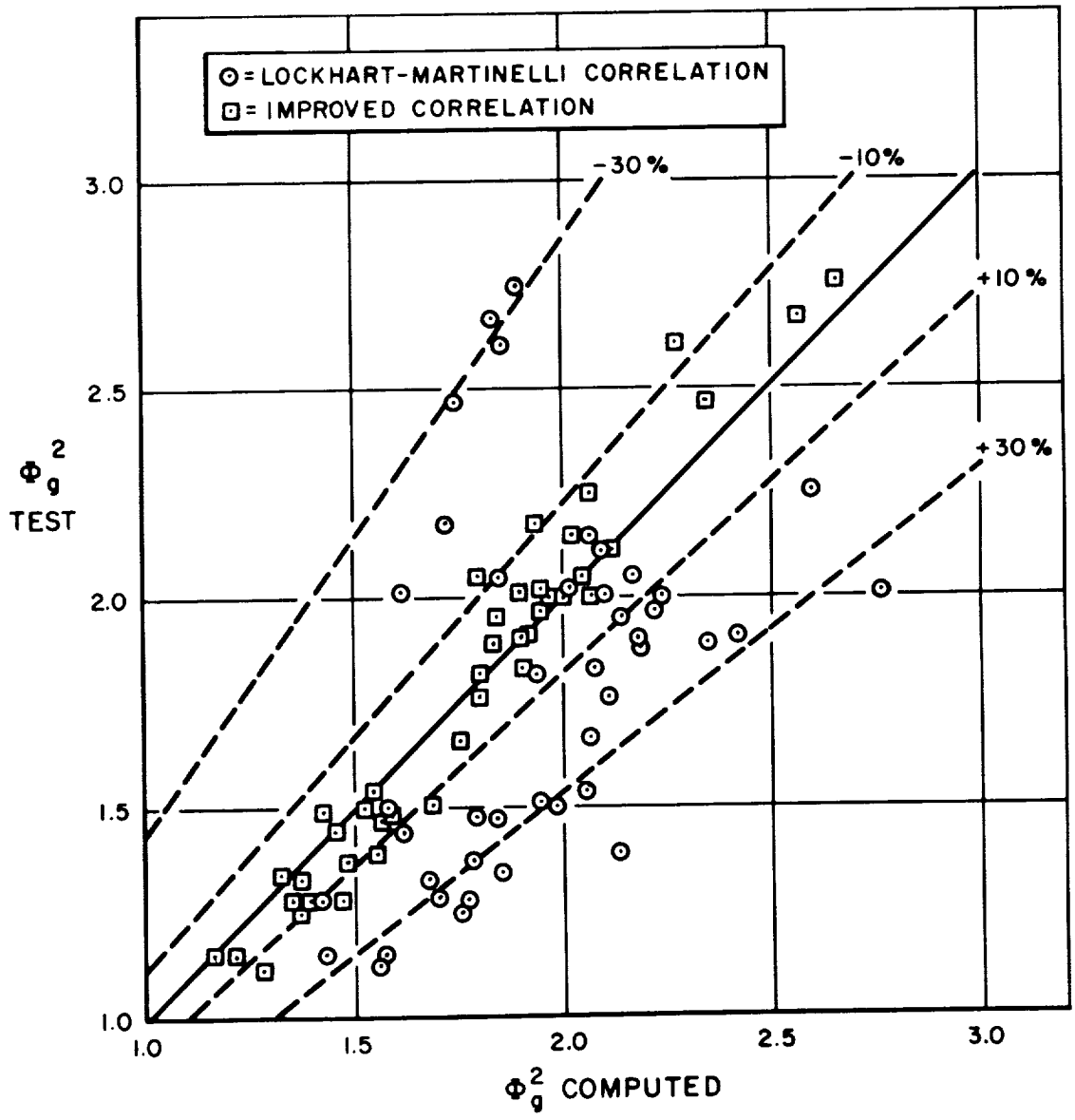

Figure 3. - Comparison of experimental data (viscous mercury, turbulent nitrogen) with Lockhart-Martinelli and improved correlation.

AEROJET-GENERAL NUCLEONICS

SNAP-8 RADIATOR DEVELOPMENT

Presented by J. R. Payne

E-1501

INTRODUCTION AND DESIGN REVIEW

The SNAP-8 system is at least one order of magnitude larger than the other two mercury Rankine cycle plants being developed today. This larger size creates some radiator design problems that require a different approach from that being used on SNAP-2 or Sunflower. For example, the physical size requires consideration of a folding radiator and the use of massive aluminum armor and fins. Also, the physical size requires that consideration be given to the mercury inventory. Figure 1 is presented to illustrate the typical operating parameters for a SNAP-8 radiator.

Considering the design parameters for SNAP-8, it is Aerojet's opinion that there are five main problem areas that require significant engineering effort:

(1) Micrometeorites

(2) Mechanical design

(3) Liquid-vapor interface stability

(4) Pressure drop

(5) Mercury inventory

By mutual agreement between NASA and Aerojet, the following ground rules are being used to analyze the micrometeorite problem:

(1) Whipple's mass distribution

(2) 90 percent probability of no puncture in 10,000 hours

(3) Bjork's penetration model

(4) Massive aluminum armor

Aerojet is not conducting any experimental work on micrometeorites, but currently is relying on other programs to provide meteorite population

and penetration information. The micrometeorite hazards and the fluid flow phenomena are, to a large extent, separate problems. A development program has been initiated to solve the remaining four problems listed above. The program is mainly devoted to experimental investigations of fluid flow stability and pressure drop but, where possible, analytical work on these topics is also being done.

In conducting a design analysis of the mercury condenser, Aerojet has found that the direct condensing radiator provided adequate performance for the SNAP-8 system. Figure 2 presents a transverse cross section of one radiator tube and fin assembly. Note that a modified Whipple bumper concept is also presented. There is some experimental evidence that this meteorite protection technique can be applied to the SNAP-8 radiator.

EXPERIMENTAL PROGRAM

Aerojet has proposed using twisted tape in the SNAP-8 condenser tubes on the basis that vortex flow will alter the flow stability and provide better inventory control. Also, at an axial velocity of 40 feet per second, a radial acceleration of approximately 60 g's will be obtained. It should be possible then to test one radiator tube in a horizontal configuration so that gravity would be normal to the flow and not significantly affect the flow behavior. With this arrangement, operation in a 1-g field would be similar to zero-gravity operation. Based on this premise, Aerojet has designed a condenser apparatus (shown schematically in fig. 3) that consists of a pot boiler, a full sized test section, and a weighing apparatus. In addition, the test section is instrumented with open mercury manometers for measuring static pressure and thermocouples. A photograph of the test apparatus is shown in figure 4.

Numerous tests have been performed with Pyrex tubes approximately 10 feet long having inside diameters of 0.375 and 0.500 inch. These tubes were tested without any inserts and/or with stainless steel tapes 10 mils thick twisted to a y value[2] of 5. Also, various subcooler configurations, either 4-inch lengths of capillary tubing or a special annular type flow passage, were tested. The purpose of the subcooler inserts is to "stiffen" the flow in much the same fashion as an orifice in a manometer prevents bouncing. A photograph of the test devices is shown in figure 5.

This test program has been under way for nearly 6 months and four significant discoveries have been made: (1) pressure drop data as shown in figure 6, (2) the importance of surface tension, (3) effect of drop size on flow behavior as demonstrated in the high-speed film, and (4) a method for obtaining interface stability, but with unsatisfactory inventory.

---

[2]The y value is the number of 180° turns per tube diameter.

Recalling the movie concerning the condensing mercury flow in a 1/2-inch tube, it was observed that mercury drops had to approach a certain critical size before the vapor drag could propel the droplets toward the subcooler. The film also showed a droplet of approximately 0.050 inch that traveled some 4 inches while hanging upside down on the tube wall. Unfortunately, films on the performance of a tube without twisted tape, as compared to a tube with twisted tape, were of such poor quality that they could not be presented. Visual observations of these tests reveal that, in the 1-g environment, the liquid flow in a plain tube is very unstable with violent pulsations produced by gravity waves in the subcooler. In the tests with the twisted tape and the annular flow subcooler, interface stability was obtained in the sense that mercury vapor did not pass through the subcooler. However, an unsatisfactory inventory situation was produced because the condensed mercury did not have enough momentum to be elevated over the lobes of the twisted tape and small flow pulsations occurred. Most of the testing was at flow rates of 40 to 80 pounds per hour as compared to the design flow rate of 125 pounds per hour. It appears that such a flow increase would result in sufficient droplet momentum to eliminate most of the pulsations mentioned above. Unfortunately, the glass test section is heat-transfer limited and higher flows cannot be achieved.

A stainless steel condenser tube with two copper fins and a glass subcooling section has been fabricated. This unit will have more pressure taps and will thus make it possible to obtain better measurements of $\Delta P/\Delta X$ as a function of quality. Also, a phase separator has been inserted between the boiler and the test section to eliminate the uncertainty of the incoming vapor quality. Testing of the glass units and the stainless steel units will continue until better pressure drop data have been obtained and a satisfactory subcooler configuration has been selected. A multiple tube test is now in the initial design stages. The special requirement that the SNAP-8 radiator shall fold required that a flexible vapor manifold be designed. It appears that a mechanical design capable of such deflection greatly influences the multiple tube operation problem.

A small-scale zero-g interface stability test has been conducted. This test consists of a short length of Pyrex tubing of 0.500-inch diameter which is oriented vertically and contains a mercury inventory. Positioned above the mercury meniscus is a spring-loaded hypodermic syringe. The test apparatus is positioned in a drop capsule along with a movie camera and suitable lighting. This capsule is shown in figure 7. Nine drop tests were performed in the Stanford University drop tower and residual accelerations of 10^{-4} g were experienced. In none of these tests did the interface appear to be unstable when the mercury droplets were impacting against the meniscus. This is considered to be sufficient evidence that the liquid-vapor interface would be stable in the SNAP-8 environment from this particular flow phenomenon. Figure 8 shows a comparison of the interface at 1 g (fig. 8(a)) and zero g (fig. 8(b)).

ANALYTICAL PROGRAM

The analytical program for radiator design has been principally concerned with radiator optimization, pressure drop calculation, and formulating a hydrodynamic model to predict inventory in flow stability. Recently the latter has been emphasized, since the testing program has provided enough information with which to construct a flow model. The SNAP-8 radiator was optimized insofar as configuration by the procedure of Callinan and Berggren (ref. 1) based upon the following inputs:

(1) Armor surface temperature equal to condensing temperature

(2) Rectangular aluminum fins

(3) Surface emissivity of 0.8

Some of the results of this optimization are shown in figure 1. A final, refined design will be made which will shape the armor, employ tapered fins, and possibly increase the emissivity. Most of the analytical work has been concerned with reducing and correlating the pressure drop data obtained in the condenser test apparatus. Several methods for correlating pressure drop have been tried, Martinelli-Lockhart's, Isbin's, and Kutateladze's. This latter correlation has the advantage of presenting the two-phase pressure drop as simply a correction factor to the single-phase pressure drop. This has the obvious advantage of being easier to work with when doing optimization studies. Figure 5 presents the test data and the analytical curves for two-phase pressure drop. There is a fair spread in the data which apparently can be partially reconciled by the uncertainty in the entering quality. Aerojet believes that this problem of quality input to the test setup must be corrected before reliable pressure drop data can be obtained.

FUTURE WORK

Bench testing with the metal condenser tube will continue for several months until an adequate pressure drop correlation is obtained. In this same test rig, various subcooler configurations will be evaluated for interface stability. Simultaneously, a parallel flow experiment will be constructed to evaluate the multiple tube stability problem. Operation of this test will depend upon the selection of an adequate subcooler configuration and a realistic vapor manifold design.

In conjunction with the experimental work, an analytical model to describe the flow behavior and interface stability is being formulated. Presently, the pressure drop and inventory portion is nearing completion. To support the interface stability analysis the drop tests are to be rerun with a faster camera and larger disturbing forces.

A final radiator optimization will be made and will include armor shaping, tapered fins, and realistic emissivity values. The latter are to be supplied from the Pratt & Whitney emissivity measuring program.

To substantiate and confirm the SNAP-8 design, a few tube condensing experiments should be performed in a zero-gravity environment.

REFERENCE

1. Callinan, Joseph P., and Berggren, Williard P.: Some Radiator Design Criteria for Space Vehicles. Preprint 59-AV-29, ASME.

FLOW RATE	7,200	lb/hr
INLET TEMPERATURE	700	°F
INLET QUALITY	90	%
INLET PRESSURE	20	psid
EXIT TEMPERATURE	550	°F
PRESSURE DROP	5	psi
TUBE ID	0.5	in.
TUBE LENGTH	368	ft
HEAT REJECTED	913,400	BTU/hr
WEIGHT	570	lb
Q/W	1540	BTU/hr-lb
ARMOR THICKNESS	0.35	in.
FIN THICKNESS	0.05	in.
PRIME AREA	110	ft^2
PROJECTED AREA	248	ft^2

Figure 1. - Snap-8 radiator operating parameters at 30 KW_e.

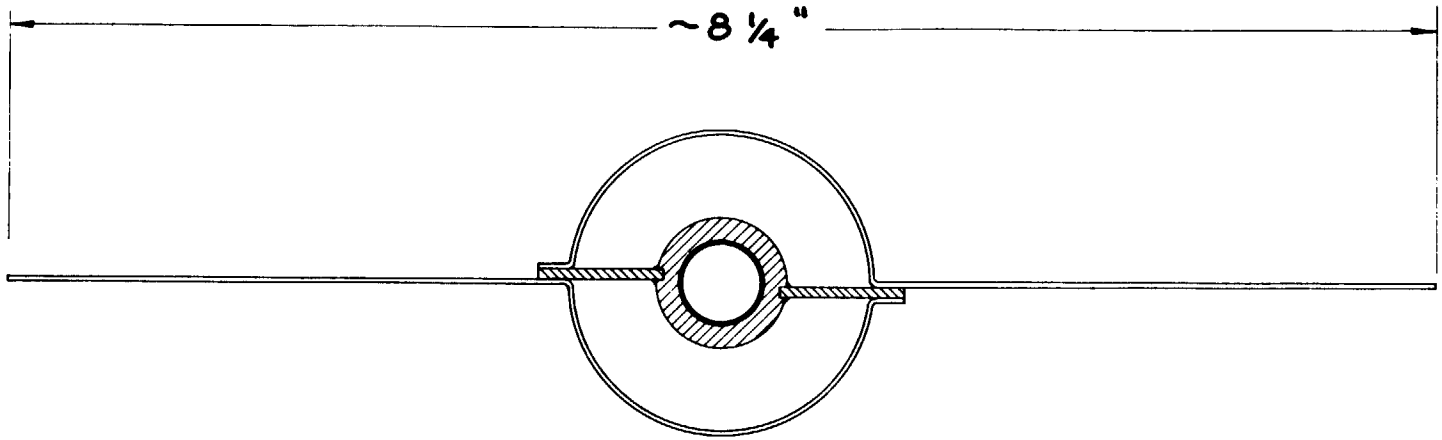

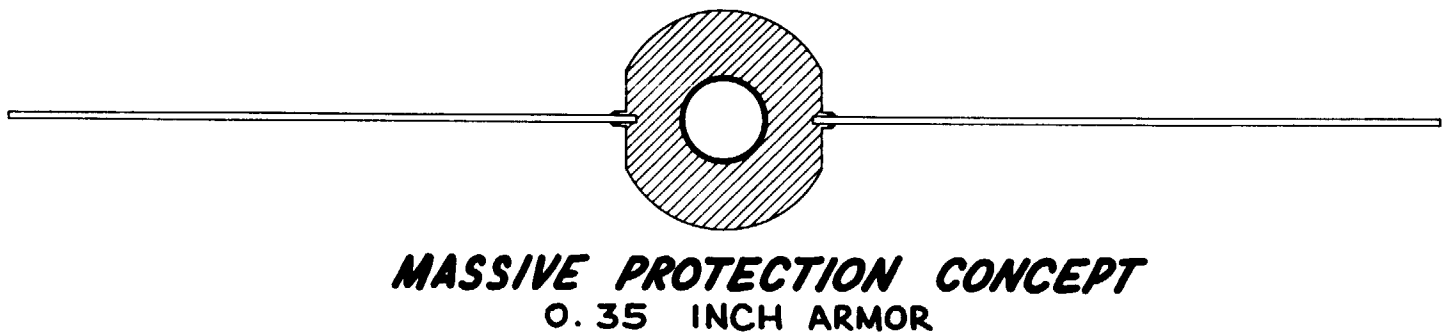

Figure 2. - Radiator tube, armor and fin cross section.

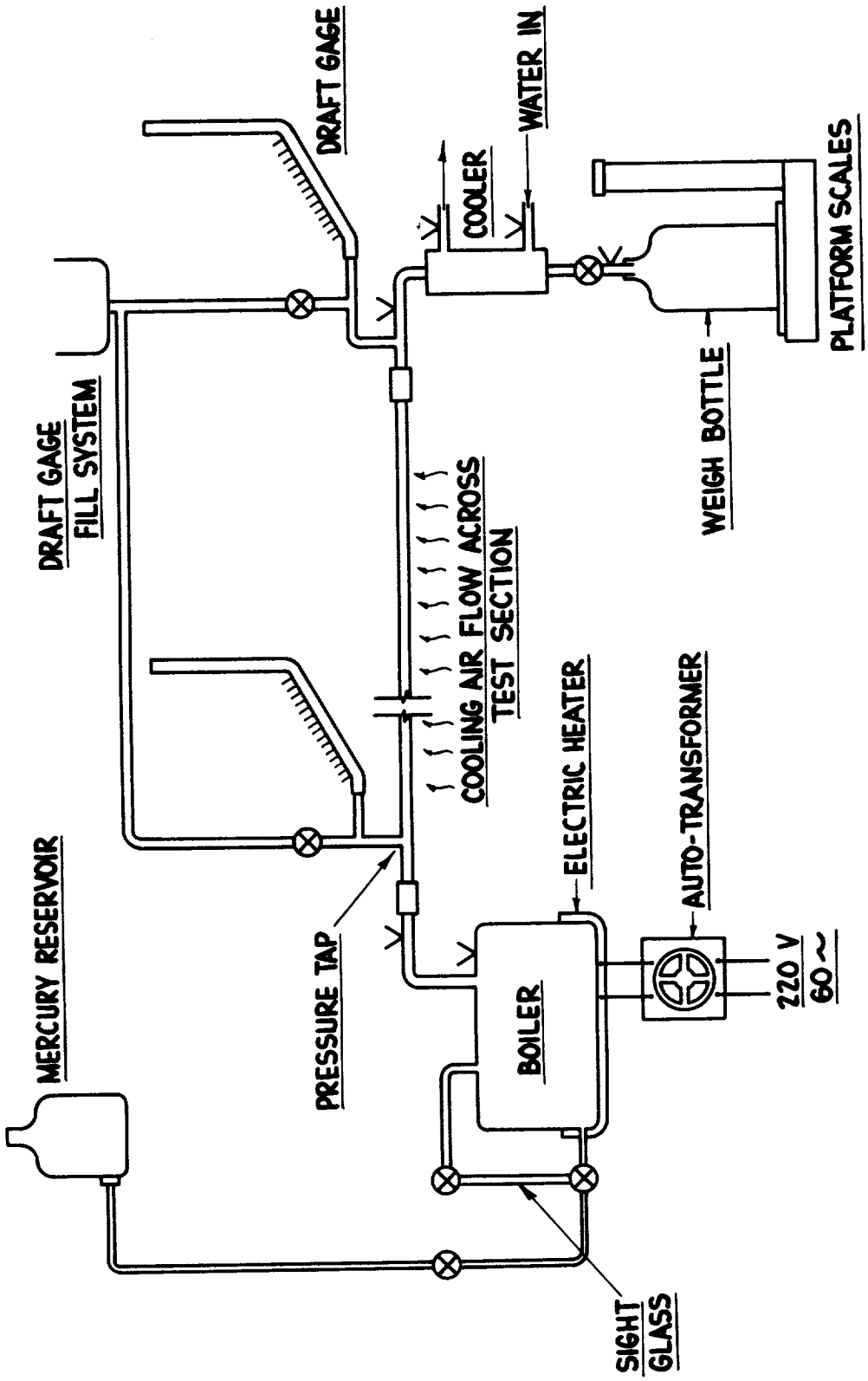

Figure 3. - Condensing flow test schematic.

E-1501

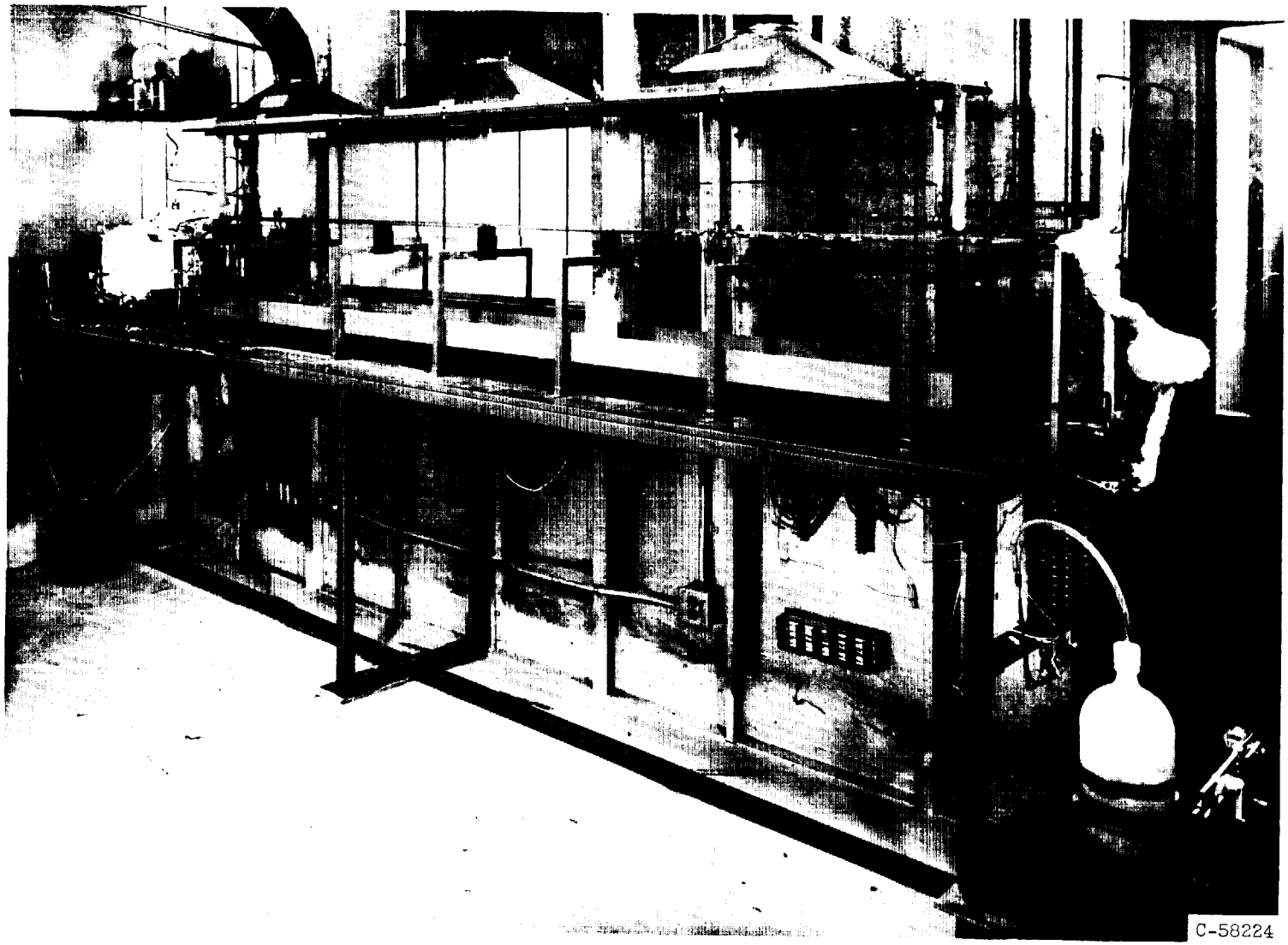

Figure 4. - Condensing flow test system.

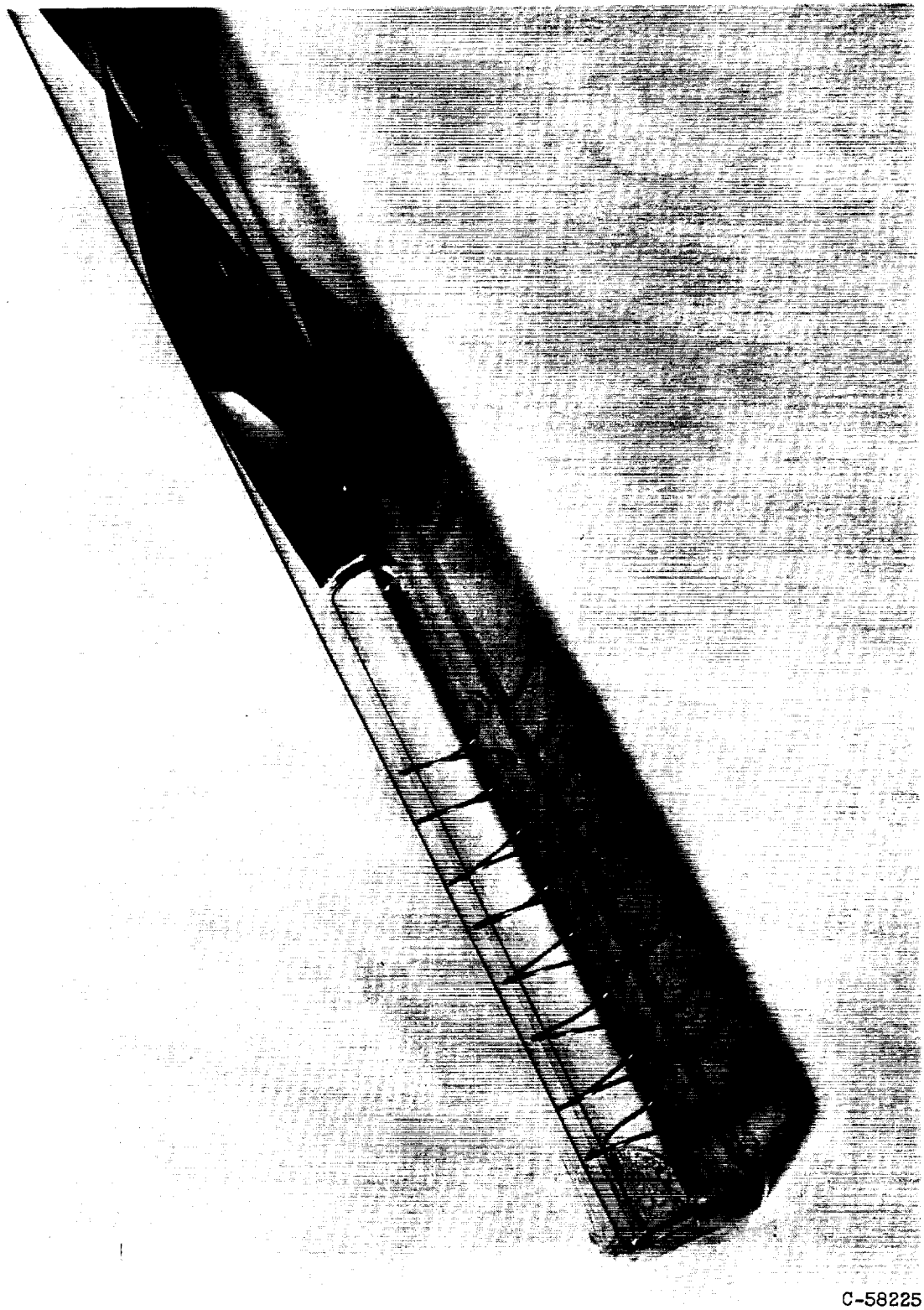

C-58225

Figure 5. - Twisted tape and subcooler assembly.

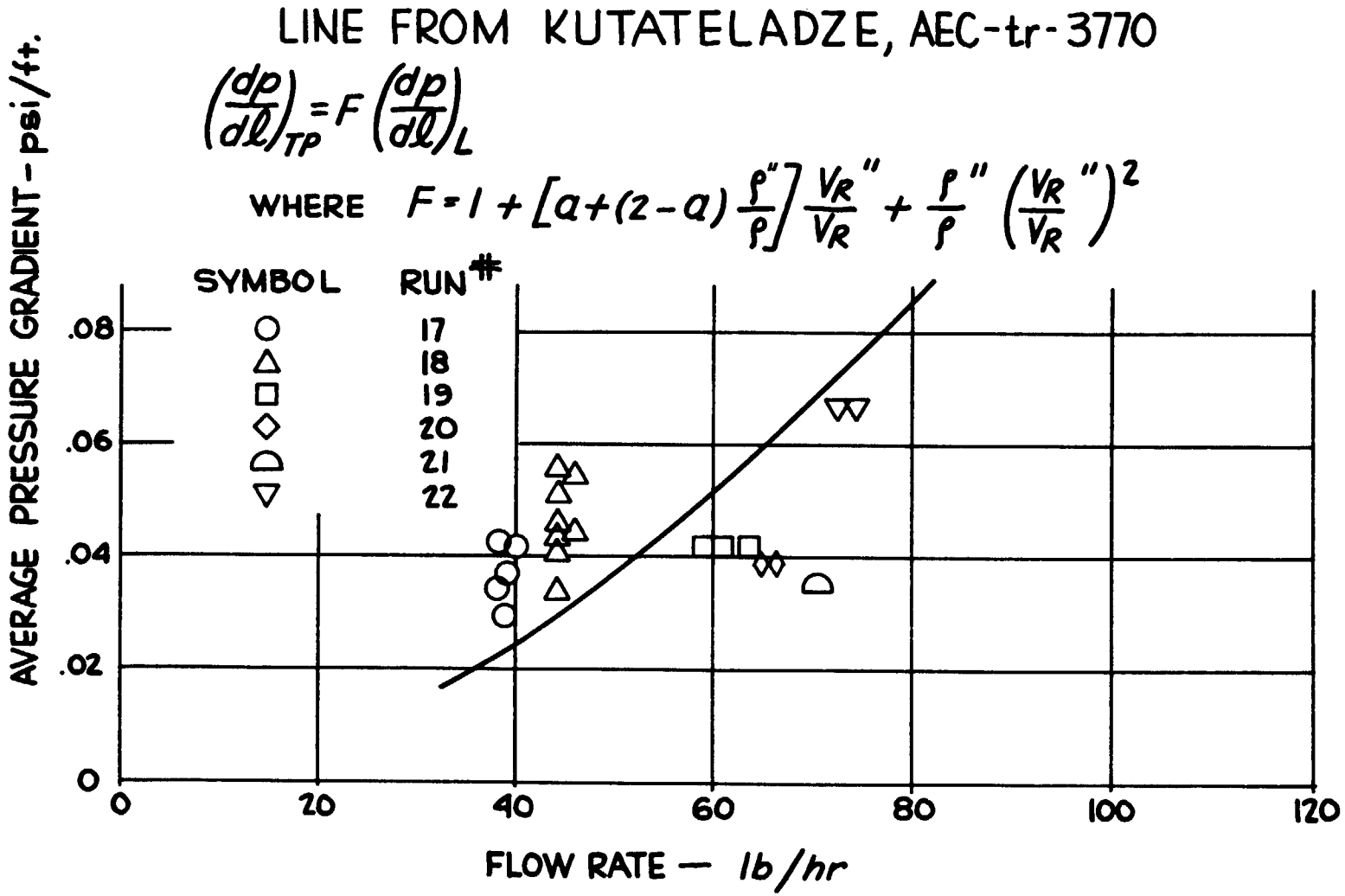

Figure 6. - Pressure drop data from test section 6.

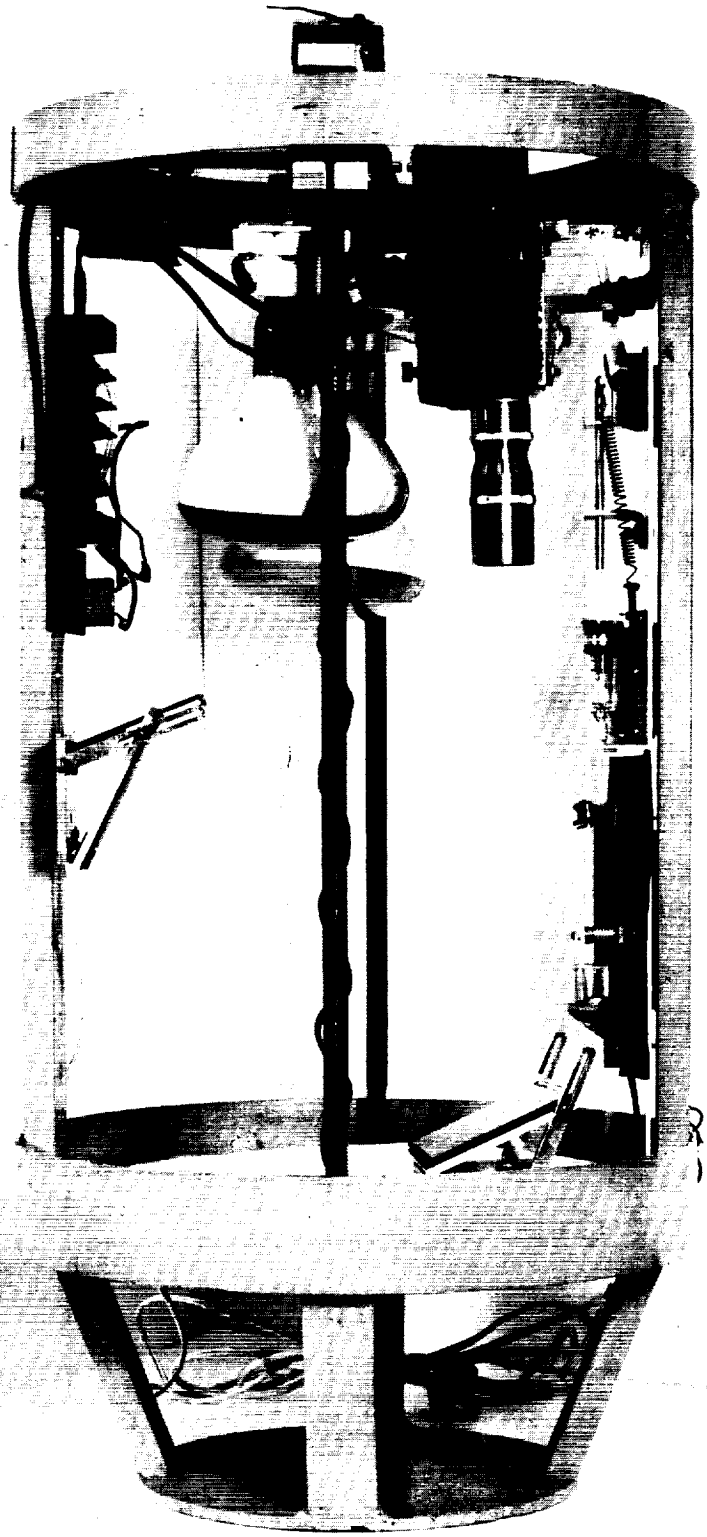

C-58226

Figure 7. - Capsule for zero-g tests.

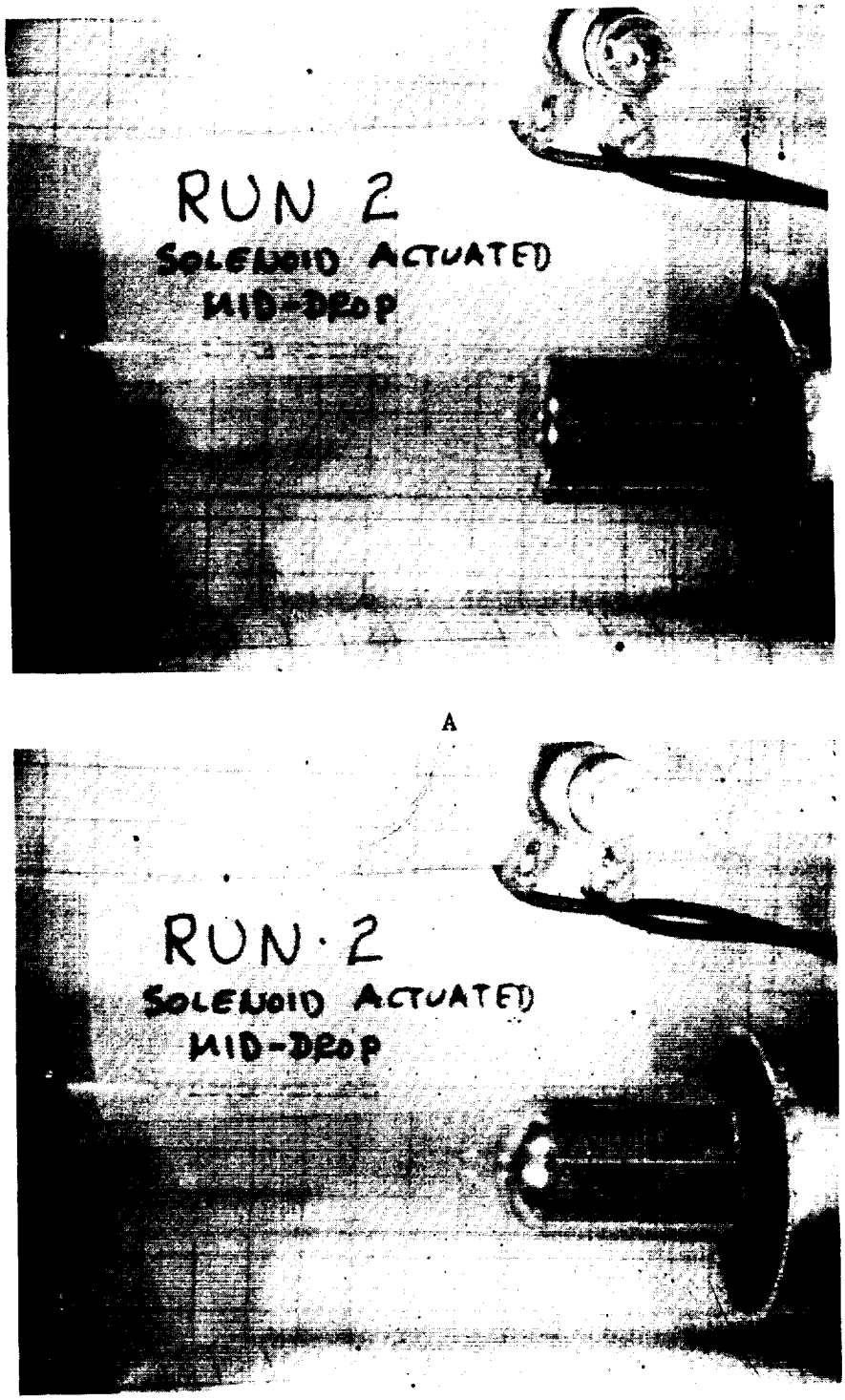

Figure 8. - Motion picture frames comparing free mercury surface in 1 g and zero g.

C-58228

Figure 9. - Half fin emissivity test sample.

ELECTRO-OPTICAL SYSTEMS, INC.

SUMMARY OF MERCURY CONDENSING WORK

Presented by J. Neustein and L. Hays

DIRECT CONDENSERS

Experimental Equipment

Before presenting a description of the test loop, some comment will be made on an earlier use of a drop tower. A completely closed Rankine cycle test loop was operated to study the effects of zero-gravity operation on direct condenser performance. However, because of the short zero-gravity time (less than 1 sec), very little useful information was obtained. As a consequence, this testing technique was discarded. Of course, useful experiments can be conducted in drop towers. Generally speaking, however, the important characteristic times of the experiment should be compared to the available zero-gravity time in order to judge the usefulness of an experiment.

The experimental test loop currently in use at EOS is shown in figure 1. In essence it is a compound loop which is used for both direct and indirect condenser investigations. The outside loop constitutes the direct condenser circuit, while the inside loop is used for spray condensing studies. The heat source consists of a pool boiler followed by a superheater. Although the superheater is shown only in the direct condensing part of the loop, it has been relocated and is now used for both direct and indirect condenser experiments. The pool boiler contains an automatic level indicator. Flow is produced by a constant-speed pump. The flow rate is controlled by throttles coupled with a bypass loop around the pump. The direct condenser test section is in effect a calorimeter. Cooling air within the transparent jacket flows countercurrent over the direct condenser tube. Appropriate measurements of air temperatures, airflow rate, mercury temperatures, and mercury flow rate provide a direct measure of the quality of the mercury vapor entering the test section. The direct condenser tube is also instrumented to give differential pressure. In addition to the single tube tests, experiments have also been made on a radiator condenser for which heat was removed directly by radiation. This investigation will be described later.

Flow rates have been measured by use of electromagnetic flowmeters and, as shown in the figure, by orifice-type flowmeters. Although two orifices were installed in the direct condenser loop, the one located directly downstream of the test section was used for flow-rate data.

Because of the thermal lag of the boiler, the orifice located at the boiler inlet was less indicative of the test-section flow rate.

Temperatures were measured with chromel-alumel thermocouples. Differential pressures were measured with manometers calibrated to read in millimeters of mercury.

As noted above, a superheater was used in the test loop. The objective was to obtain various degrees of quality at the inlet of the test section. In this regard it is essential, for proper interpretation of the test results, that a direct measure of inlet quality be made. In a film, which shall be described shortly, the effects of liquid entrainment on interface stability are shown. It is important to note that liquid separation alone is insufficient to ensure high quality vapor entering the test section. Small liquid droplets, of micron size, are often entrained in the flow and, moreover, are not easily removed by liquid separators. As a result, relatively low qualities may exist even though the large visible liquid drops have been removed. In the direct condenser tests, quality was determined by the calorimeter technique noted above. In the most recent modifications to the test loop a separate calorimeter is located immediately downstream of the superheater in such a way as to provide a continuous record of vapor quality.

Experimental Results

The results of the investigations, including compilations of test data, are given in three reports. The analytical and survey type work is presented in reference 1. The experimental work is reported in references 2 and 3. It should be noted that references 2 and 3 contain the recorded laboratory data. Since, in the field of heat transfer, data correlation is a never-ending objective, it would be helpful if all those working with liquid-metal heat-transfer investigations would publish the laboratory data and thereby make possible the use of such data by persons attempting to achieve correlations. As is known, curves and plotted data are usually insufficient for use in new correlations.

Reference 2 describes the investigation of a multitube radiator-condenser for use in a space environment. Reference 3 deals with several types of condensers with primary emphasis being given to the spray-type condenser. Currently, a second 6-month report describing the continuation of both direct and spray condenser studies is being prepared.

In the direct condenser studies attempts were made to control geometric, hydrodynamic, and thermodynamic variables. The geometric variables include tube shape, that is, straight and curved tubes (6-in. rad. of curvature), and tube inside diameter (0.06 to approximately 1/4 in.). The results obtained with straight tubes confirm those

reported earlier by TAPCO; namely, that stable condensation can be accomplished in horizontal straight tubes as long as the internal diameter is less than approximately 0.2 inch. The multitube condenser reported in reference 2 incorporated tubes with an internal diameter of approximately 0.06 inch and tube lengths of 27 inches, with seven tubes being used in parallel.

The range of variables covered includes the following:

Hydrodynamic variables	
Reynolds number	
Single tubes	1200 to 36,000
Multiple tubes	2000 to 7000
Mach number	0.02 to 0.4
Vapor velocity, ft/sec	10 to 40
Flow rate, lb/hr	
Single tubes	5 to 25
Multiple tubes	17 to 36
Thermodynamic variables	
Liquid-vapor density ratio	400 to 1800
Vapor temperature, °F (saturated)	
Single tube	700 to 750
Multiple tubes	700 to 1000
Inlet quality	0.1 to 1.0
Superheat, °F	up to 100

Inasmuch as the detailed results have been described in the documents cited above, only a brief review will be presented here. As noted earlier, for horizontal straight tubes without insertions such as turbulators or orifices, the maximum inside diameter for which stable flow has been obtained is approximately 0.16 inch, which, again as noted above, corresponds to the results reported by TAPCO. It is important to note, however, that this is a laboratory result which does not in any way describe the upper limit of tube diameter, which, in a true zero-gravity field, can be used to achieve stable flow. In fact, much larger tube diameters should be practical for the zero-g applications. This expectation raises the question of the necessity for using orifices, swirl devices, and so forth in systems intended for zero-g operation, even though such devices appear necessary for the investigation of larger tube sizes in ground-based laboratory test loops.

The problem of stability is one with which EOS has been concerned. However, stability is a term oftentimes used very loosely. Generally speaking, it is difficult to discuss the stability of a condenser without identifying the influence of the remainder of the test system. In this connection, it would be very helpful if the persons concerned with hardware system development would identify the types of stability problems which are considered important. Similarly, the factors which are unimportant with respect to stability should also be identified. For example, the occurrence of slugs leads to vapor collapse and subsequent pressure pulsations. The question to be asked in this case is, "Are these pulsations important in an actual power system?" Such pulsations, of course, may be identified as a form of instability. However, more generally, stability in a dynamic system is associated with perturbations which cause the system either to seek a new operating point or to acquire a completely random or uncontrolled state. If one accepts the latter definition of stability, or perhaps more correctly, instability, then, according to our experimental results, no instability occurred in tests with any tube having a diameter less than 0.16 inch, whether the tube was straight or curved. Therefore, it would be concluded that, in 1-g horizontal operation, stable flow can be obtained with tubes of such size; and, as will be noted later, this conclusion includes both multiple and single tubes.

Another interpretation of instability is associated with the movement of the vapor-liquid interface. Films have been taken showing the interface movements in a single tube. At this point, however, it is important to observe that the movement of an interface should be related to the movement of fluid in other parts of the system. For example, consider the case for which a constant-pressure reservoir exists downstream of the test section. If, upstream of the interface, a change in pressure occurs because of, for example, a change in heat-transfer rate or the collapse of bubbles, then a force exists for moving fluid either into or out of the constant-pressure reservoir, thereby causing interface movements which are a direct reflection of the existence of the downstream reservoir. However, if the system incorporated a pump immediately downstream, the interface movements would differ, since, in order for the interface to move upstream or downstream, a change in flow rate through the pump would be required. Such a change, however, would depend upon the characteristics of the pump as well as the dynamics of the remainder of the flow system. Thus, in general, movements of the interface should be identified with the system in which tests are being conducted.

The following pages review briefly the experimental investigations which have been conducted. Reference is first made to the multiple-tube investigation. At the time this program was started, little published information was available on the subject of mercury condensation in condensers which would be useful for a space environment. As a consequence, at the outset, an analysis was developed for determining the combination

of parameters leading to the minimization of radiator weight for a specified heat-rejection rate. From this analysis the tube diameter, tube length, and fin width were established. The use of curved tubes was based on the objective of minimizing the effect of 1 g in a ground laboratory experiment. Thus, by use of sufficient curvature to produce a 40- to 50-g acceleration of liquid drops traveling at the vapor velocity, the effect of Earth's gravity on the condensation process would be expected to be minimized. However, at the vapor-liquid interface, the presence of 1-g is still important, even for curved tubes. However, experiments indicated that this effect was relatively unimportant for small tubes. Thus, the small tube diameter satisfied both the weight minimization requirement and the restriction imposed by 1-g laboratory operation. Of course, it was recognized that in practice other factors such as corrosion effects, fabrication problems, and the like might dictate the necessity for using larger diameter tubes. Nevertheless, the multiple tube radiator-condenser was successfully fabricated and operated for many hours without the occurrence of any noticeable effects of corrosion or blockage from any other causes.

The design incorporated curved stainless steel tubes welded to tapered stainless steel manifolds and brazed to a steel radiation fin. The test unit, designed to reject approximately 1 kilowatt of heat was tested in the closed-loop laboratory system described in figure 1 above. Both wet and superheated vapor conditions were used. Flow rates were adjusted over a range of values at each inlet temperature in order to move the vapor-liquid interface from a position near the radiator condenser outlet manifold to a position near the inlet manifold. In this connection it is important to note that the experiments were not conducted in a vacuum environment. As a consequence, free-convection effects were present. In fact, the heat-transfer rate had to be suppressed by use of insulation in order to place the vapor-liquid interface at various positions along the condensing tubes. Transparent sections were installed at the inlet and outlet of the condenser.

The results demonstrated that a curved tube radiator condenser of the type investigated can be used to condense mercury vapor in a space power system over a relatively wide range of operation conditions. For the range covered in the investigation, vapor-free liquid flow was obtained at the condenser outlet.

A very simple method was employed for locating the position of the interface within the condensing tubes. A series of 41 thermocouples was attached over the surface of the radiator. These thermocouples were placed both along the surface of the tubes and on the fins between the tubes. Measurements were made during startup and transient and steady-state operation. The plots of temperature versus position along the tubes are shown on pages 2-4 through 2-16 in reference 2. As expected, the temperature remains essentially constant until the position of the

interface is reached, at which point an abrupt reduction in temperature occurs. An examination of the heat balance at the interface will show that the rapid reduction in temperature is to be expected. During the course of the given experiment, the temperature data were observed continuously with the aid of an automatic temperature recorder. Thus, it was possible to observe any large-scale movements of interfaces within the tubes. With this technique, for all test conditions in which the interfaces were between the inlet and outlet manifolds, no large-scale interface movements could be detected. This result was obtained, moreover, even though the interface locations, measured from the inlet manifold, were at different lengths in each of the seven tubes. Temperatures were also measured during startup. The results indicated that, within approximately 1 minute after the initiation of boiling, the temperature readings along the condenser were at approximately steady-state conditions. No damage from thermal stress was apparent after repeated operation.

As noted above, tapered manifolds were incorporated at the inlet and outlet of the condenser. No direct measure of the distribution of flow rate among the tubes was available.

In connection with multiple tubes, it may be of interest to note that the use of honeycombs as stabilizers in large tubes (~3-in. I.D.) has been investigated. The honeycomb was investigated as an interface stabilizer in a negative 1-g environment. The results of this work are described in reference 4. In general, the honeycomb is a useful stabilizing element. However, investigations in a ground laboratory environment are difficult, since instability associated with ground operation can occur. The reasons for this are described in reference 4 and are similar to those noted earlier by TAPCO in connection with the use of dual tubes oriented vertically. With considerable care during startup and steady-state operation, the honeycomb could be used to maintain a stable vapor-liquid interface for a period of many hours. In a zero-g environment, it appears that, if desired, the honeycomb can be used as a stabilizing device.

As noted by others, the Martinelli correlation is generally used to estimate pressure drop in a condenser. EOS experimental pressure drop values have been compared to those obtained by use of the Martinelli correlation. The most interesting experiments, however, are currently being obtained. The results will be reported as soon as they are available. The past data had a number of deficiencies which have been eliminated from the current work. The principal factor concerns the accurate measurement of quality entering the condenser. In some of the past work, a considerable deviation between the calculated and experimental pressure drops was found. An example of this is shown in figure 2. These results are to be considered as preliminary only. The abscissa is the ratio of the frictional pressure drop calculated by Martinelli's method to that

which was obtained from the experiments. The ordinate contains an empirically determined correlation factor consisting of the product of the inlet vapor quality and the vapor Reynolds number each raised to a separate power. The range of vapor Reynolds numbers was 11,000 to 36,000. Two tube diameters were tested, and vapor qualities were varied from approximately 0.1 to 0.6. These results suggest that, for the indicated range of Reynolds numbers and quality, the pressure drop is significantly influenced by these two factors. Both of these factors, moreover, affect the flow regime referred to earlier by TAPCO. Current experiments are devoted to a closer examination of the influence of each of the factors noted here.

In the multiple tube experiments measured surface temperatures were used to estimate the heat-transfer coefficient. The values obtained varied from approximately 200 to 2000 Btu per hour per square foot per ^{o}F. These results are reported in reference 2.

It is desirable to add a few remarks on gravity effects. In horizontal flow within straight tubes, gravity influences the fluid dynamic and thermodynamic boundary conditions. In zero g, liquid mercury formed at the wall of the condenser is removed either by vapor drag or by impact caused by other liquid drops. The presence of gravity causes the drops to move in a spiral motion, while in the absence of gravity spiral motion will not occur. Thus, the different particle paths along the walls should produce corresponding differences in heat-transfer and friction coefficients. These effects, moreover, may be greater the larger the tube diameter.

Gravity certainly influences the interface shape. This influence is especially significant in the case of large tubes. Finally, the presence of gravity is particularly important in vertical flow systems, particularly in the negative 1-g systems. In such systems the occurrence of reverse flow is due to the presence of gravity; reverse flow would not exist in the absence of gravity.

The film selected for demonstrating mercury condensation shows a particularly interesting feature not noted in any of the other work described here. In the experiment, a transparent direct condenser is housed within a transparent jacket. Cooling is produced by air flowing through the jacket. In the film, mercury vapor is flowing from left to right and is being condensed continuously. The condenser tube internal diameter is approximately 0.16 inch, and the condenser length is approximately 10 inches. Other conditions of the experiment are the following:

Vapor Reynolds number at the inlet	8200
Vapor velocity, ft/sec	76
Vapor temperature, ^{o}F	715

The heat rejected in the test section, as determined by the calorimeter method described earlier, was 1500 Btu per hour. Under these operating conditions, there occur flowing from left to right, large irregularly shaped collections of liquid. The origins of this liquid were not traced, since in later experiments it was eliminated. However, very likely the liquid represents a combination of that which emerges from the boiler and the condensation which occurs in the lines between the boiler and the test section. The surfaces appear to have a shape similar to that observed by TAPCO in their experiments. As these liquid surfaces travel downstream, they scrape additional liquid from the walls of the tube. The surfaces appear to fall downward and then to rebound. Thus, even at 1-g, a mechanism exists to cause liquid to move in a direction opposing gravity. The liquid surface finally impacts on the vapor-liquid interface, which appears to behave in part like an inelastic wall; that is, at impact a reverse flow of liquid emerges from the interface. This jet curves toward the bottom of the tube and breaks into smaller masses, each of which continues to move upstream until slowed by friction, vapor drag, and the impact of downstream-moving liquid. Eventually the liquid which originated at the interface begins to flow downstream, back to the interface. Additional liquid is scraped from the walls, and in some instances the liquid accumulation and motion is sufficient to block the entire flow passage. Under these circumstances a slug is formed. Thus, a slug-forming mechanism is observed which can occur independently of the condensation in the tube and, in fact, is attributed to the presence of large amounts of liquid entrained in the flowing vapor. In a practical situation, entrainment may be characteristic of the fluid emerging from the turbine and passing into the condenser. Aside from the possible instability effects, the presence of such large liquid entrainment leads to an eventual pressure loss, since the momentum in the reverse jet is eventually dissipated in friction. Also to be noted in the film is the spiral sweep of the liquid which has condensed along the wall. In addition, the steadiness of the vapor-liquid interface except in the instances referred to above is to be noted. Incidentally, the total real time of the film sequence is approximately 1 second.

In the continuing work on direct condensers, efforts are being devoted to careful measurements of pressure drop with controlled and carefully measured inlet quality and heat-transfer rates. In addition, a mercury test loop is being constructed for use in the KC-135 zero-g airplane. A combination loop, such as that described earlier in figure 1, will be used, thereby providing the capability for testing both spray condensers and direct condensers. The direct condenser, to be enclosed in a vacuum chamber, can be operated simultaneously with the spray condenser. This latter program is now at the state where the design is being finished and parts are being ordered.

In closing, some of the problem areas which are believed to remain in connection with the condensation of mercury will be noted. First of all, there exists the problem of determining or verifying an accurate method for prediction of pressure drop. On the basis of the information presented here today, this problem remains unsolved. The stability problems and their importance have yet to be clearly identified. The problem of tube size remains unresolved. The essential matter here is that of trying to establish scaling laws. Finally, the problem of non-condensables, about which TAPCO has published some information, remains to be clarified. No results have been published which establish quantitatively the effects of noncondensables on the condensation process associated with mercury.

SPRAY CONDENSERS

The general way in which a spray condenser would be used in a Rankine cycle system can be illustrated by reference to figure 1. In a spray-type system, a boiler would be located in the position indicated, with the turbine being downstream of that component. Vapor is exhausted from the turbine into the spray condenser, and at the same time a stream of subcooled liquid is injected to cause condensation of the vapor from the turbine. The resulting flow, which may be entirely liquid, is circulated through a liquid radiator, which corresponds to the cooler in the test loop, and then to the pump. The liquid is then pumped back to the spray condenser with a portion of the flow equal to the vapor flow being bled off and returned to the boiler.

Some of the possible advantageous features of spray condensers can be summarized as follows:

(1) The length of vapor run from the turbine to the condenser or within the condenser can be made relatively short (compared to the dimensions of a direct condenser). As a result, a given percentage change in condensation distance produces a very small change in the total liquid inventory in the system. The condensation length can change by a factor of 2 or 4 and not significantly change the fluid inventory in the system.

(2) As a second advantage, the injected fluid can be used to provide pressure augmentation. Several space power systems currently being developed apparently require the use of a jet pump upstream of the boiler feed pump in order to boost the pressure and thereby prevent pump cavitation.

(3) As a third advantage the design and operation of the radiator (which would be a liquid radiator for this system) is simplified, since only one phase flow occurs.

(4) For some applications the use of a liquid radiator can reduce the sensitive area (i.e., the area which would be sensitive to meteoroid penetration) and thereby reduce the total system weight. This result is characteristic of the lighter alkali metals. However, for some low-pressure applications with mercury, a weight advantage may also be gained with a spray condenser system.

Three important disadvantages pertain to spray condensers:

(1) The first is due to the large ratio of injected liquid flow rate to vapor flow rate (10 to 40) which increases pumping power.

(2) The second disadvantage stems from the subcooled state of the liquid in the radiator. The liquid is therefore less effective per unit area in rejecting heat than the direct condenser.

(3) As a third disadvantage, the use of the liquid radiator increases the liquid inventory weight compared to that required for a direct condenser.

Some of the results which will be described for spray condensers were obtained in the earlier program which is summarized in reference 1. In addition, some of the results of the 6-month investigation reported in reference 3 will be described. Finally, some of the important results which have been obtained in the current NASA program will be discussed.

The early investigation had three main objectives. The first was to demonstrate the feasibility of achieving rapid condensation in a relatively simple spray condenser. It was necessary to determine whether subcooled liquid could be injected into the spray device, cause rapid condensation, and result in a steady vapor-free outlet flow. The second objective was to investigate different methods of injecting the subcooled liquid into the vapor. The third objective was to establish the hydrodynamic and heat-transfer characteristics of these devices for several simple geometric units.

The experimental investigation was carried out with both mercury and water, in order to introduce a wider range of fluid variables. However, the results of testing with mercury mainly will be reported.

The test loop (fig. 1) contains a pool boiler and a superheater in the vapor section. In addition, a second heating element is wrapped around the lines before the test section in order to maintain superheat up to the test section. Present tests being conducted in this loop allow the attainment of entrance quality equal to unity. Thermocouples are used to measure vapor temperature, in addition to outlet and inlet liquid temperatures. A manometer across the spray condenser records

differential pressure. The cooler is used to lower the temperature of the condensate liquid mixture in order to protect the pump. Although the pump is rated at 600° F, it was operated at lower temperatures in order to minimize repair time.

The division of flow is regulated by valves when the loop is operated closed cycle. It was also operated with the condensed vapor flowing into the reservoir, and the return leg of the boiler being shut. A heater is located before the point of liquid injection into the condenser in order to increase the temperature of the injected fluid to the desired operating point. Pressure gages are located on the injected fluid leg and in the vapor leg, and an orifice-type flowmeter is placed in the injection leg.

The range of variables covered for mercury during this program is summarized here and in reference 3.

Geometric variables	
Tube inside diameter, in.	0.190
Angle of injectors measured from vertical, deg	35
Jet diameter, in.	1/32 to 1/64
Number of jets	8
Hydrodynamic variables	
Vapor Reynolds number	10^4 to 2×10^4
Injected liquid flow rate / Vapor flow rate	7:1 to 35:1
Thermodynamic variables	
Vapor pressure, lb/sq in. abs	20 to 50
Vapor temperature, °F	700 to 860
Liquid-to-vapor density ratio	1000 to 2300
Subcooling of injected liquid, °F	100 to 400
Heat exchange in test section, kw	0.4 to 1

Although the discussions in these papers are limited to mercury, some of the results obtained with water will be presented briefly for explanatory purposes. In figure 3 experimental data obtained for water indicate the usefulness of particular parameters for describing spray condenser performance. The ordinate is a nondimensional spray temperature, which is equal to the temperature of the jet at any distance x from the point of injection, minus the temperature of the jet at the

point of injection, divided by the vapor temperature minus the temperature of the jet at the point of injection. This quantity can be interpreted as the enthalpy change of the injected fluid at any point x divided by the maximum enthalpy change which would occur if, during the condensation process, the jet temperature were raised to vapor temperature. The abscissa is the approximate residence time of the spray or jet in the presence of vapor and is equal to the distance x divided by the axial component of the jet velocity. The data points on the curve are obtained from temperature measurements taken inside the liquid core of a water spray condenser. The calculated curves are determined from the transient heat conduction into liquid spheres. Only the steeply rising parts of the calculated curves are appropriate for comparison with the experimental data.

The comparison shows the usefulness of the temperature parameter and suggests that, in instances where the jet is cylindrical, the jet temperature history can be estimated.

Based on these results an overall performance parameter is defined by substituting the final jet temperature (or mixture temperature when complete condensation occurs) for the local jet temperature. This parameter, designated as the spray utilization factor X, is used to describe the performance of the mercury spray condensers.

In figure 4, X as ordinate[3] is given as a function of condensation length (i.e., the length measured from the point of injection to the point at which an interface occurs). Curves 1 and 2 in this figure correspond to injector hole sizes of 1/64 and 1/32 inch, respectively. The comparison shows that, for a given value of X, shorter condensation lengths are achieved with the smaller jets. Condensation lengths L_c varied from less than 0.06 to 3 inches, which was the length of the transparent test section. For smaller jets, figure 4 also demonstrates that, at the same values of vapor Reynolds number and X, shorter condensation lengths are obtained with mercury than with water.

For the test conditions indicated in figure 4, the condensation length is seen to be very sensitive to small changes in X, or in other words to changes in injected fluid temperature or to injected mass-flow rate. This sensitivity is undesirable in a power system. However, data not shown in figure 4 demonstate that, for smaller values of X, L_c is insensitive to X. As an example, for the conditions of curve 1, a variation of X from 0 to 0.9 causes an increase in L_c of only 0.05 inch. Thus, for design purposes, the value of X should be selected to correspond to a low sensitivity in L_c.

[3]The quantity X is the independent variable (cf. fig. 6).

Curves 3 and 4 in figure 4 have been included to indicate the effect of vapor Reynolds number on condensation length. For a given value of X, lower values of L_c are obtained with higher values of Re_v.

Water data are again used in figure 5 to indicate the influence of injection angle on condensation length. Injection angles, measured from the vertical, of 10°, 35°, and 45° were used. As might be expected, the condensation length decreases with lower injection angles.

Data obtained with a mercury condenser incorporating a single central injector are presented in figure 6. In this case the condensation length is shown as the dependent variable, while X is the independent variable. The near-vertical part of the curve identifies the sensitive L_c versus X region (cf. figs. 4 and 5). However, for $X < 0.85$, L_c becomes relatively insensitive to changes in X.

Compared to the impinging jet design, the central injector is simpler and less likely to be eroded or plugged. For the conditions listed in figure 6, larger values of L_c, for given values of X, occur with the central jet than with impinging jets. Comparisons at other conditions are currently being made.

One of the useful features of a spray condenser is the augmentation of the inlet vapor pressure. In figure 7 the pressure recovery ratio is presented as a function of mass-flow ratio. The pressure recovery ratio is defined as the pressure rise divided by double the velocity pressure of the injected liquid. Data points are shown and compared to the calculated curve of pressure ratio (for no frictional losses in the spray condenser). Figure 7 shows test data for the spray tube with 1/64-inch jets. Smaller jet sizes or lower values of the area ratio of the injected liquid to vapor result in lower values of the recoverable pressure. Figure 8 presents the results for a larger jet size (larger ratio of area occupied by liquid to that of the vapor). The pressure ratio has increased considerably from that for the smaller jet size (for the same value of mass-flow ratio).

The pressure drop associated with the injection of the subcooled liquid ranged from about 5 to 20 pounds per square inch for the larger jet size. For the smaller jet size, the injection pressure drop ranged from about 10 to 100 pounds per square inch.

For the remainder of this discussion, a film showing condensation in a mercury spray condenser will be presented. The film speed was 8000 frames per second and the total elapsed real time of the entire film is approximately 1 second. As shown in the film, the impinging jets form, in effect, a central jet which breaks into large, relatively discrete masses. Complete condensation is effected in a very short distance. Although small vapor pockets form at the top of the tube, they

subsequently disappear. The fluid leaving the condenser shows no evidence of vapor being present. The vapor-liquid interface is relatively steady, the movements which do occur being in part associated with the existence of the constant-pressure reservoir downstream of the condenser.

The important design considerations involved in spray condensers are described in EOS reports. Here it should be noted that the spray condenser must be integrated with the remainder of the power system in order to achieve the best compromise between weight, condensation length, pressure augmentation, and so forth.

REFERENCES

1. Analysis and Development of a Space Heat Rejection System and Its Optimum Integration into a Space Vehicle. EOS Final Rep. 250, Dec. 15, 1959. (Prepared for ABMA under Contract DA-04-495-ORD-1473.)

2. Radiator Condenser for Space Environment. EOS Final Rep. 310. (Prepared for WADD under Contract AF33(616)-6520, Proj. 3084 Task 30405.)

3. Condenser Space Heat Rejection Systems. EOS Final Rep. 500. (Prepared for AMBA under Contract DA-04-495-506-ORD-2007.)

4. Analysis and Development of a Space Heat Rejection System and Its Optimum Integration into a Space Vehicle. Supplement to Semi-Annual Tech. Summary Rep. (Prepared for ABMA under Contract DA-04-495-ORD-1473, Feb. 29, 1960.)

FILMS AVAILABLE

1. Mercury Spray Condenser - 200 ft of steady-state operation of a spray condenser with mercury. Slug-free flow is shown with condensation distances from 1/2 to $1\frac{1}{2}$ in. (8000 ft/sec).

2. Mercury Direct Condenser - three 100-ft rolls of operation of a mercury direct condenser with low quality vapor (<0.50). Interface oscillations and liquid impact shown in detail (8000 ft/sec).

3. Mercury Spray Condenser - 75 ft of startup of a mercury spray condenser. Liquid is injected into a test section initially filled with flowing vapor. The resulting formation of an interface and attainment of steady-state conditions are shown (2000 to 4000 ft/sec).

4. Water Spray Condensers - Several 100 ft rolls showing different aspects of spray condensers operating with water.

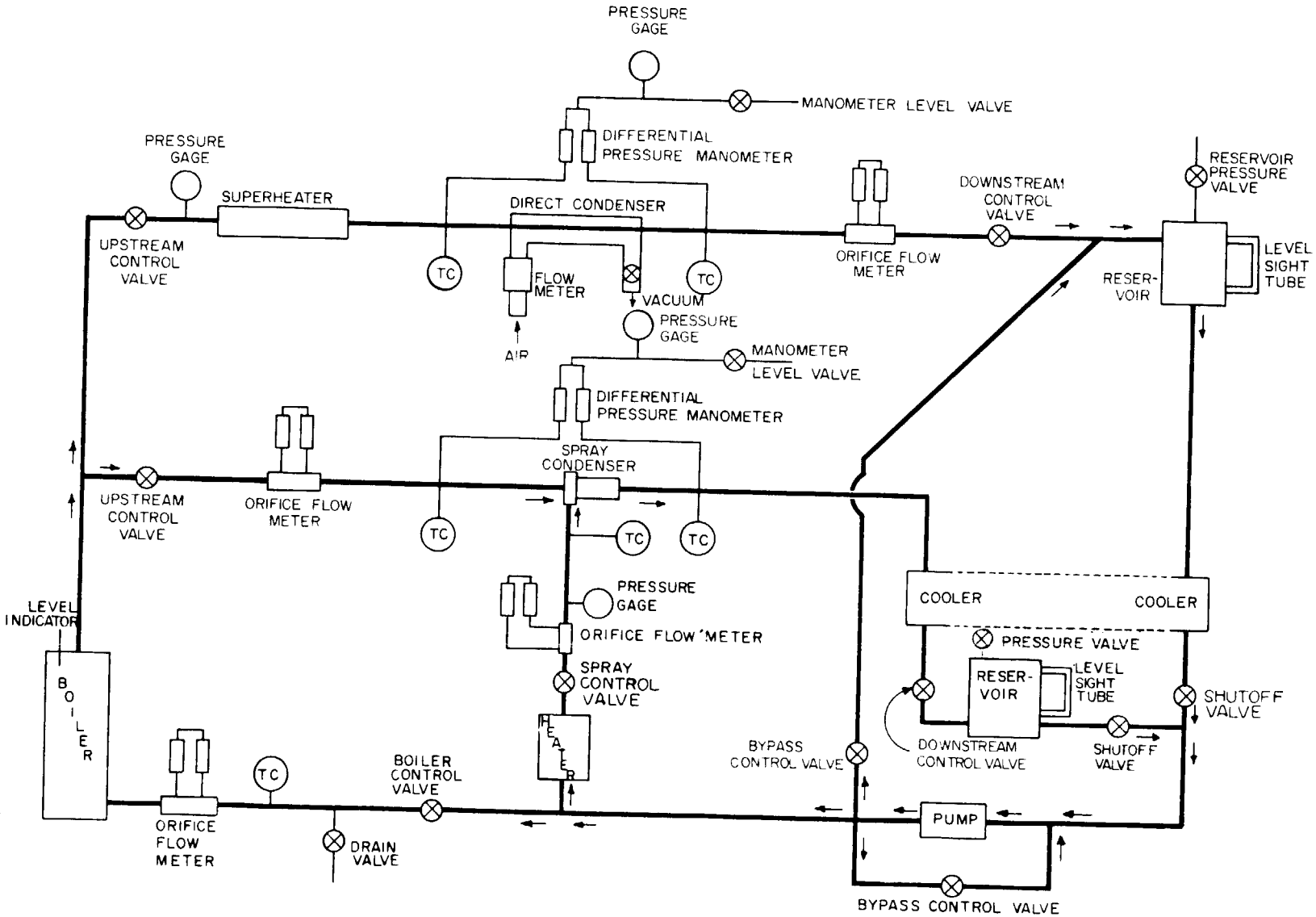

Figure 1. - Mercury condenser test loop schematic diagram.

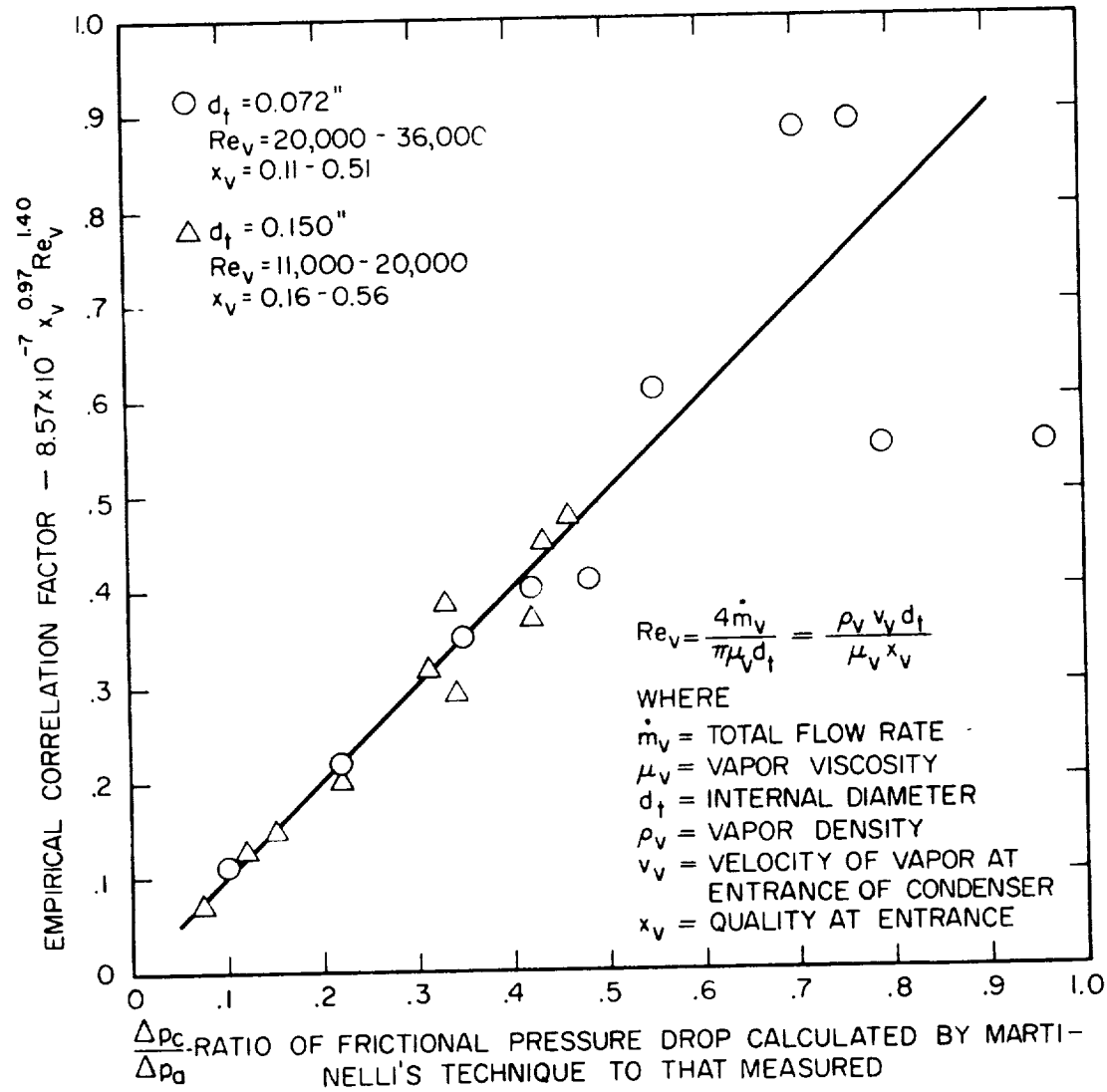

Figure 2. - Ratio of Martinelli pressure drop to measured against quality and Reynolds number. Factor for two geometries for condensing mercury (700° F).

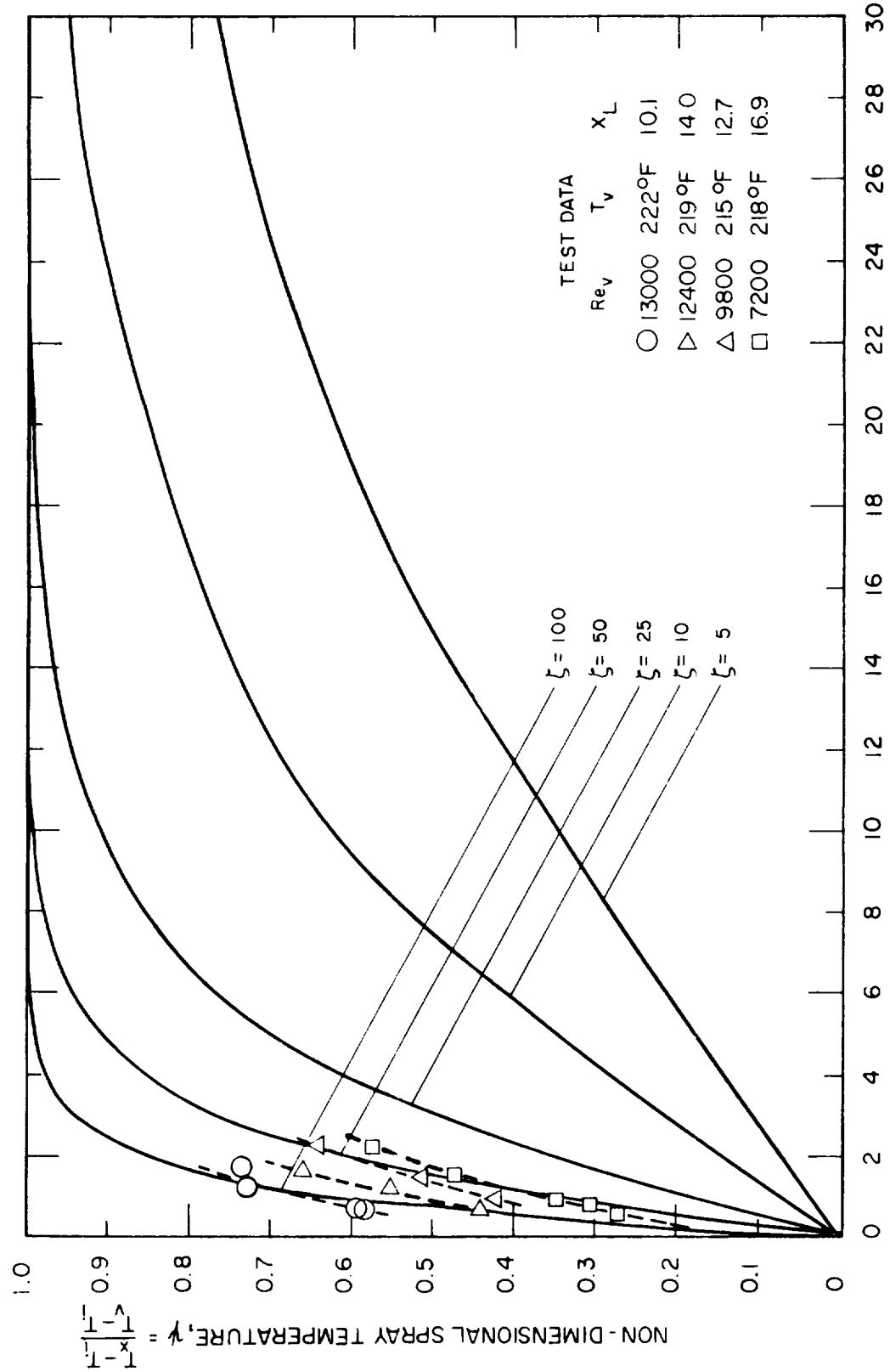

Figure 3. - Temperature of spray as a function of spray residence time in condensing chamber (calculated on basis of spherical geometry, lines of constant $\zeta = (\alpha + \alpha_T)/s^2$, sec^{-1}).

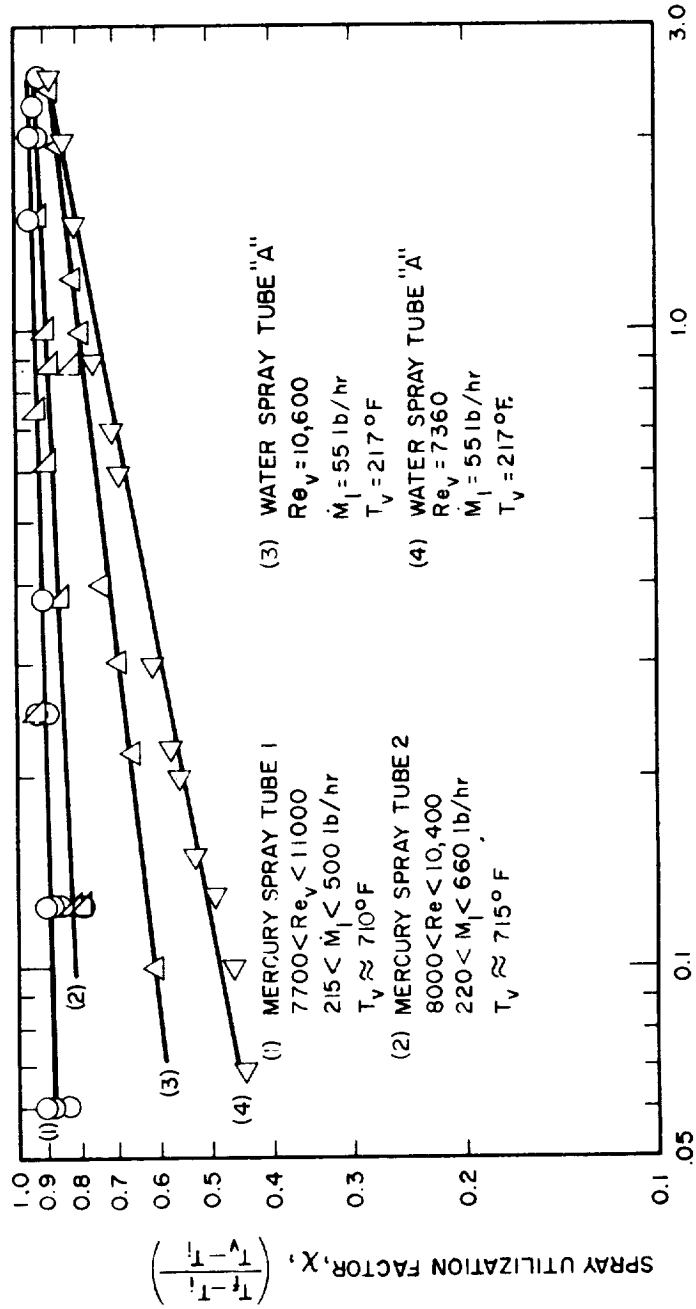

Figure 4. - Condensation length against spray utilization factor for mercury and water. Spray condensers (varying vapor Reynolds number and injector size).

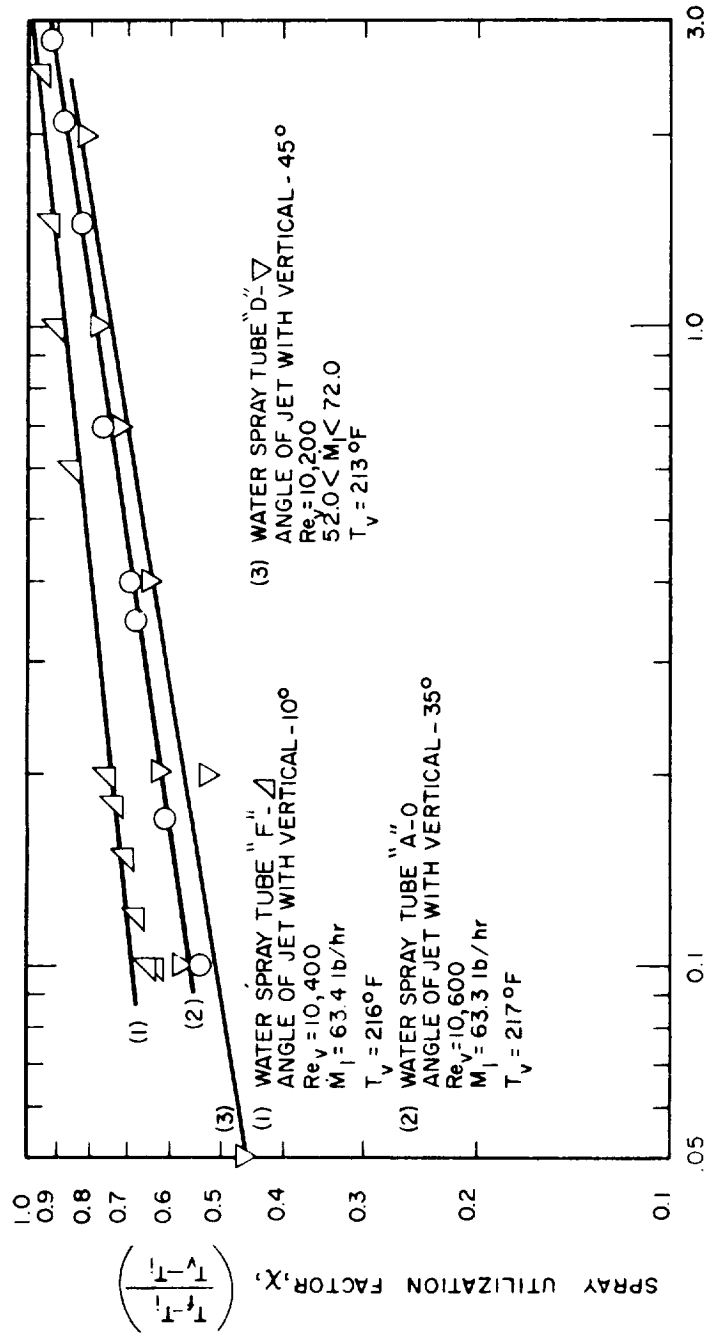

Figure 5. - Condensation length against spray utilization factor for water spray tubes with different angles of injection.

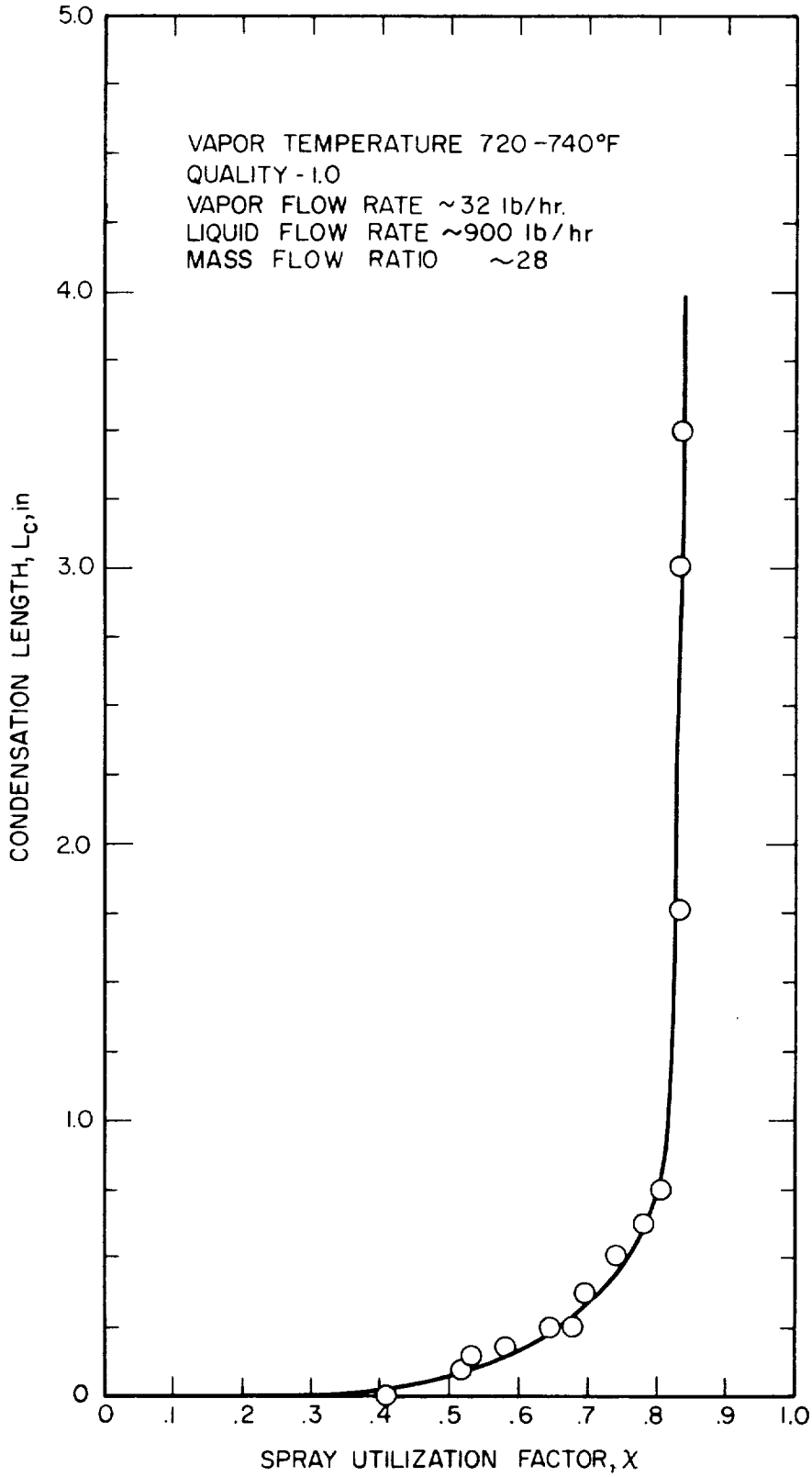

Figure 6. - Condensation length against spray utilization factor for central injector mercury spray tube. Injector diameter, 0.044 inch; tube diameter 0.190 inch.

E-1501

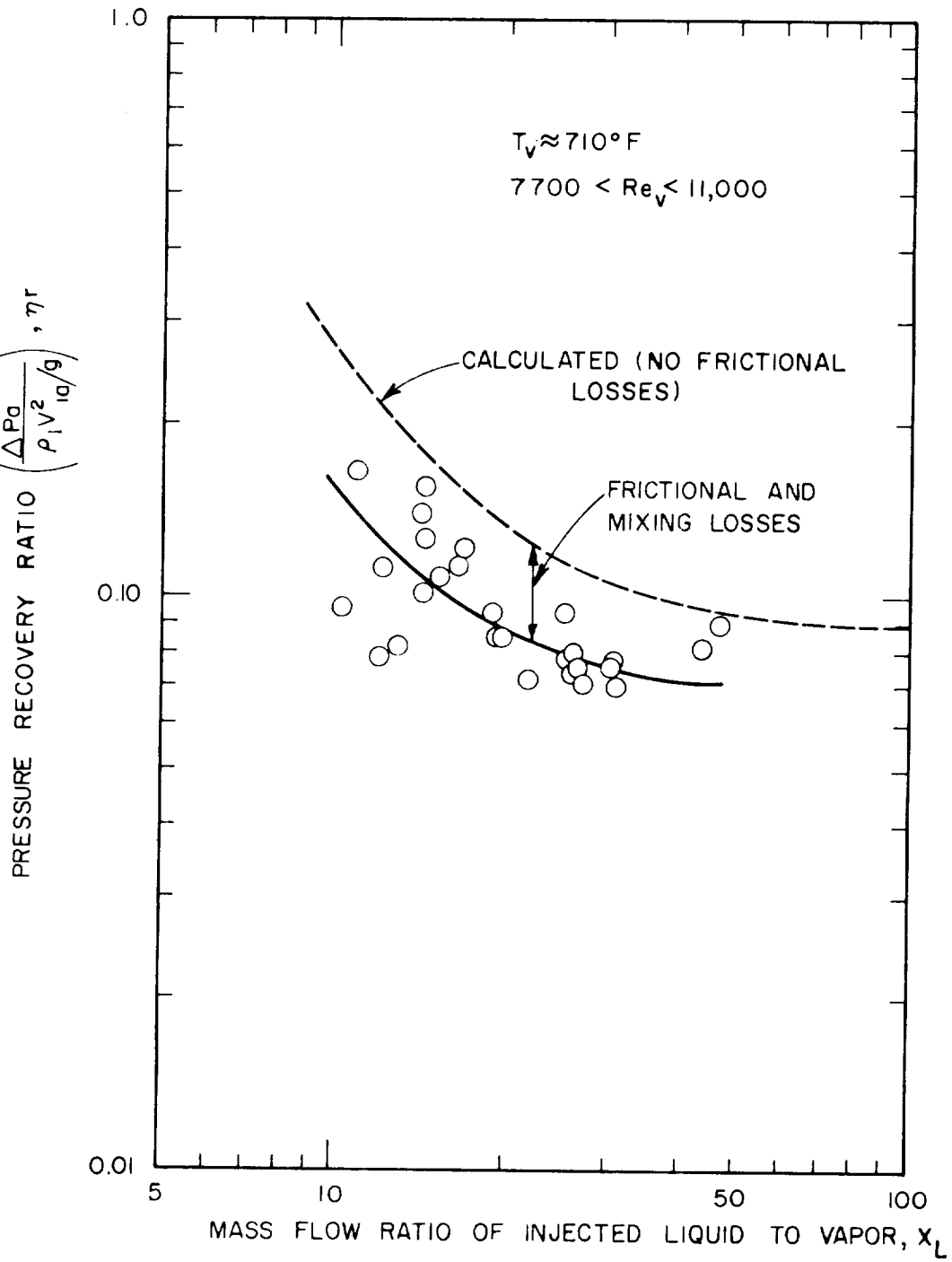

Figure 7. - Pressure recovery ratio against mass flow ratio for mercury spray tube 1.

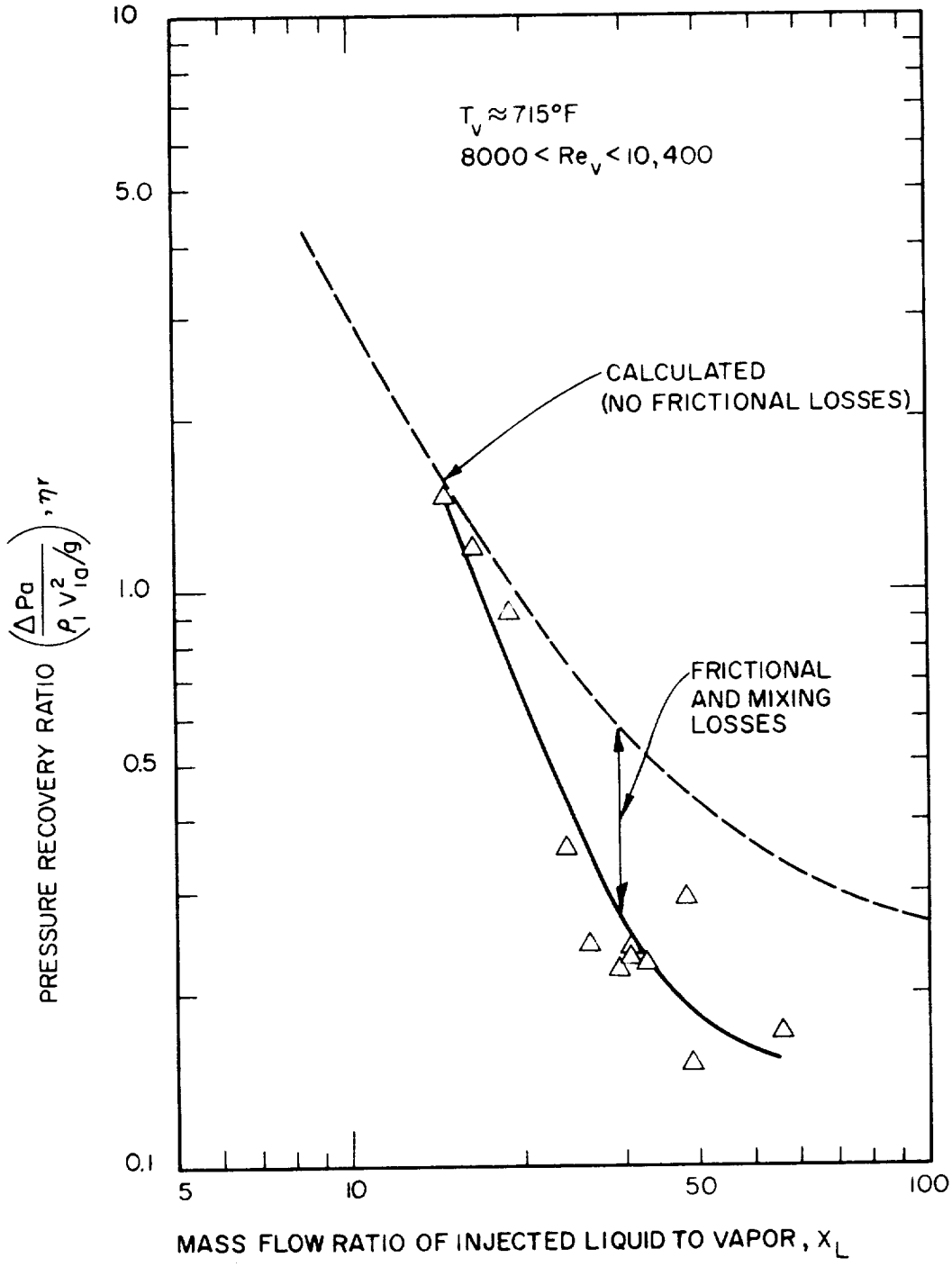

Figure 8. - Pressure recovery ratio against mass flow ratio for mercury spray tube 2.

UNITED STATES AIR FORCE

AERONAUTICAL SYSTEMS DIVISION PROGRAMS IN MERCURY CONDENSING

Presented by Lt. Lloyd M. Hedgepeth

SOLAR POWER UNIT DEMONSTRATOR (SPUD)[4]

Objective

The objective of the project was to design, fabricate, and test a ground demonstration model of a closed-loop mechanical conversion solar power system utilizing mercury in order to demonstrate its feasibility.

Design Philosophy

This was to be a breadboard type system with no attempts made to optimize any of the system components. In keeping with this philosophy, only existing techniques, knowledge, and hardware were utilized.

Supplemental Agreement

Under the supplemental agreement, the turboalternator rotating assembly was successfully operated for a period of 2500 hours to demonstrate endurance. The test time was terminated at the request of ASD.

Redirected SPUD Program

The endurance test was halted by ASD in order that the SPUD type hardware could be designed into a test capsule to be launched on a ballistic shot. The shot will demonstrate the feasibility of zero-gravity operation of a closed-loop Rankine cycle power system. The redirected effort is under Contract AF 33(616)-7979.

Report

Rough draft reports have been submitted on the basic contract and the supplemental agreement; however, they will not be published. Because of the purpose and nature of the contract, these reports contain

[4]Contract No. AF 33(616)-6625 and Supplemental Agreement 2(61-122); contractor, Thompson Ramo Wooldridge Inc.; ASD project engineer, George E. Thompson.

very little condensing information. A report on the 2500-hour test will be published as ASD Technical Report 61-113. The final report on the ballistic shot should contain quite detailed information on the condenser design philosophy as compared with the actual results.

Remarks

The flight capsule experiment will be contained in a side pod of an Atlas vehicle that will be launched in a ballistic trajectory sometime in late 1961 with 15 to 30 minutes of zero-gravity time expected. The flight-capsule test hardware consists of a complete mercury Rankine cycle utilizing a SPUD type turboalternator rotating package and a battery heat source. Principal components are battery heat source, boiler, superheater, turbine, alternator, radiator, and pump. Thermocouples will be provided in the boiler and along some of the radiator tubes and pressure drop will be measured across the condenser. Turbine speed and alternator output will also be measured. Since the capsule will not be recovered, no photographs of the condensing will be taken.

The loop will be started on the ground and will operate during the launch and zero-gravity periods. The pod will be ejected from the vehicle probably just prior to the retrorocket firing. Ejection will be very slow in order to prevent the pod from tumbling; thus the gravity level will be very close to zero.

The radiator-condenser will comprise roughly half of the pod external surface and will be vertically oriented. Vapor will enter at the top, and liquid will be removed at the bottom. The tubes will be tapered. Analyses indicate proper functioning during the cooling and heating portions of the launch period. Although static head in the radiator and pump will be increased during vehicle acceleration, boiler pressure and operation (upward flow) are not expected to be materially affected.

RADIATOR CONDENSER FOR SPACE ENVIRONMENT[5]

Objective

The objective of this program was to determine basic design parameters for space radiators and methods of evaluating future radiator-condenser type heat-rejection devices.

[5] Contract No. AF 33(616)-6520; contractor, Electro-Optical Systems, Inc.; ASD project engineer, Charles L. Delaney.

Final Report

WADD TR 61-20; Abstract. - A radiator condenser for a Rankine cycle space power system was designed to condense and subcool superheated mercury vapor. The weight of the radiator condenser was to be minimized at design conditions. The design incorporated curved stainless-steel tubes welded to tapered stainless-steel manifolds and brazed to a steel radiation fin. A test model radiator condenser, designed to reject approximately 1 kilowatt of heat, was tested in a closed-loop laboratory system over a range of vapor inlet temperatures from 810° to 964° F. Both wet and superheated vapor conditions were used. Flow rates were adjusted over a range of values at each inlet temperature in order to move the vapor-liquid interface from a position near the radiator condenser outlet manifold to a position near the inlet manifold.

The results demonstrated that a curved tube radiator condenser can be used to condense mercury vapor in a space power system over a relatively wide range of operating conditions. For the range covered in the present investigation, vapor-free liquid flow was obtained at the radiator condenser outlet, and relatively stable conditions occurred in the radiator condenser. Performance demonstrated the validity of the design method, except that measured pressure drops were considerably lower than those predicted by currently available analytical methods.

Remarks

At the time that the work was first started on this contract at Wright Field, interest was in condensing temperatures around 950° F, which is higher than current thinking for mercury systems. Also, sulfur was being considered as a working fluid; however, early results negated the use of sulfur, and most of the contract effort was concentrated on mercury.

DESIGN AND TESTING A SPRAY-TYPE CONDENSER FOR ZERO-GRAVITY OPERATION[6]

Objective

The objective of the contract is to design, fabricate, and test a spray-type condenser that will operate at the same design conditions as the curved-tube radiator condenser that was designed and tested under

[6]Contract No. AF 33(616)-7533; contractor, Electro-Optical Systems, Inc.; ASD project engineer, Charles L. Delaney.

Contract No. AF 33(616)-6520. The spray condenser would also utilize mercury as the working fluid, and this would allow a direct comparison of the results of the curved tube and spray condensers. Under this contract, the contractor will build the spray condenser and the curved tube condenser into a capsule which can be flown under zero-gravity conditions aboard the ASD zero-gravity aircraft. These flights are considered to be proof of feasibility since it is felt that the characteristics of these two types of condenser will be stable in zero-g conditions if they are stable for 1-g conditions.

Progress to Date

Because of the unrealistic temperatures and the difficulty in designing the capsule for flight testing at the temperatures and pressures at which the curved tube condenser was operated, it has been decided that the condensing temperature will be reduced to 650° F. Tests will also be run on the curved tube condenser at the new operating conditions in order that a comparison of the results can still be made.

Remarks

This work represents an in-flight companion program to the spray condenser laboratory investigations currently being funded by NASA as previously described. Zero-gravity flights in a KC-135 airplane are expected later in the year.

OFFBACE (ORBITAL FORCE FIELD BOILING AND CONDENSING EXPERIMENTS)[7]

ASD Participation - Zero-Gravity Flight Tests

In this program, ASD provided the coordination and the test facility which made the zero-gravity test flights possible. The OFFBACE test unit consisted of a simulated Rankine cycle utilizing mercury as the working fluid. The vapor entered the parallel tube condenser at approximately 3 to 6 pounds per square inch absolute and 0° to 10° F superheat and left the condenser at approximately 2 to 5 pounds per square inch absolute and 300° to 400° F. The range of flow rates was 0.2 to 0.6 pound per minute.

---

[7]Atomic Energy Commission contract; prime contractor, Atomics International; subcontractor, Thompson Ramo Wooldridge, Inc.; ASD project engineers, Charles L. Delaney and Lt. Lloyd M. Hedgepeth.

Report

The results of these tests will be published and distributed by the AEC.

Remarks

Figure 1 shows the Mark I rig that was flown in a 131 airplane. It contains a pot-type boiler as used by Thompson Ramo Wooldridge, a superheater, and a single-tube condenser. The condenser tube is glass along the straight section with a Pyrex end section and stainless-steel return leg. The valve could be closed off to build up liquid in the leg prior to the run. Cooling was obtained by blowing air over dry ice. Results of these tests were discussed earlier by the TRW representatives.

Figure 2 is a schematic of the Mark II loop. This system contains a nozzle to simulate turbine pressure drop and a desuperheater to provide vapor conditions that would correspond to those of the SNAP 2 system at the condenser inlet. The pump and the motor are the same as that in the SNAP 2 package. The condenser in this loop is a four-tube, parallel, air-cooled arrangement as shown in figure 2. Photographs of the condenser and boiler are shown in figures 3 and 4, respectively. The condenser tubes were oriented vertically in the airplane with flow entering the top. Good pressure-drop measurements were difficult because of the short tube length and the need to use absolute pressure gages. (Differential pressure gages could not operate properly at the low pressure levels.)

About four or five flights have been made in a KC-135 airplane. Reports of the results are being prepared for transmission to Atomics International and finally to the AEC.

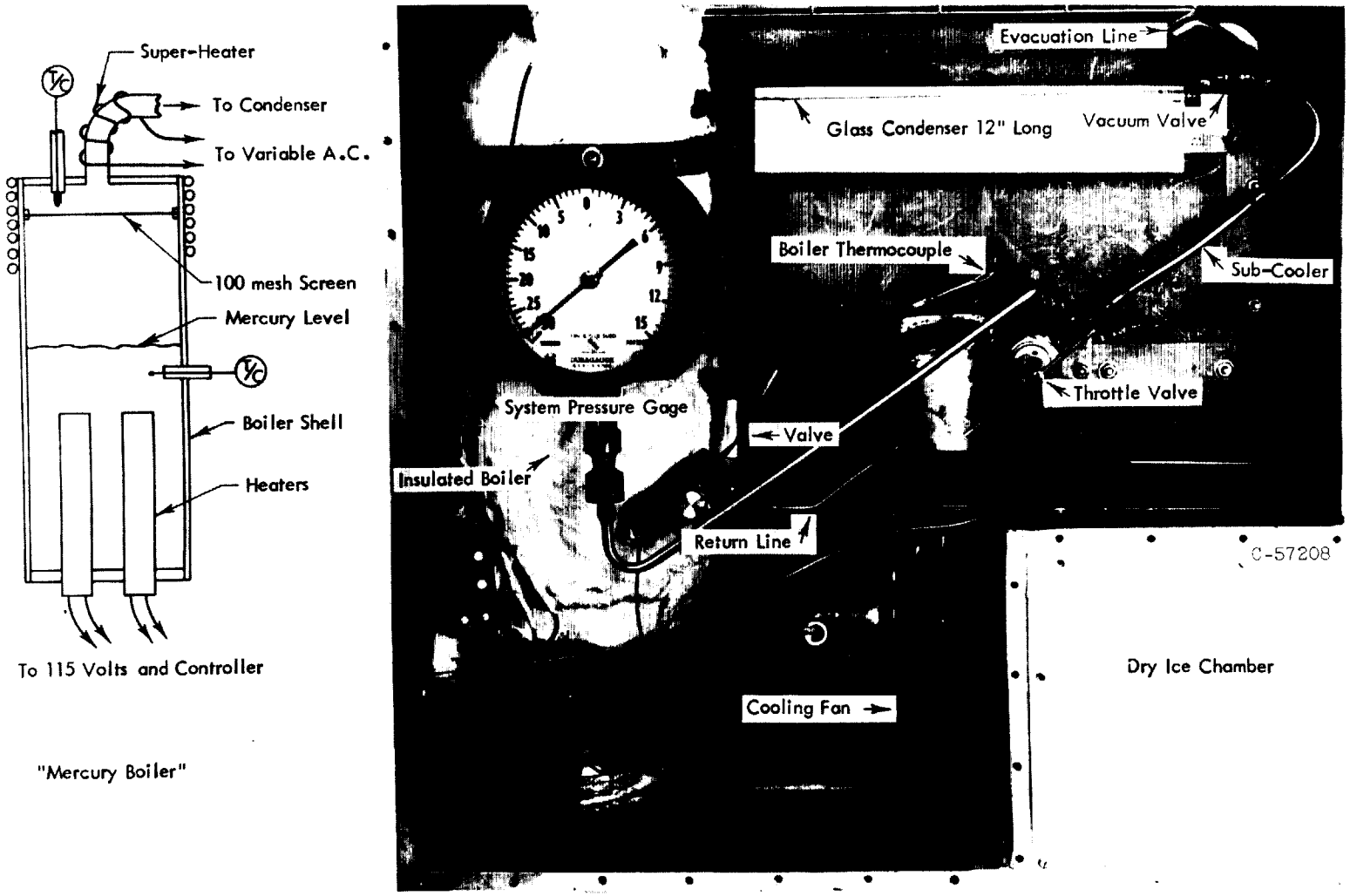

Figure 1. - Mark I loop.

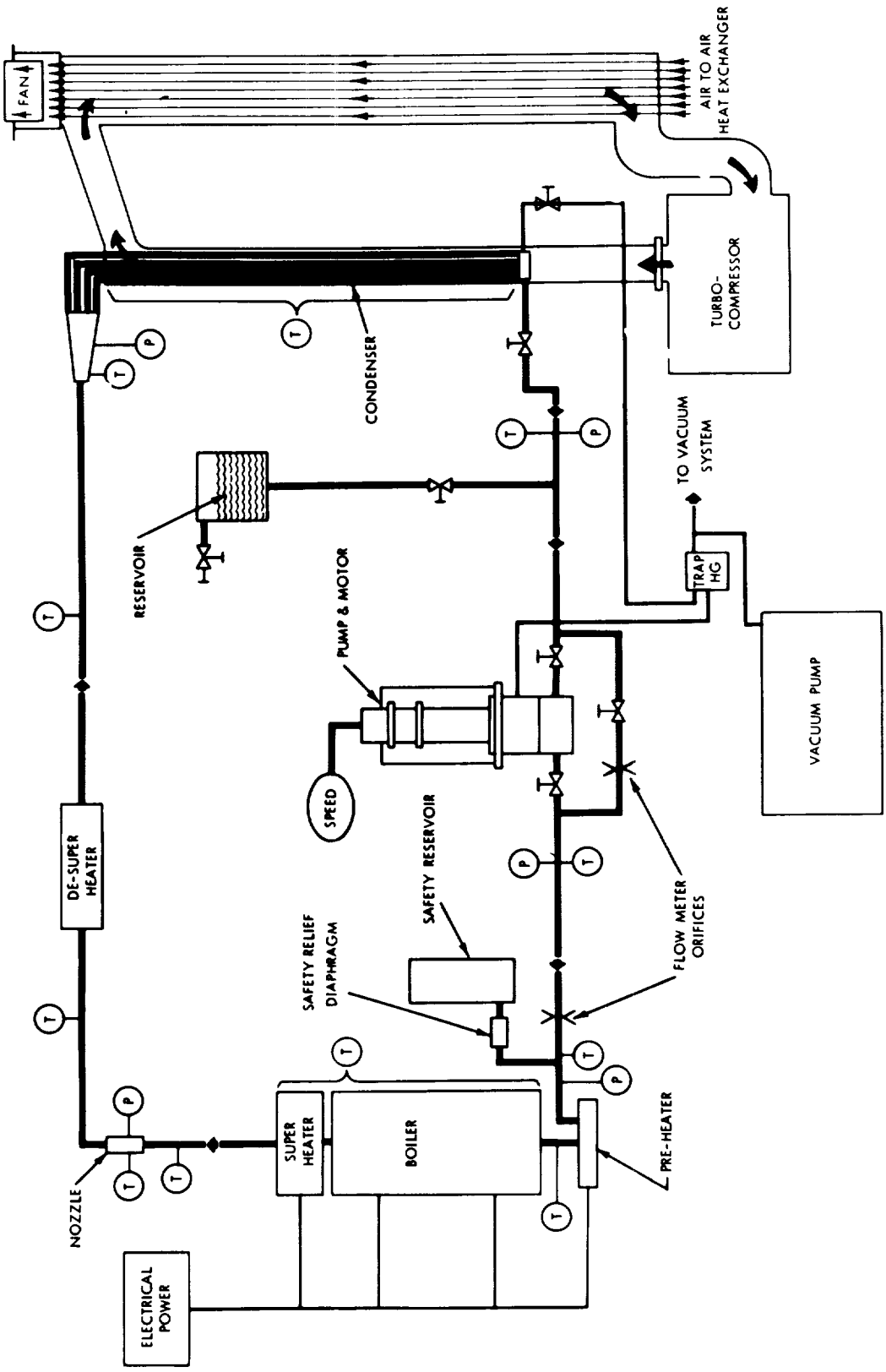

Figure 2. - Mark II OFFPACE loop schematic.

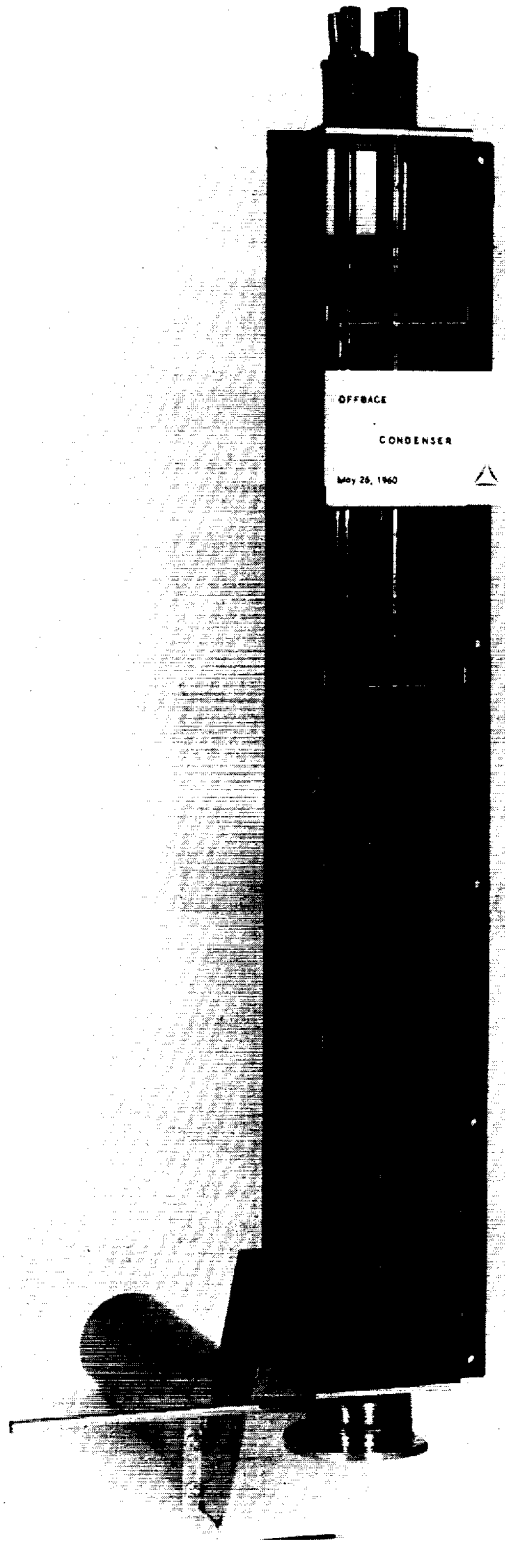

C-57210

Figure 3. - OFFBACE condenser.

E-1501

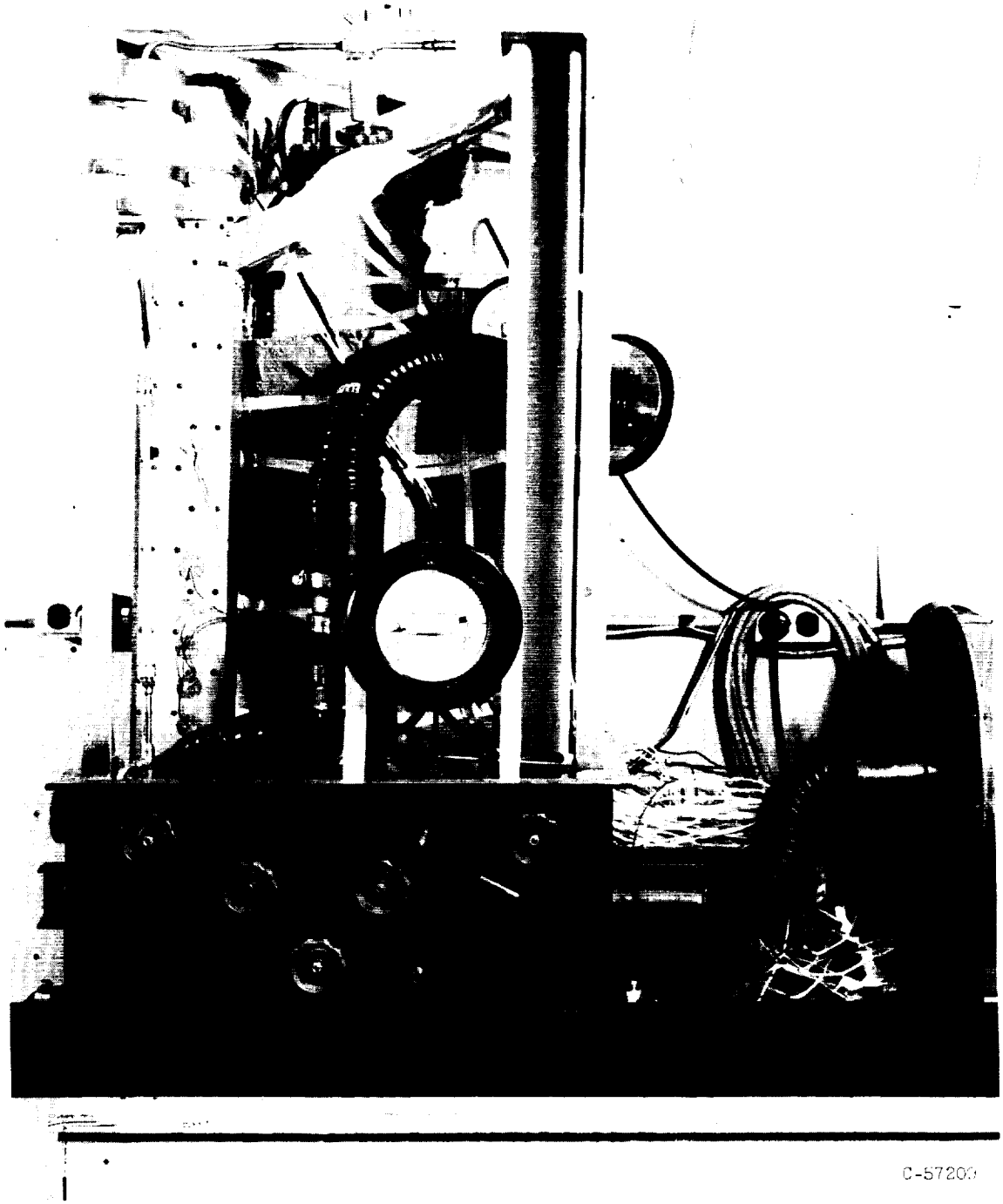

C-57203

Figure 4. - OFFBACE boiler.

SUMMARY OF DISCUSSION PERIOD

Following the individual presentations by the contributing organizations, an informal round-table session was held among the participants to discuss further some of the important questions and problems in mercury condensing. The specific topics discussed were space requirements and ground testing; test apparatus and measuring techniques; pressure drop; flow stability; effect of noncondensable gases; and physics of condensing.

This section presents a condensation of the principal comments and salient factors brought out during the discussions.

SPACE REQUIREMENTS AND GROUND TESTING

The topic SPACE REQUIREMENTS AND GROUND TESTING relates to the various requirements imposed on the design of the condensing system by the space environment and the problems involved in determining system performance under simulated or actual space conditions. The principal environmental factors influencing condenser design and performance were considered to be startup in orbit, operation at zero gravity or near zero gravity, and resistance to launch loads and vibrations.

The Sunflower condenser design considers a vibration frequency against amplitude spectrum and operation at 1 g in all directions. The requirement for the SNAP 2 condenser, however, is primarily a zero gravity force field. Accelerations arising from attitude control were estimated to be negligible. The SNAP 8 condenser also has to survive boost accelerations and the vibration spectrum of the launch vehicle with a maximum orbit g force of 10^{-3} or 10^{-4}. Some thought has also been given in these designs to balancing out sloshing forces in the piping systems.

In orbital startup, the condensing system must be primed and preheated. Priming concepts involve the use primarily of an excess fluid inventory. Preheating considerations require systems with low thermal capacity, which is inconsistent with the requirement of protection against meteoroids. Although many ways are possible, preheating may be accomplished through the use of selective surface coatings that have high absorptivity to solar radiation and low emissivity at low surface temperature. Shrouds or skins can also be used to accomplish this purpose or to act as heat retainers for the condenser. Another consideration in startup is that an adequate net positive suction head must be maintained at the condensate pump in order to avoid cavitation.

It was believed certain that mercury condensation and removal of condensate can be accomplished under conditions of zero gravity. The

problem is basically that of obtaining the necessary knowledge on how to design for such operation and how to overcome the various problems involved, such as flow instability, shifting interface location, and excessive pressure drop.

The principal problem involved in laboratory testing of space mercury condensing systems is eliminating or minimizing the effects of gravity. The current approach is to work with configurations in which forces substantially larger than the gravity force are introduced; thus the effects of gravity become negligible. Principal techniques employed involve capillary forces by using small (critical) diameter tubes (as in SNAP 2) or plugs in the ends of the tubes, or large centrifugal forces by using twisted ribbons or other swirl producing elements (as in SNAP 8). These devices, required solely for effective ground testing, are believed to be unnecessary for space operation. Thus, penalties in weight, pressure drop, and power may unnecessarily be incurred with the use of these devices. If the penalties are relatively small, however, meaningful laboratory tests can be made.

The most significant method of condenser testing is in the zero-gravity environment. Simulated zero-gravity experiments using the drop tower, airplane maneuver, or ballistic trajectory, however, have their individual shortcomings in brevity of time, varying initial conditions and accelerations at the start of the zero-gravity period, and limitations of equipment and measurements. Thus it is not generally possible to obtain exact correspondence between ground and simulated zero-gravity experiments. A mercury-condensing capsule designed for both ground and airplane tests is currently being prepared for such investigation by Electro-Optical Systems for Air Force use. However, it was agreed that all methods of laboratory and zero-gravity tests can yield useful information if the limitations and influencing factors of the approach are clearly understood and accounted for.

Since it may be advantageous in some applications, for fabrication and other reasons, to use larger diameter tubes than indicated by critical stability requirements (< 0.2 in. diam.), the question of scaling was raised. Although it has not yet been demonstrated, it was believed there should be no difficulty in operating bare large diameter tubes for true zero-gravity operation. However, such large diameter tubes could not be effectively laboratory tested on the ground. For other than strictly zero-gravity conditions, the use of artificial body force generators may be indicated for large tube diameters. It is also not clear how to scale tubes with body-force generators from small to large diameter. A compromise can be obtained by considering tubes with continuous or stepped taper so that a critical diameter is provided at the interface location.

TEST APPARATUS AND MEASURING TECHNIQUES

In reporting results of experimental investigations, it was indicated that complete descriptions of the apparatus, test procedures and conditions, and instrumentation used should be given. In particular, information on inlet vapor quality was deemed desirable. It was stressed that the original raw data should also be presented in order to enhance the correlation and comparison of data from different sources.

As far as specific measurements are concerned, the need for more accurate differential pressure transducers operating with mercury at low pressures was expressed. It was believed that low-temperature pressure gages can be used if the taps are properly filled and cooled; response times, however, might be reduced. Temperature measurements, on the other hand, were considered to be adequate with developments in process in industry for very accurate temperature-measuring devices. Gear pumps presented fewer operating problems than centrifugal pumps.

PRESSURE DROP

The prediction of pressure drop in mercury condensing systems was considered to be unsatisfactory. More accurate pressure-drop measurement and better controlled and identified experiments specifically directed toward pressure-drop studies are needed. The development of Martinelli type, two-phase, two-component correlations in conjunction with a step-by-step integration procedure for the tube length was considered a good approach to the problem. This procedure allows for variation of tube diameter and heat flux and may promote a better understanding of the process. The basic correlation data, however, should be based on mercury results. Significant differences in the condensing mechanism and friction effects may occur with different (especially wetting and nonwetting) fluids.

In making pressure-drop measurements, the interface location must be known accurately in order to account properly for the momentum pressure recovery. Friction pressure drop is difficult to measure accurately in short tubes with pressure taps located downstream of the interface because the friction drop will be small compared with the momentum pressure rise. Future tests should include variations in inlet vapor quality as well as Reynolds number. Somewhat different droplet - boundary layer relations may be obtained for different qualities.

The importance of using checks of the measurement accuracy was stressed. As a control, checks should be made with all-vapor and all-liquid runs and the results compared with established pressure-drop data. Runs with varying inlet quality without condensing should also be made to establish the basic adiabatic two-phase friction pressure drop.

Limiting pressure-drop magnitude can be determined as a control by assuming all vapor flow with instantaneous condensation at the pressure tap location.

As part of the pressure-drop studies, information is also desired to permit prediction of the vapor-liquid fraction along the tube. Such information is needed to determine fluid inventory weight so that the right amount of working fluid can be introduced to assure correct interface location.

In addition to the pressure drop along the condensing tubes, information is also needed about pressure losses in the inlet and outlet headers of the condenser. For the low-power-level mercury systems, headers were designed for constant diameter. This approach was taken for simplicity and reasonable assurance of achieving relatively constant pressures. High-power systems would have to consider tapered or stepped manifolds in order to optimize weight. Some of the manifold designs contained estimates of the pressure losses in both the header and the transition from the header to the individual tube (90° turn and sudden contraction). The transition losses can be a large fraction of the condensing pressure drop, depending on the condenser tube velocity. If the condenser tube velocity is much higher than the header velocity, the transition and overall pressure drop will not vary significantly for all tubes in the circuit.

In the previous header loss calculations, saturated vapor was considered at the entrance to the tubes. For wet vapor entering, the usual loss factors assuming gas flow can be computed and the appropriate Martinelli two-phase pressure-drop correction can be applied. Unfortunately, there are currently no data available on pressure losses in two-phase flow through bends, valves, and orifices. Furthermore, significant condensation can occur in the inlet header, and in all likelihood the condensed liquid will not pass equally into all tubes; most would be expected to go down the last tube. However, if it is true that the entrance loss is primarily a function of tube inlet vapor velocity, the effects on pressure drop should not be marked.

It was pointed out that header-loss investigations should also take practical fabrication considerations into account. Such factors as the type and "cleanness" of tube to header joint as well as fabrication and dimensional irregularities and compromises can adversely affect the pressure drop. The margin of control introduced by good theoretical header design can easily be lost in the final fabricated configuration.

Flow Stability

In the discussion of flow stability, attempts were made to define or identify the various stability phenomena that might be important in the flow through multiple parallel tube condensers. The first was the location and fluctuation of the liquid-vapor interface. Since the interface defines the start of the subcooling region, it is important to be able to fix its location within limits so that a continuous adequate subcooling can be provided for the pump, especially if the margin is small. It was also felt that any upstream movement of the interface could also cause difficulties, since such motion would tend to bleed fluid out of the boiler. This could be compensated by an inventory reservoir, but such a system might impose weight penalties.

Tests of multitube radiators oriented vertically would not be expected to produce realistic indications of interface location stability because of the inertia effect of the liquid static head. In the zero-gravity environment, slight pressure inequalities can be reflected in gross changes in liquid level. A substantial part of the static-head effect can be eliminated by the use of a horizontal orientation, but this would not represent a true zero-gravity situation. The system developers were aware of these considerations, and plans for the horizontal testing of all system components were indicated in some cases.

Opinion was not uniform on the prognosis of interface location stability in multitube condensers. Entirely uniform flow and liquid level could be expected theoretically only if there was essentially zero pressure drop in the inlet and outlet headers. Some feeling existed that the condenser is a self-stabilizing system to a large extent because the equal heat flux on all parts of the tubes tends to limit the extent to which the condensing length can change with equal flow in each tube. However, opinion was also expressed that design situations involving a large number of small diameter tubes feeding off a long header might easily produce large tube-to-tube flow nonuniformities and possibly local reversed flows. Such sensitivity could be reduced, it was believed, by using large headers. Large headers, however, would increase radiator weight. Header weight was not significant at the SNAP 2 and Sunflower power levels, but could be important at SNAP 8 and greater power levels.

The second factor in stability considerations is the influence of pressure perturbations in the condenser on other parts of the system, notably the pump and the boiler. Since mercury pumps for vapor cycles operate under comparatively large head rises, pressure fluctuations arising from slug formation and vapor bubble collapse in the condenser would not be expected to affect pump performance materially. If interface movement and shift in fluid inventory accompanied the fluctuations, however, serious effects in pumps operating close to cavitation and in boilers operating at the saturated condition could occur. In this

respect, it was noted that analog studies showed that boiler stability could be improved by operating in the superheat region.

A third form of instability is concerned with the response of the flow pattern or regime to outside disturbances such as vibrations and changes in body forces. Considerable further testing will be necessary, however, in order to define and understand the complete stability situation. Such investigation should involve tests of both components that are artificially disturbed and complete systems.

NONCONDENSABLES

Although mercury has negligible solubility for gases, noncondensable gases can be trapped by surface tension effects in which comparatively high pressures can be developed to contain the gas bubbles. Experience with mercury test loops has indicated that sizable quantities of noncondensable gases can occur and have significant effects for a long term operation. Effects of noncondensable gases have been observed at the pump and condensing interface. Entrained gas bubbles are not expected to have a noticeable effect on flowing fluid heat transfer since the controlling resistance in mercury radiating condensers is generally the outer-surface heat transfer. The gas bubbles, however, will tend to collect in the region of the interface and build up a concentration over long periods of time. This concentration will locally reduce heat transfer to the tube wall and interface and result in a local region of lowered temperature. It was not clear whether the gas concentrations tended to promote plug formation. Such concentration, however, is not believed likely to occur for spray condensers because of the agitation and dispersing effects of the mixing action.

Considerable difficulty can be experienced if slugs of noncondensable gases reach the comparatively small size pumps of mercury systems. If the gas slug is large and the liquid inertia low, the slug will stop at the inlet of the inducer or impeller, where it can materially alter the operating point of the pump and possibly cause cavitation. In this respect it was pointed out that even entrained bubbles could affect the minimum net positive suction head of the pump. The slug might also impose a flow control similar to a cavitating Venturi, such that the pump operating point might not be attained.

It was agreed that further investigation of effects of noncondensable gases is needed. Also, it would be well to try to eliminate all gases and work specifically with the fluids and materials of the system application. Entrained gases can be removed or reduced by means of ultrasonic agitators and frequent loop circulation and fill under hard vacuum. For space systems, hard vacuum purge can be obtained by leaving the system open and then sealing in orbit by means of an explosive valve. It was not known how to measure noncondensables or what might constitute an excessive amount.

PHYSICS OF CONDENSING

Experimental work to date in mercury condensing has produced only gross data and phenomena. For specific system applications, it was felt that such data are adequate. However, it was also recognized that a better understanding of the actual mechanism and detailed physics of the condensing process is desirable. Such knowledge would be useful in several ways: in determining how best to scale results; in enhancing ability to correlate and predict; and furthermore, in evaluating the differences in nonwetting and wetting condensation. It was the feeling that in actual systems where mass transfer may occur, the tubes will eventually become wetted. Further studies will be needed to determine whether this transition will produce a large order effect.

NASA TN D-1188
National Aeronautics and Space Administration.
GOVERNMENT-INDUSTRY CONFERENCE ON MERCURY CONDENSING, APRIL 18, 1961, PASADENA, CALIFORNIA. February 1962. 163p.
OTS price, $3.00.
(NASA TECHNICAL NOTE D-1188)

This report contains a collection of presentations on current developments by government and industrial organizations actively engaged in research and development on condensing components for Rankine cycle space power systems using mercury as the working fluid. A summary of a general discussion period treating specific topics in mercury condensing is also included.

Copies obtainable from NASA, Washington

I. NASA TN D-1188

(Initial NASA distribution: 20, Fluid mechanics; 35, Power sources, supplementary; 37, Propulsion system elements.)

NASA

NASA TN D-1188
National Aeronautics and Space Administration.
GOVERNMENT-INDUSTRY CONFERENCE ON MERCURY CONDENSING, APRIL 18, 1961, PASADENA, CALIFORNIA. February 1962. 163p.
OTS price, $3.00.
(NASA TECHNICAL NOTE D-1188)

This report contains a collection of presentations on current developments by government and industrial organizations actively engaged in research and development on condensing components for Rankine cycle space power systems using mercury as the working fluid. A summary of a general discussion period treating specific topics in mercury condensing is also included.

Copies obtainable from NASA, Washington

I. NASA TN D-1188

(Initial NASA distribution: 20, Fluid mechanics; 35, Power sources, supplementary; 37, Propulsion system elements.)

NASA

NASA TN D-1188
National Aeronautics and Space Administration.
GOVERNMENT-INDUSTRY CONFERENCE ON MERCURY CONDENSING, APRIL 18, 1961, PASADENA, CALIFORNIA. February 1962. 163p.
OTS price, $3.00.
(NASA TECHNICAL NOTE D-1188)

This report contains a collection of presentations on current developments by government and industrial organizations actively engaged in research and development on condensing components for Rankine cycle space power systems using mercury as the working fluid. A summary of a general discussion period treating specific topics in mercury condensing is also included.

Copies obtainable from NASA, Washington

I. NASA TN D-1188

(Initial NASA distribution: 20, Fluid mechanics; 35, Power sources, supplementary; 37, Propulsion system elements.)

NASA